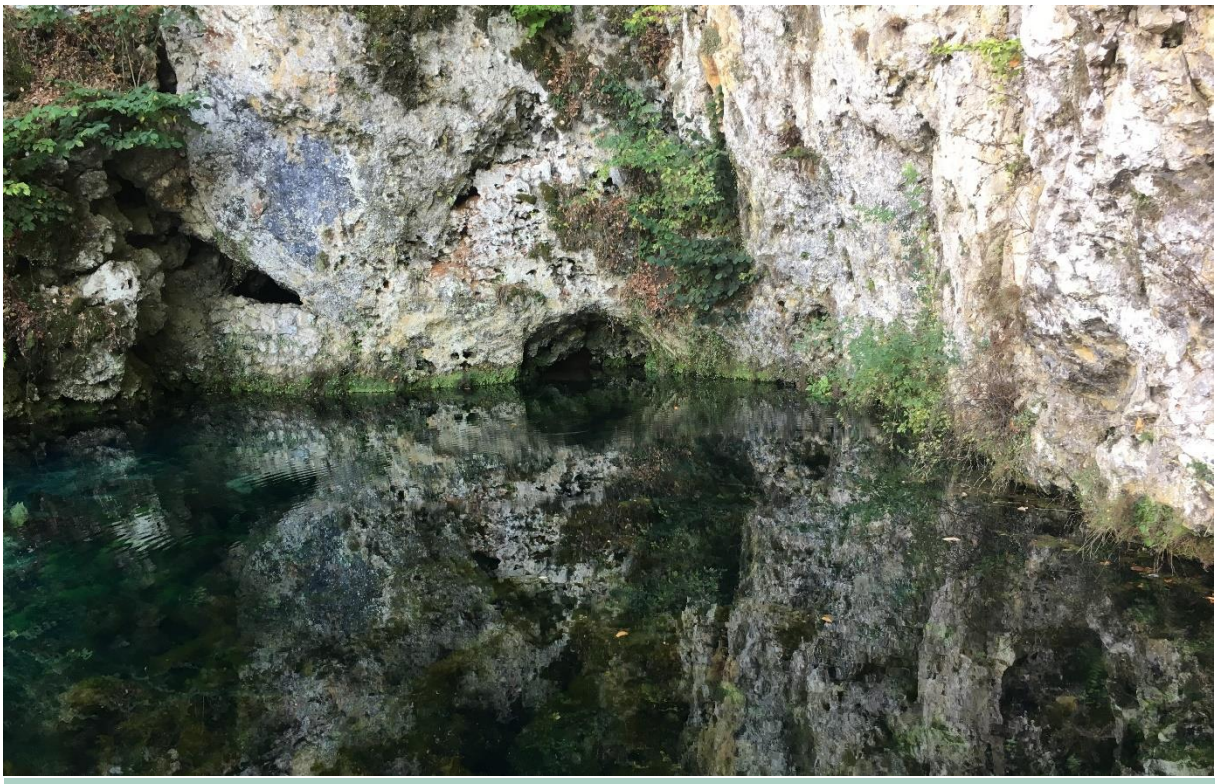

Evaluation of Darcy Flow Velocities Obtained from Borehole Dilution Tests

Johanna Lundin

Division of Engineering Geology
Faculty of Engineering
Lund University

MSc Thesis, 30 ECTS

ISRN LUTVDG/(TVTG-5159)/1-76/(2019)

Thesis work for Master of Science, 30 ECTS
Engineering Geology
Faculty of Engineering
Lund University

Evaluation of Darcy Flow Velocities Obtained from Borehole Dilution Tests

Johanna Lundin

Division of Engineering Geology
Faculty of Engineering
Lund University

in collaboration with

Institute of Applied Geosciences,
Division of Hydrogeology,
Karlsruhe Institute of Technology

Supervisors
Dr. Gerhard Barmen, Division of Engineering Geology
Prof. Dr Nico Goldscheider, Institute of Applied Geosciences
Dr. Nadine Göppert, Institute of Applied Geosciences
Examiner
Dr. Jan-Erik Rosberg, Division of Engineering Geology

Abstract

The project is part of a larger investigation of the water protection area *Donauried-Hürbe*. This area is a recharge zone used by one of Germany's biggest water supply companies, the *Zweckverband Landwasserversorgung* (LW). The freshwater supply originates from a 200 m thick karst aquifer in the Swabian Alb (*Schwäbische Alb*) and flows southest towards the *Donauried* and into a porous aquifer. The long-term research goal of the investigation is to define the flow time and flow path for the water moving from the recharge area to the main discharge area, to update protection zone boundaries and prevent contamination.

Groundwater flow patterns are being studied using tracer tests. However, finding suitable borehole for tracer inputs requires knowledge of subsurface flow behavior in these boreholes. This knowledge can be obtained by carrying out *single borehole dilution tests* (SBDT). The focus of this project was to determine the flow connections between several candidate boreholes and the aquifer, by calculating the Darcy flow velocity (also called filtration velocity) obtained from SBDTs. In some wells, sections with particularly high groundwater flow were detected. Such identified locations would therefore be recommended for tracer tests.

Based on results of the electrical conductivity development, total salt quantity development and Darcy flow velocity, four wells were identified as suitable for tracer tests (measurement wells 5303, 5312, 7721 and 7733). Another studied well (measurement well 2301) was identified as less suited for tracer tests due to low Darcy flow velocity. Even though Darcy flow velocity is normally used for groundwater flow in non-karstic aquifers, it seems to work relatively good for the karst aquifer wells 7721 and 7733.

Three different injection methods (stocking method, hosepipe method and point injection method), and two different measurement methods (Electrical Conductivity Meter and CTD-Diver) for SDBTs were investigated. Compared to the stocking method, the hosepipe method did not deliver any greater improvements for equally distributed salt injections. Due to this and the advantages that the stocking method has in terms of costs, technique handling, and preparation, it is a preferred injection method. The point injection method worked relatively well, based on problems met in the experiments of this thesis, but will work better in the future by developing an improved point injection device. Handling a CTD-Diver compared to an Electrical Conductivity Meter is more practical and time effective. However, the Electrical Conductivity Meter is preferred for SBDTs in boreholes where the groundwater flow characteristics are still relatively unknown. Based on information from point injection tests in a lab hall, density effects during SBDTs could be neglected.

In future experiments, SBDTs should be carried out in the field by combining different factors such as seasonal differences, salt quantity, and injection method. This would increase the understanding of how the filtration velocity may vary depending on different factors. From the results, it seems as if a more reliable model of the salt development quantity might be obtained when the measurements of electrical conductivity are made more frequently and during a longer time.

Keywords

Single borehole dilution tests (SBDT), Darcy flow velocity, karst aquifer, porous aquifer, Donauried-Hürbe, Germany

Acknowledgements

For the success of this master thesis I would like to thank my supervisors Prof. Dr. Nico Goldscheider, Dr. Nadine Göppert and M. Sc. Nikolai Fahrmeier at the *Institute of Applied Geosciences* (AGW) at *Karlsruhe Institute of Technology* (KIT). They have provided me with valuable guidance and necessary measuring equipment for field and lab work as well as a computer workplace. They and other staff at AGW have been very welcoming towards me and allowed me to be part of their team during these months. I would also like to express my gratitude to my academic supervisor Dr. Gerhard Barmen at the *Division of Engineering Geology* at *Lund University* (LTH), who gave me constructive feedback during the writing process.

Johanna Lundin
February 2019
Karlsruhe, Germany

Terminology

aquifer	a geologic unit that can store and transmit water at rates fast enough to supply reasonable amounts to wells
recharge area	the subsurface volume through which groundwater flows towards a specific discharge zone
Darcy flow velocity	groundwater velocity that has been calculated through Darcy's Law
Donauried	south-eastern part of the water catchment *Donauried-Hürbe* containing a gravel aquifer
electrical conductivity	measures a material's ability to conduct electric current, SI unit: Siemens per meter (S/m)
Electric Contact Meter	a tool that can measure electrical conductivity, water temperature and water level
The European Watershed	surface run-off divide that separates the water catchments of rivers discharging into the Atlantic Ocean, the North Sea and the Baltic Sea from those discharging into Mediterranean Sea, the Adriatic Sea and the Black Sea
Jurassic	the geological time period taking place 145-201 million years ago (before the Cretaceous period and after the Triassic period) during the Mesozoic era
karst	soluble sedimentary rocks with cavities and caves that have been formed by groundwater flows containing CO_2systems with sinkholes and cavities
molasse	a clastic sedimentary rock mainly consisting of sandstone from shore deposits
Quaternary	the youngest geological time period of the Cenozoic era, taking place from 2,6 million years ago until today
SBDT	abbreviation for Single Borehole Dilution Test
Swabian Alb (Schwäbische Alb)	south-western part of the water catchment *Donauried-Hürbe* containing a karst aquifer
Water Protection Zone	a designated area of a catchment area with specific land use restrictions, usually divided into three zones with different levels of protection needs
Zweckverband Landwasserversorgung	German water-supply company that prepares and distributes drinking water from the aquifer of Donauried-Hürbe

Contents

List of Figures

List of Tables

Chapter 1

Introduction

1.1 Background

In most parts of the world, karst aquifers are a pivotal contributor to freshwater supply. Roughly 20-25 % of the Earth's total population depend largely or completely on drinking water from these sources (Ford and Williams, 1989). In some European countries, karst aquifers contribute up to 50 % of the total freshwater supply. For many European regions, groundwater from karst aquifers is the only accessible drinking water source (Europea, 1995).

Karst aquifers form when groundwater containing carbon dioxide (CO_2) flows through soluble sedimentary rock. The CO_2 dissolves the carbonatic material, and leaves cavities and caves in the rock (Goldscheider et al., 2007). Many karst systems are hydraulically linked and distributed across large areas. These uniqe hydraulic fractures make them particularly vulnerable to contamination and difficult to manage (Ford and Williams, 1989). A contaminant which is released in one part of the aquifer can spread rapidly and negatively affect other parts of the aquifer (Goldscheider et al., 2010). Karst aquifers therefore require system-wide exploration and protection in order to be well understood and sustainably managed (Chen et al. 2017). For example, different protection zones should be defined for different parts of a karst aquifer system where each protection zone has specific restrictions regarding land-use (Goldscheider, 2005).

As a result of their high heterogeneity and anisotropy, karst aquifers generally cannot be studied using classical hydrology modeling. In some parts of the aquifer there might be large cavities with high groundwater flows and high discharge capacity, whereas in other parts there are basically no voids and a non-existent discharge capacity (Bakalowicz, 2005). Tracer tests, however, can be used as a reliable method to analyse and characterize flow velocities and flow paths in karst aquifers. This is why the Institute of Applied Geosciences (AGW) at Karlsruhe Institute of Technology (KIT) and the Zweckverband Landwasserversorgung are doing a long-term research project with tracer tests within the water protection area and karst aquifer of Donauried-Hürbe. A few tracer tests have already been carried out and more are planned. To choose suitable input points for the tracer, information regarding flow velocities and flow paths in the aquifer is needed. This information can be obtained by (multiple) Single Borehole Dilution Tests (abbr. SBDT) (Fahrmeier, 2016).

1.2 Purpose and aim

The purpose of this master thesis is to evaluate groundwater characteristics for the water protection area Donauried-Hürbe, so that contamination risks in the water discharged for drinking water purposes can be further assessed.

The main aim is to investigate the *depth-dependent Darcy flow velocity* (also called filtration velocity) of several boreholes at different hydrological conditions by conducting single borehole dilution tests (SBDT).

Other objectives consist of evaluating different SBDT injection methods (stocking method, hosepipe method and point-injection) and measurement methods (CTD-Diver and Electrical Conductivity Meter). Another objective is to investigate factors whether density effects might have significant impacts on a SBDT.

1.3 Project approach

The Darcy flow velocities occuring in the aquifer of Donauried-Hürbe were investigated by conducting SBDTs in the field. Previous SBDTs were looked at, optimized if possible and executed again if necessary. Relevant reports, expert opinions, research work and maps were studied.Groundwater measuring points occuring downstream of the injection point were observed, because an increasing electrical conductivity indicates the connection between these points and effective flow velocities can be calculated and compared to the Darcy flow velocities.

SBDTs based on different methods were carried out in a lab environment: "stocking method", "hosepipe method" and "point injection". With help from these results, the reliability of each method were evaluated and the factors with significant impacts for a SBDT were investigated.

Chapter 2

Theory

2.1 Introduction to study area

The study area Donauried-Hürbe is located in the eastern part of the German Federal State *Baden-Württemberg* and parts of the eastern Swabian Alb as well as the Donauried (Regierungspräsidium Freiburg Landesamt für Geologie, Rohstoffe und Bergbau, 2007). The exact location of the study area is presented on the map in Figure 1 for the location. It extends 36 km in east-west direction and 21 km in north-south direction. The main part of the water protection area is located within the rural districts of Alb-Donau (*Alb-Donau-Kreis*) and Heidenheim (*Landkreis Heidenheim*). The area also covers some parts of Ulm municipality (*Stadtkreis Ulm*) and the rural district of Göppingen (*Landkreis Göppingen*). The western part of the protection area, i.e. the Swabian Alb, has a ground elevation between 710 and 760 m.a.s.l., whereas the southeastern part, i.e. the Donauried, include elevations between 450 and 460 m.a.s.l. (Landesamt für Geologie, Rohstoffe und Bergbau Baden-Württemberg 2002).

Figure 1: Map of central Europe pointing out the location of the study area Donauried-Hürbe in southern Germany. (Source: Esri, DigitalGlobe, GeoEye, Earthstar Geographics, CNES/Airbus DS, USDA, USGS, AeroGRID, IGN, and the GIS User Community)

Across the study area, there is a well-developed network of state and district roads as well as important railway connections. A federal road ("Autobahn") is located along the southern border of the study area. The industry in the area mainly consists of small and medium-sized companies in the fields of mechanical engineering, vehicle construction and precision mechanics. However, the area is characterized by agriculture: mainly cereals (wheat and other winter cereals, spring barley and oats) and fodder crops. A major part of the Swabian Alb consists of farmland and forest. The southeastern part, i.e. the Donauried, mainly consists of farmland and greenland. The Donauried-Hürbe also comprises garden land, heathland, bog and swamp, groves and water bodies (Landesamt für Geologie, Rohstoffe und Bergbau Baden-Württemberg 2002). A detailed map of land usage in the study area can be found in Appendix 6.

2.2 Geology

Geologically, the study area can be divided into two main sections:

- **Jurassic limestone and Jurassic marl** in the Swabian Alb
- **Limestone with Tertiary and Quaternary sediments** in the Donauried

All geologic layers older than the Upper Jurassic are not relevant for the project and therefore not presented in this report (Regierungspräsidium Freiburg Landesamt für Geologie, Rohstoffe und Bergbau, 2007). A geologic overview map of the study area can be found in Appendix 6 and each relevant formation is presented with its corresponding abbreviation, summarized in Appendix 6.

2.2.1 Jurassic stratified formations in the Swabian Alb

During the time that a sea emerged in the Jurassic period, extensive marine deposit layers with a thickness of up to 600 m appeared in southern Germany. As the sea retracted, the sedimented limestone was subject to intense weathering and karstification (Udluft et al., 2000). In the part of the study area belonging to the Swabian Alb, a 400 m thick layer of this sedimentary rock from the Upper Jurassic period can be found. The layer dips slightly southeast, i.e. towards the Donauried. It consists of stratified facies and reef limestone facies in both horizontal and vertical directions. The lowest stratigraphic level relevant for this project is the *Lacunosa marl* formation. It mainly consists of layered marlstone and has a thickness of up to 50 m. Since the *Lakunosamergel* is almost incapable of karstification, it is considered as the aquifer base of the area (Regierungspräsidium Freiburg Landesamt für Geologie, Rohstoffe und Bergbau, 2007). See Table 1 for detailed description.

Table 1: Relevant Jurassic stratified formations in the part of the study area belonging to the Swabian Alb (Regierungspräsidium Freiburg Landesamt für Geologie, Rohstoffe und Bergbau, 2007).

	Formation	Facies	Thickness
Jurassic	Zementmergel-Formation (ki5)	dark grey marl, limestone marl and limestones	up to 140 m
	Liegende Bankkalk-Formation (ki4)	light grey layered limestones with marlstone interlayers	40-60 m
	Obere (Upper) Felsenkalk-Formation (ki3)	light grey, banked limestones with thin marl joints, pebble nodules	25-30 m
	Untere (Lower) Felsenkalk-Formation (ki2)	light grey, banked limestones with mostly thin marlstone joints	150 m
	Lacunosamergel-Formation (ki1)	dark grey marlstones with limestone and limestone marlstone banks	36-49 m

The *Liegende Bankkalk-Formation* (ki4), the *Untere Felsenkalk-Formation* (ki2) and the *Obere Felsenkalk-Formation* (ki3) are karstifiable and have undergone a relatively high amount of karstification. The most karstified formation is, however, the *Massenkalkfazies* coral reef limestone facies occuring in large quantities, with an expansion with a large vertical and horizontal extent, mostly found in Germany. It occurs as an additonal formation between the *Liegende Bankkalk-Formation* (ki2) and the *Zementmergel-Formation* (ki5). The *Massenkalkfazies*, abbreviated as joM, consists of light-grey to yellow-grey mass limestone, often classified as pure. Sponge-algae reef limestones, carbonate sands, and grey dolomite rocks can also be found. The *Massenkalkfazies* are divided into an upper and lower massive coral reef formation: *Obere Massenkalk-Formation* (joMo) and *Untere Massenkalk-Formation* (joMu), which together make up a thickness of 200 m (Regierungspräsidium Freiburg Landesamt für Geologie, Rohstoffe und Bergbau, 2007). The *Massenkalkfazies* shows strong karstification in the study area. In the northern part of the study area, the main karstification levels are to be found relatively deep in the geological formations, whereas in the southern part, it appears in younger and higher geological layers (Landesamt für Geologie, Rohstoffe und Bergbau Baden-Württemberg 2002).

2.2.2 Tertiary molasse formations in the Swabian Alb and the Donauried

Concurrently with the Alpine orogeny during the early Tertiary, tectonic uplifts as well as depressions of the molasse basin occured in southern Germany. The changes were accompanied by filling with alpine debris. The tertiary molasse reaches up to the Swabian Alb, where limnic, fluvial, brackish and marine deposits can be found. The molasse sediments have a thickness of between <0,5 m and 90 m. The layer thickness increases in the southern direction and therefore is thinnest in the northern part of the study area (Regierungspräsidium Freiburg Landesamt für Geologie, Rohstoffe und Bergbau, 2007). Due to changing deposition conditions, the geological surface cover consists of alternating layers of clay, silt, sand, gravel and marly rocks (Udluft et al. 2000).

In the middle of the study area, molasse appears in small, isolated spots at the surface. The molasse occurence becomes more frequent further south. In the Donauried, it covers the Jurassic formations almost completely (Landesamt für Geologie, Rohstoffe und Bergbau Baden-Württemberg 2002). As a result of premolassic reliefs in the Swabian Alb, the thickness of the tertiary layers varies largely and at some spots the tertiary molasse is completely absent (Regierungspräsidium Freiburg Landesamt für Geologie, Rohstoffe

und Bergbau, 2007).

The Tertiary molasse formations can be divided into two types:

- The Tertiary molasse formations occuring in the eastern part of the Swabian Alb
- The Tertiary molasse formations occuring beneath the Quaternary molasse in the Donauried

See Tables 2 and 3 for more detail.

Table 2: Molasse formations in the Swabian Alb (Regierungspräsidium Freiburg Landesamt für Geologie, Rohstoffe und Bergbau, 2007). *Locations shown on map in Appendix 6.

	Formation	**Facies**	**Distribution area**
Jurassic	Jüngere Nagelfluh, (J2)	fluviatile pebbles from Upper Jurassic limestone - a type of conglomerate only existing in southwestern Germany	south of Gerstetten, east of Langenau*
Tertiary	Obere (Upper) Süßwassermolasse, (tOS)	freshwater limestone, greenish marl, fine-grained yellow-brown-greenish grey sands, sandy marl, sand marl	small scale; for example by Gerstetten-Dettingen and Gerstetten-Heuchlingen*
	Obere (Upper) Meereswassermolasse, (tOM)	yellow-brown and greenish micaceous fine-grained coarse-grained sands, clayey sands, sand marls	south of the cliff line (*Klifflinie*)*
	Untere (Lower) Süßwassermolasse, (tUS)	yellow to greenish-grey clays and silt, yellow-brown fine-grained sands, sandy marls, freshwater lime	southeast of Lonetal

Table 3: Tertiary molasse formations in the part of the study area belonging to the Donauried (Regierungspräsidium Freiburg Landesamt für Geologie, Rohstoffe und Bergbau, 2007). *Locations shown on map in Appendix 6

	Formation	**Facies**	**Distribution area**
Tertiary	Obere (Upper) Süßwasser- (Freshwater) molasse, (tOS)	micaceous fine sands (Flinz)	southeastern Donauried
	Brackwasser- (Brackish water) molasse, (tOM)	Kirchberg strata (fine-grained deposits with organic layers and pyrite), Grimmelfingen strata (marley sands with partly high pyrite contents)	eastern, middle and western Donauried
	Untere (Lower) Süßwasser- (Freshwater) molasse (tUS)	grey, greenish or red clayey-merky facies, fine sands	eastern and western Donauried

2.2.3 Division of the Swabian Alb into *Kuppenalb* and *Niedere Flächenalb* along the *Klifflinie*

The *Obere Süßwassermolasse* (tOS) and the *Untere Süßwassermolasse* (tUS) were deposited in lakes. In the Donauried, the *Obere Meeresmolasse* (tOM) was eroded before the *Brackwassermolasse* (tBM) started to form (Regierungspräsidium Freiburg Landesamt für Geologie, Rohstoffe und Bergbau, 2007). As the *Obere Meeresmolasse* was deposited, the tertiary *Molassemeer* extended as far as to the Swabian Alb. The coastline that existed at that time is still visible along the *Klifflinie* (Eng. cliff line) in the form of an abrupt terrain level change of 50 m. The *Klifflinie* divides the Swabian Alb into two sections:

- The *Kuppenalb* north of the *Klifflinie*
- The *Niedere Flächenalb* south of the *Klifflinie*

The *Kuppenalb* landscape is characterized by its peak- and bowl-shaped formations, which developed as a result of the different erosion susceptibilities of the *Bankkalk* and the *Riffkalk*. The *Niedere Flächenalb* demonstrates in contrast a flat land surface in which the streams *Lone*, *Hürbe*, *Brenz* and *Egau* flow (Landesamt für Geologie, Rohstoffe und Bergbau Baden-Württemberg 2002).

2.2.4 The different layers of Quaternary sandy gravel in the Donauried

In the Donauried (and some parts of the Swabian Alb), the Jurassic and Tertiary rocks are covered by Quaternary deposits, mainly originating from the Alps but also partly from the Swabian Alb. In the dry valleys (without regular surface flows) of the Swabian Alb, there are for instance considerably large thicknesses of alluvial loam. At some spots in the Donauried, the Tertiary layers are overlain by a Quaternary sandy gravel cover of up to more than 11 m, consisting of three different depositional layers (Regierungspräsidium Freiburg Landesamt für Geologie, Rohstoffe und Bergbau, 2007, Anlage 5)

- The oldest of these sandy gravel deposits developed during the Riß-Würm Interglacial Stage (a major division of the Pleistocene) and today build up the high terrace at the southern edge of the Swabian Alb
- The second oldest sandy gravel deposit originates from the Würm glaciation, forming a *lower terrace*
- The youngest layer consists of redistributed sediments and riverbed sediments

(Encyclopedia Britannica, 2009; Regierungspräsidium Freiburg Landesamt für Geologie, Rohstoffe und Bergbau, 2007).

In almost the whole study area, gravel overlays the tertiary molasse. In the north of the Donauried, however, the tertiary molasse eroded, and due to this the quaternary gravel can be found directly above the Jurassic limestone (Udluft et al. 2000). Smaller spots where the molasse has eroded can be found in the middle of the Donauried, for example at *Fassung 2* and *Fassung 4*, see Appendix 6. The Quaternary deposits in the Donauried are overlain by a top layer up to 7 m thick (Regierungspräsidium Freiburg Landesamt für Geologie, Rohstoffe und Bergbau, 2007).

2.3 Hydrogeology

2.3.1 Hydrogeological description

The study area can be divided into two hydrogeological parts:

- One **Upper Jurassic karst aquifer** located across the Swabian Alb and underneath the molasse
- One **Quaternary gravel aquifer** which overlays the molasse and at some points has direct contact with the underlying Upper Jurassic karst aquifer (Landesamt für Geologie, Rohstoffe und Bergbau Baden-Württemberg 2002)

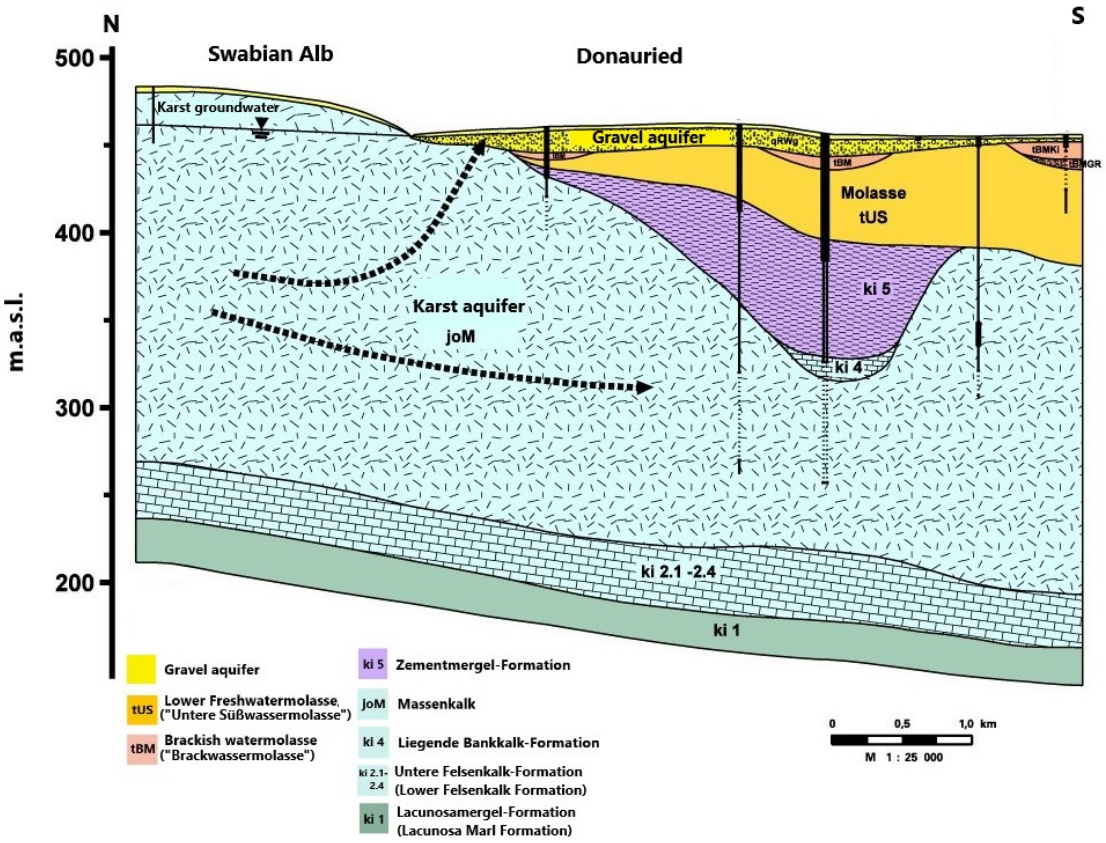

Figure 2: Hydrogeological cross-section through the study area from Langenau to discharge container ("Fassung 3"). The Swabian Alb (German: Schwäbische Alb) is located to the left in the figure and Donauried to the right. The exact location of the cross-section can be found in Appendix 6. (Soure: Regierungspräsidium Freiburg Landesamt für Geologie, Rohstoffe und Bergbau, 2007; Anlage 8.5)

The karst aquifer is a continuous and highly heterogeneous aquifer with a thickness of up to 200 m (Udluft et al. 2000). It is the most productive aquifer in Germany, with particularly high water flow velocities in strongly karstified zones and separation joints. Lower, but still influental, groundwater flow takes place in smaller matrix porosities. Due to this, a wide range of groundwater velocities exist in the aquifer. Pollutants can be temporarily stored in the aquifer and not re-mobilized until after a long period of time. Recharge into the aquifer mainly occurs via percolation through karstified subsoil, e.g. in sinkholes and dolines. At several

locations along the karst aquifer, groundwater deposits can be found on top of an impermeable surface layer. This water drains at the fringe of the karst aquifer or into small springs, and eventually ends up in the karst aquifer (Landesamt für Geologie, Rohstoffe und Bergbau Baden-Württemberg 2002).

In the northwestern part of the water protection area Donauried-Hürbe, the European watershed divides the karst aquifer into two sections:

- One section located **north** of the line of the European Watershed, where water from precipitation eventually flows into the **Rhine** and later ends up in the **North Sea**
- One section located **south** of the line of the European Watershed, where water from precipitation flows towards and along the **Danube**, and then further to the **Black Sea**

The exact position of the divide may alter with changing groundwater levels in the karst aquifer. Since the karst groundwater level varies depending on the time of the year, there is no fixed boundary. Low groundwater levels occur in late autumn and early winter, whereas high levels appear in late winter and early spring as a result of ice and snow melting (Landesamt für Geologie, Rohstoffe und Bergbau Baden-Württemberg 2002).

For the part of the study area located south of the European watershed, the alluvial recharge into the aquifer takes place far above the aquifer base level. As a result, this part of the aquifer is denoted as deep karst. Here, the most rapid groundwater velocities for the study area (approx. 100 m/s) occur, due to particularly notable karstification. The groundwater flowing south-east is partly disharged into overflow springs, e.g. the Nau springs (German: *Nauquellen*) in Langenau. High water levels in these springs indicate a high groundwater level in the karst, and vice versa. A significant amount of the water that doesn't flow into the springs, flows instead where there is an absence of molasse, and into the Quaternary gravel aquifer (Landesamt für Geologie, Rohstoffe und Bergbau Baden-Württemberg 2002). Groundwater flowing from the karst aquifer into the gravel aquifer has a velocity of 3.5 - 3.8 m^3/s (Schloz 1993). The groundwater mostly flows horizontally into the gravel aquifer. However, in the central parts of the Donauried where the molasse surface cover is very thin or absent, there is vertical groundwater flow directly from the underlying karst aquifer (Landesamt für Geologie, Rohstoffe und Bergbau Baden-Württemberg 2002).

Concerning groundwater level fluctuation, there is an important difference between the karst aquifer and the gravel aquifer. Due to higher water storativity in the gravel aquifer, it has experienced 2-4 m of recorded groundwater level fluctuations, whereas levels in the karst aquifer may vary by more than 20 m (Landesamt für Geologie, Rohstoffe und Bergbau Baden-Württemberg 2002).

2.3.2 Groundwater contamination risk

Due to open conduits, karst aquifers are particularly vulnerable to contamination. Contaminants can be transported quickly and over long distances with little dilution. Sinking streams, sinkhole drains, and open fractures in the bedrock provide little or no filtration for incoming water (Vesper et al., 2001). Less permeable top layers, such as for example the molasse, help protect the underlying karst aquifer through filtration and microbial degradation to a certain degree. The presence of such top layers should be reflected in the locations of the different water protection zones. Areas with high protection capacity include areas with molasse layers, and vice versa. The water protection capacity in the study area is, however, still limited. Zweckverband

Landwasserversorgung faces many challenges with intensive agricultural and forestry activities as well as settlement, industry, raw material mining and landfills that are present in Donauried-Hürbe (Landesamt für Geologie, Rohstoffe und Bergbau Baden-Württemberg 2002).

2.4 Water protection zones

2.4.1 General definitions

A recharge area is usually divided into three water protection zones. The zones have certain restrictions regarding land-use and infrastructure installations in order to minimize the contamination risk and ensure good quality for the discharged water. An area where the risk of groundwater contamination is higher (in case of for example chemical pollution) is assigned more land-use restrictions and vice versa. By analyzing the hydrogeological situation (flow direction, flow velocity, hydraulic conductivity and transmissivity of the aquifer) as well as the annual groundwater recharge, the size and location of the protection zones can be determined. Usually, areas closer to a discharge well are assigned stricter water protection regulations. During the past decades, Germany has been active in improving contamination prevention for water wells. For example, more than 25% of the land surface of Baden-Württemberg today water lies in protection zones. (Zhu and Balke 2008)

The restriction for the different zones are specified below:

- *Water Protection Zone III*: well field management zone. Guarantees the protection of a well from non-degradable or heavily degradable chemicals and radioactive pollutants. Covers the hydrological and hydrogeological recharge area of a well.
- *Water Protection Zone II*: attenuation zone. Protects a well from pollutions specifically caused by microorganisms such as bacteria, germs and viruses. Since most of the microorganisms introduced into the groundwater are eliminated after 50 days because of dying off, decay and absorption, the boundaries of protection zone II have to be located within the so-called "50-day-line", i.e. a line from which it takes 50 days for flowing groundwater to reach a discharge well.
- *Water Protection Zone I*: remedial action zone. Protects the direct vicinity of a well against contamination and destruction. German regulations state that it should cover an area of at least 10 meters from the well in all directions. Within this area, unauthorized entry is prohibited. (Zhu and Balke 2008)

2.4.2 Water protection zones in the study area

The location of the water protection zones in the study area are presented on a map in Appendix 6. Protection zone II of Donauried-Hürbe is located in the southeast part of the catchment and has an approximate length of 16 km and width of 2-4 km, with a total area of 38,6 km^2 (Landwasserversorgung Stuttgart Kommunaler Zweckverband, 2012). The area corresponds to the gravel aquifer from which almost all groundwater for the Landeswasserversorgung is discharged. The discharge wells are divided into six capture zones which have been assigned with protection zone I due to their immediate contact with the boreholes. The rest of the water protection area belongs to protection zone III. (Landesamt für Geologie, Rohstoffe und Bergbau

Baden-Württemberg 2002) With better knowledge of the hydrogeological situation of Donauried-Hürbe, the current borders of the different water protection zones can be re-evaluated and be more accurately defined in order to protect the water wells even better.

2.5 Zweckverband Landwasserversorgung

The Zweckverband Landwasserversorgung (LW) is one of Germany's largest water-supply companies. It started its first installations in 1917 and today provides drinking water for about three million people in southern Germany, including cities such as Stuttgart and Ulm (Zweckverband Landwasserversorgung, 2017). They extract water from the Buchbrunnen Spring at Dischingen, the river Donau, and the gravel aquifer in the Donauried. The water is then treated before being distributed to the consumers.

Today, the Zweckverband Landwasserversorgung take their water from over 200 production wells, which are divided into six discharging areas (so-called container systems, in German *Fassung*) in the gravel aquifer of Donauried. Two of the wells located outside of these six areas are deep wells reaching the karst aquifer beneath the gravel layer. One of Germany's largest groundwater protection areas (>500km^2), was established for the well recharge area. (Landesamt für Geologie, Rohstoffe und Bergbau Baden-Württemberg 2002). In the groundwater protection area, more than 600 groundwater measuring points were built in the last 100 years.

Current boundaries of the water protection area Donauried-Hürbe were defined in 1967 by the Zweckverband Landwasserversorgung. Since then, there has been extensive geological and hydrogeological mapping, investigations, and numerical modelling of the groundwater conditions but few updates of the water protection zone boundaries (Regierungspräsidium Freiburg Landesamt für Geologie, Rohstoffe und Bergbau, 2007).

2.6 Single Borehole Dilution Test (SBDT)

Borehole dilution techniques can improve understanding of the spatial flow distribution of an aquifer, which gives valuable insight into contaminant transport. This technique is based on determining the depths at which water enters and leaves a borehole. At each of these locations, the in- and outflow rates can be determined. Since a SBDT is carried out in an undisturbed borehole under natural head conditions, it is a much simpler and cost-effective method than other commonly used techniques that require pumping. A SBDT also makes it possible to identify fractures that may be undetected by temperature and electrical conductance logging (Maurice et al., 2011).

Borehole dilution tests are a relatively widely used tracer technique (Fitts, 2002). The theory behind the method is well established (Halevy et al., 1967; Drost et al. 1968; Gaspar 1987). The principle consists of adding a specific amount of salt into a water well and measuring how fast it disappears into the rest of the aquifer (Pitrak et. al., 2007). This is done either using a uniform distribution of salt along the whole water saturated depth of a borehole, or a point-emplacement of salt at a specific depth in the borehole (Maurice et al., 2011). As groundwater flows into and out of the well, the electrical conductivity is measured. From the salt dilution curve, groundwater velocity can be derived. A detailed explanation of how to execute a SBDT, including different injection and measurement methods, is described in section 3.2. A detailed evaluation

approach of the results from a SBDT is described in section 3.3.

2.6.1 Injection methods

There are three possible injection methods used in SBDTs: the stocking method, the hosepipe method, and the point injection. The first two create a uniform distribution of salt whereas the latter injects salt only at a specific section along the borehole. All methods can identify flowing fractures. Usually, examination of a borehole starts with uniform-emplacement SBDT, which provides an understanding of the general flows throughout the saturated water depth. An additional point-emplacement SBDT may be necessary to clarify uncertainties at different sections of the borehole. The combination of uniform-emplacement and point-emplacement gives more understanding of the flow characteristics than either method alone (Maurice et al., 2011). See section 3.2.1 for more details.

2.6.2 Measurement methods

Several different measurement tools can be used in SDBT:s. These include Electrical Conductivity Meters and CTD-Divers. Both help measure the electrical conductivity at different water depths. With an Electrical Conductivity Meter, the electrical conductivity values are shown on a display and are then manually written down (Solinst, n.d.). With a CTD-Diver, the electrical conductivity is directly recorded as a digital file (van Essen Instruments, 2016). See section 3.2.2 for more detail.

2.7 Darcy Flow Velocity

The filtration velocity is a key parameter to evaluate pathways for contaminant transport in an aquifer. It is derived from the definition of Darcy flux or groundwater flux q, introduced by Henry Darcy in France in 1856. According to Pitrak et al. (2007), the dilution technique is the only reliable method for investigating the filtration velocity of a borehole. Other experimental methods with for example Doppler scattering or optical tracing of suspended particles have been proven to be unreliable for such purposes (Pitrak et al., 2007). In most parts of the aquifer belonging to the study area, there is both horizontal and vertical groundwater flow. In this master project, however, the focus for the SBDTs lies in estimating the filtration velocity of groundwater in the surrounding aquifer. In order to calculate the horizontal flow, the vertical component of water flow can be averted by using a packer. Another possibility is to detect intervals where vertical flow occurs in the borehole, and exclude them in the filtration velocity calculations. Darcy flow velocity can be determined by deriving the decline in the average salt concentration from a SBDT. The horizontal flow velocities in a well generally range between 1×10^{-6} m/s and 1×10^{-4} (Pitrak et al., 2007). The Darcy flow velocity calculation procedure is explained in further detail in section 3.3. Darcy flow velocity is primarily targeted for porous aquifers, however, according to previous experience within the research project which this master thesis is a part of, it could give valuable information also for karst aquifers.

2.8 Concerns

2.8.1 Density effects

Theoretically, all added salt dissolves directly into the water in the borehole. In reality, this doesn't happen instantly, and salt is more dense than water, so some salt could sink by gravity before it is dissolving. Even though the salt is finely ground to minimize these effects, they are still a concern. According to Lamontagne et al. (2002), density effects during salt solution injection can be negligible. However, according to the well-cited article by Ogilvi (1958), usage of NaCl can indeed face some obstacles. To evaluate whether density effects during solid salt injection should be taken into account, some SBDTs were executed in a lab environment.

2.8.2 Improper release of salt

To properly analyze the results from a SBDT using the stocking method or hosepipe method, it is important that the salt is injected as uniformly as possible. Obtaining a homogeneous mixing of salt has been a challenge for this project. Several improvements have been tried, such as pulverizing the salt so that it dissolves faster and thereby making the duration of injection shorter.

2.8.3 Environmental risks

Typical quantities of salt used are 25-100 g for shallow wells (10-20 m depth) and up to 800 g for deep wells (40-75 m depth). The wells injected with smaller amounts of salt are located approximately 1 - 2,5 km from the Landwasserversorgung's discharging wells, whereas the same distance for the deep wells is around 4 - 5 km. As mentioned, the catchment from which the discharged water originates from, has a total area of $>500\text{km}^2$. In comparison to the volume of groundwater flowing through the aquifer, the salt quantities used in the SBDTs are very small. As long as only a few tests are carried out on the same day, the environmental risks of the salt are therefore negligible.

Chapter 3

Material and Methodology

3.1 Information base

Information about the water protection area Donauried-Hürbe has mainly been extracted from documents of Zweckverband Landwasserversorgung's large existing inventory. GIS-shapefiles including valuable data about the area, were provided by Zweckverband Landwasserversorgung for this thesis. The GIS shapefiles include border limits of the water protection area, Donauried-Hürbe as well as a geological map of the region. The GIS data also included information about the location of groundwater wells. Additional information was collected from various reports and scientific articles (see Reference section).

3.2 SBDT execution

First, the ambient background electrical conductivity must be measured throughout the whole saturated water column at different depths in a monitoring well (Pitrak et al., 2007). Groundwater normally has an electrical conductivity of 50-2000 µS/cm, whereas seawater has values between 45 000 and 55 000 µS/cm (Langguth and Voigt, 2004). Electrical conductivity values can be converted into salt concentrations by creating a calibration for each borehole. The concentration over time can be used to calculate Darcy flow velocity for each depth (Pitrak et al. 2007).

Next, an initial salt concentration condition is applied to the total water-saturated depth of the well with either a *hosepipe* or a *normal nylon sock*. The uniform condition should consist of an evenly distributed concentration of a specific measurable substance, such as salt (Pitrak et al., 2007). Another possible injection method used in SBDT is *point injection*, in which salt is only applied at a specific depth of the well and not uniformly throughout the whole borehole.

During the injection, the salt increases the electrical conductivity of the well water. Afterwards, the electrical conductivity is measured at different depths and times until it returns to background condtions, i.e. the well conditions that existed shortly before the salt was applied. The rate of which concentration decrease gives information about the connection between the well and the surrounding aquifer. Special attention should be paid if different sections of a groundwater measurement point show a different behaviour or an unequal decrease. (Pitrak et al. 2007)

3.2.1 Injection methods

Stocking

A weighted nylon stocking is filled with a specific mass of dry salt and then lowered into the monitoring well. It is moved up and down until all the salt had been dissolved. This is done throughout the whole water saturated depth of the well in a steady pace in order to distribute the salt as evenly as possible (Fahrmeier, 2016). The sock is moved throughout the borehole at a pace of approximately two-three seconds per meter. Usually the stocking has to be lowered into the well several times before the salt is completely dissolved. A setup of the tools is presented in Figure 3.

1: A thin nylon stocking.

2: A specific mass of salt (NaCl).

3: Tape line to lower the salt-filled sock into the well. Here, the metric tap of an old electrical contact meter is used.

3: *TLC Model 7* Electrical Contact Meter from *Solinst* for measuring water level and electrical conductivity.

Figure 3: Setup of tools and material used in a SBDT performed with the stocking method.

To prevent any salt from trickling out when using the stocking method, the stocking is lightly wetted before inserting the salt into it. The stocking is attached to a thin rope, marked to indicate the total depth of of injection. The lower edge of the depth range corresponds to the bottom of the groundwater well, and the upper edge corresponds to the point at which the filter pipe starts. Figure 4 shows a nylon stocking filled with salt and an illustration of a salt filled stocking inserted into a measuring well.

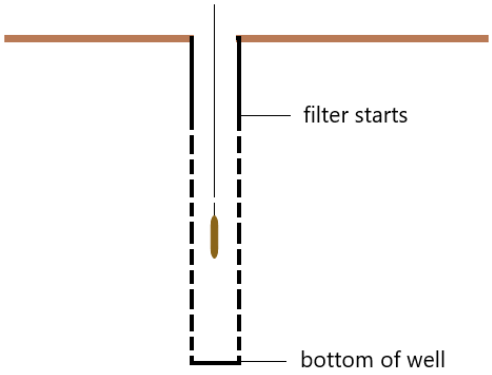

(a) Illustration of stocking in measuring well.

(b) Nylon stocking filled with salt.

Figure 4: Injection with the stocking method.

Hosepipe

In the hosepipe method, a weighted hose was inserted into the borehole. The hose was filled with a salt solution up to the filter level. As the hose was pulled out in an even and relatively fast pace, an even distribution of salt over the desired depth could be achieved (Maurice et al., 2011). In this project two types of hosepipes were used: one hosepipe with a diameter of 5 cm made out of soft, thin plastic, and one normal garden hosepipe with a diamater of approximately 1 cm made out of harder, thicker, and more unflexible plastic. In lab experiments, the salt quantites injected through salt solution are 65 g and 180 g. No hosepipe method was carried out in the field. Figure 5 anf 6 shows a setup of tools for each of the two hosepipe methods. Figure 7 illustrates a hosepipe being inserted into a measuring well and Figure 8 shows how to prepare for a SBDT with the hosepipe method.

1: Hosepipe made of thin plastic material.

2: Plastic cup that is fixed to the bottom of the hosepipe in order to prevent unvoluntary water leakage before the moment of the salt injection.

3: Salt solution to fill the hosepipe over the saturated length of the borehole.

4 and 5: Some type of tape line (here the metric tape line of an old electrical contact meter) and metal weight object used together as tool to lower the hosepipe into the well.

6: *TLC Model 7* Electrical Contact Meter from *Solinst* for measuring water level and electrical conductivity.

Figure 5: Setup of tools and materials used in a SBDT performed with the hosepipe method (type 1).

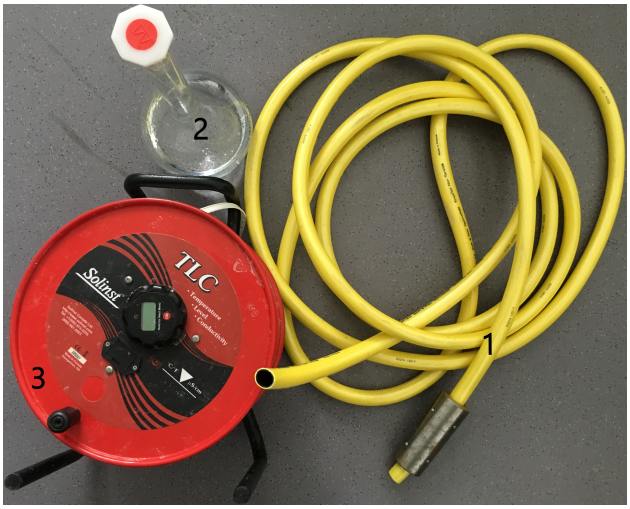

1: Hosepipe made of thick plastic material.

2: Salt solution to fill the hosepipe over the saturated length of the borehole.

3: *TLC Model 7* Electrical Contact Meter from *Solinst* for measuring water level and electrical conductivity.

Figure 6: Setup of tools and materials used in a SBDT performed with the hosepipe method (type 2).

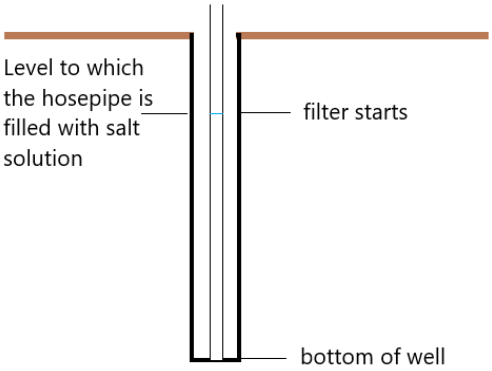

Figure 7: Illustration of hosepipe in a measuring well.

(a) Plastic hosepipe cut at a length so that it reaches from the bottom of the measured borehole depth to the top of the borehole opening.

(b) A beaker, which is attached to a heavy anchor, fixed at the bottom of the plastic hose. The beaker seals the bottom of the plastic hose during preparations and before injection of salt solution application.

(c) Salt solution being applied into the plastic hosepipe in the borehole by using a funnel.

Figure 8: Preparation of a SBDT performed with the hosepipe method (type 1).

Point Injection

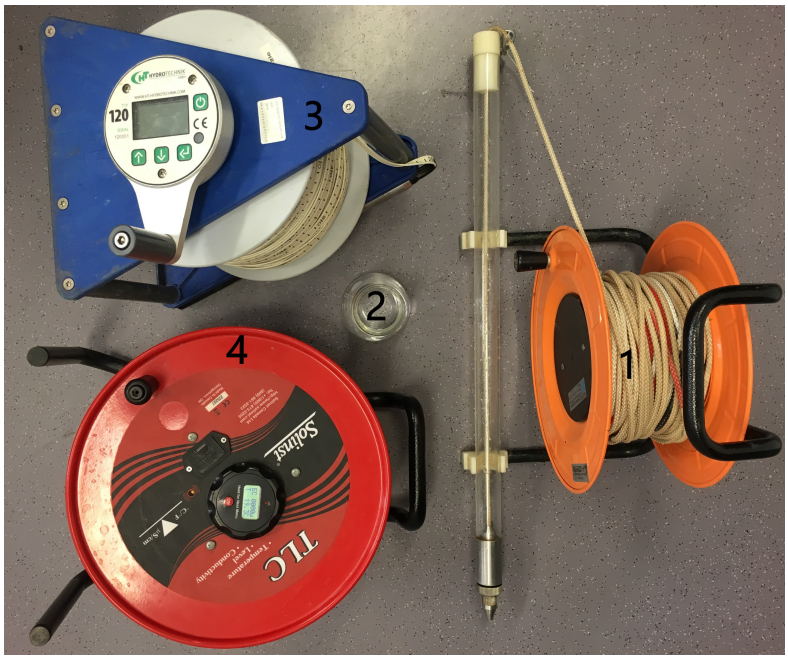

1: Point injection device. In this project a water sampler from *Glötzl* is used as injection device. The device includes a plastic pipe with a partly open upper part where salt solution can be inserted and a bottom part that is to be removed at the moment of salt injection.

2: 250 ml of salt (NaCl) solution that is to be filled into the point injection device.

3: Some type of tape line (here the metric tape line of an old electrical contact meter) used as tool to lower the point injection device into the well.

4: *TLC Model 7* Electrical Contact Meter from *Solinst* for measuring water level and electrical conductivity.

Figure 9: Setup of tools and materials used in a SBDT performed with the point injection method in this master project.

Similar to the stocking method, the point injection device is attached to a thin rope marked to indicate the point at which the injection should be carried out (see setup of tools in Figure 9). The rope is also attached to the lid of the injection device. If the rope is held straight (as shown in Figure 10b), the lid is in tight contact with the bottom opening of the device and prevents any water to leaking out. When holding the device by the rope and letting it hang freely, the weight of the device will keep the rope straight. The device can then be lowered to a specific depth in the borehole without undesirable leaking. To inject the salt, the device is pulled out with help of a second rope attached to it. The first rope is then loosened, which causes the bottom lid to open, releasing the salt solution. Figure 10a illustrates a point injection device being inserted into a measuring well.

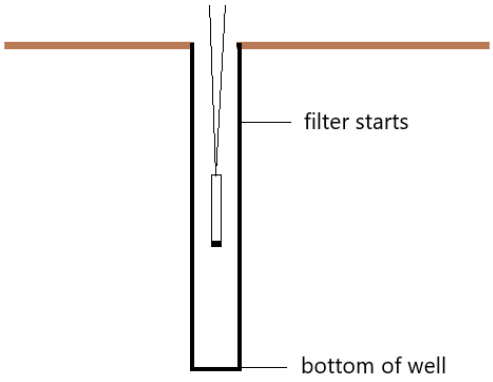

(a) Illustration of point injection device in a measuring well.

(b) Point injection device held in a way that prevents the liquid from pouring out. (Photo: Nikolai Fahrmeier)

Figure 10: Injection with the point injection method.

3.2.2 Measurement methods

Electric Contact Meter

For this project an electric contact meter of *TLC Model 7* from the company *Solinst, n.d.* was used. It has a total length of 150 m and is able to measure the groundwater level, temperature and electrical conductivity. The electrical conductivity is automatically calculated for a temperature of 25°C. It is presented along with the measured temperature on the integrated display (Solinst, n.d.). The TLC determines the electrical conductivity c (µS/cm) of the water by measuring the resistance between two electrodes installed in the probe.

$$c = \frac{l}{A \cdot R} \tag{1}$$

where A corresponds to the cross sectional area of the electrode in cm^2, l to the distance between the electrodes in cm and R to the electrical resistance of the water in Ohm (Hölting and Coldewey, 2013).

CTD-Diver

Additionally, a CTD Diver® from *van Essen Instruments* was used once for control of the resulting measured values from the electric contact meter. The CTD Diver records the electrical conductivity and the pressure every second. The data can be directly transferred into an Excel file. The exact water depths at which the different conductivity values are measured can be calculated from the measured pressure by using the relationship cmH_2O (centimetre of water) = 98,0665 Pascals (van Essen Instruments, 2016). Figure 11a

shows a picture of the CTD Diver, and Figure 11b illustrates its usage principle. The red arrow represents the up- and downward movement of the diver along the borehole and the green graph represents the pressure measured at different depths.

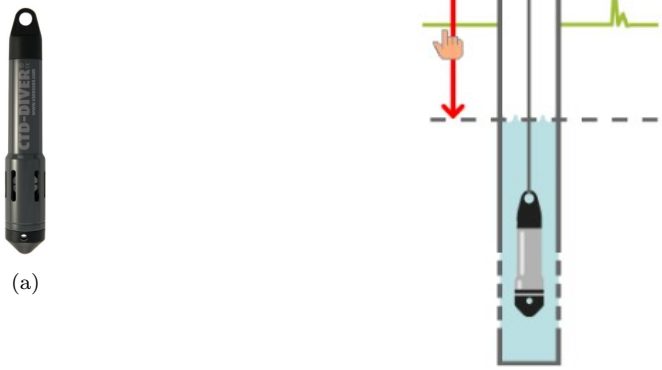

(a)

Figure 11: CTD-Diver® from van Essen Instruments. (Source: van Essen Instruments, 2016.)

3.2.3 SBDT in the lab

One purpose of the SBDTs carried out in the lab is to evaluate the stocking method and hosepipe method. Since the lab well is not exposed to any external factors such as in- or out flow, the salt distribution during injection will only depend on the injection procedure. If the electrical conductivity has similar values along the whole well (i.e. an equal distribution of salt) directly after salt injection, the injection method is reliable and suitable for SBDTs in the field. If the stocking method can give a relatively equal distribution of salt similar to the salt distribution occuring when using the hosepipe method, it can be regarded as a more easy and cost-effective alternative to the hosepipe method in the field.

The second purpose of the SBDTs executed in the lab is to investigate the impacts of density effects from the salt. This can be done by carrying out a point injection. After injection, the salt will strive for equilibrium and start to dissolve in the borehole. The electrical conductivity is measured at different time intervals shortly after the injection. If the early measurement show a faster increase of electrical conductivity below the point of the injection compared to above the point of injection, density effects (caused by the fact that the salt solution has higher density than water) can be shown to have an impact on the results in an SBDT.

As shown in Figure 12, a cylindric and transparent PET pipe with a diameter of 70 mm is fixed with two ropes along a wall to the ground. The open side of the pipe directed towards the ground is made watertight with a pipe conjoiner. Along the pipe there is a measuring rod to help identify the depths of the pipe during the SBDT executions. Between the SBDTs, the water containing salt solution is pumped out so that the pipe can be refilled with new tapwater. The pipe is filled with water to a height of almost 6 m.

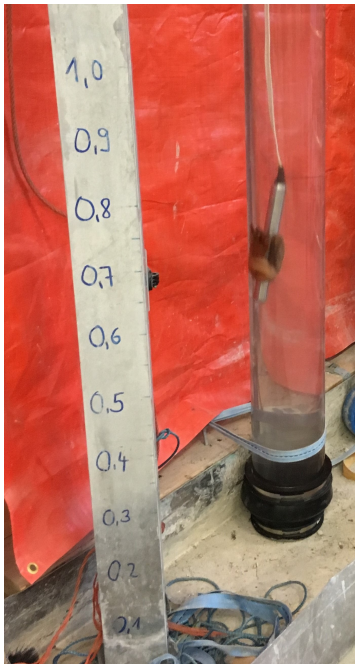

(a) Measuring rod (left) and cylindric PET pipe (right).

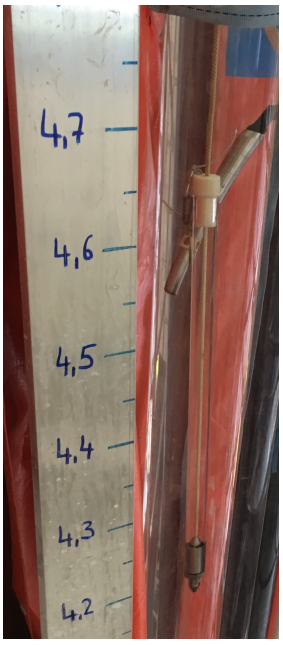

(b) Point injection device being lowered into the pipe during point injection.

(c) Water pump.

Figure 12: Explanatory illustration of execution of SBDT in lab environment.

3.2.4 Calibration of borehole water

The electrical conductivity measured with an Electrical Contact Meter or a CTD Diver can be converted into salt concentration by calibration. Also, the injected salt quantity for each SBDT in a borehole in the field was chosen based on results achieved from calibration of borehole water. The electrical conductivity and the salt concentration are proportional with a calibration factor. For the calibration, a specific amount of water was taken from the actual borehole in which a SBDT was executed. The tools used during the calibration is shown in Figure 13. Small amounts of a specific salt solution were added bit by bit with a pipette into the water sample. For each addition, the electrical conducivity was measured so that the linear relationship between the electrical conductivity and the salt concentration for the water could be determined. This relationship is the calibration factor. One example of how the calibration factor was calculated for one of the boreholes in this project is illustrated by the plotted graph and linear regression in Figure 14. See section 3.3 for more detail.

- Beaker
- Graduated cylinder
- Salt solution of 20 g/L
- Manual pipette

Figure 13: Tools and materials used for salt calibration.

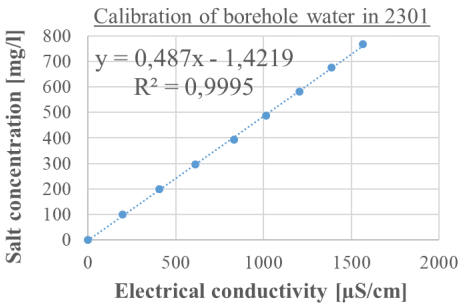

Figure 14: Example graph: a linear regression of the measured values of salt concentration at different electrical conductivity values for monitoring well 2301, showing a regression slope (calibration factor) of 0,487.

3.2.5 Selected boreholes

The location of the measurement wells evaluated in this project are presented in Appendix 6. Detailed information for each borehole can be found in Table 4.

Table 4: Measurement wells evaluated through SBDT in this project.

Aquifer type	**Well number**	**Borehole diameter [mm]**	**Depth [m]**	**Filter top [m]**	**Filter bottom [m]**
Gravel	2301	125	10	4,6	7,6
	5303	125	19,8	4,77	16,77
	5312	125	18	3,21	15,21
Karst	7721	125	75	16,7	74,6
	7733	125	40	19,8	39,8

All wells were chosen because of their location in the eastern part of the catchment area, since a tracer test is planned to be carried out there. SBDTs have already been done in the selected boreholes, however, more SBDTs are required in order to compare several tests for the same borehole, confirm previous findings, and get new information.

3.3 Evaluation of SBDT

3.3.1 Graphs displaying salt concentration development

The data provided from the results of the SBDTs can be presented with graphs showing the salt concentration throughout the whole borehole at different times. By studying the feature of such a graph, the type of vertical and/or horizontal flows occuring in the borehole can be determined. Figure 15 shows simulation results for boreholes with different horizontal flows whereas Figure 17 shows simulation results for boreholes with different vertical flows, obtained by Maurice et al. (2011). Graph line number 1 in each diagram corresponds to the first measured values (directly after salt injection) and the highest number corresponds to the last measured values. The explanation of the different types of vertical flows are presented in Figure 16 (Maurice et al., 2011).

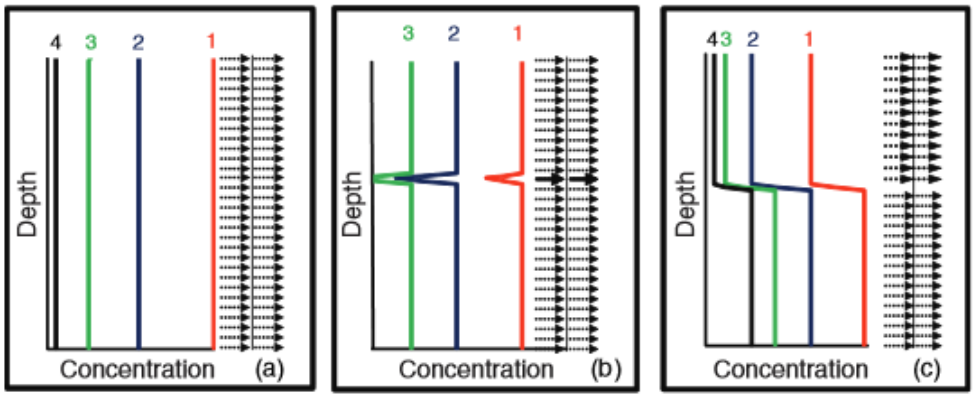

(a): Uniform diffuse horizontal flow

(b): Generally uniform diffuse horizontal flow, except for in the middle where a stronger horizontal flow creates a nick

(c): Boundary between one upper, uniformly high flow rate section and one lower, uniformly low flow rate section

Figure 15: Theoretical SBDT simulation results in boreholes with different types of horizontal flows. (Source: Maurice et al., 2011).

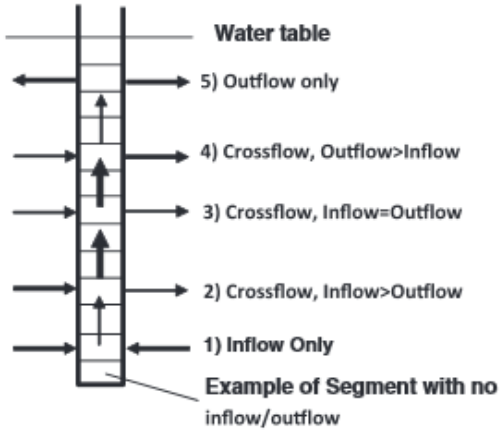

Figure 16: Scheme showing five possible flow types occuring in a borehole with vertical flow. (Source: Maurice et al., 2011).

Figure 17 shows more theoretical graphic examples of results from SBDTs and how they can be interpretated. Graph line number 1 corresponds to the first measured values, graph line number 2 to the second measured values etc.

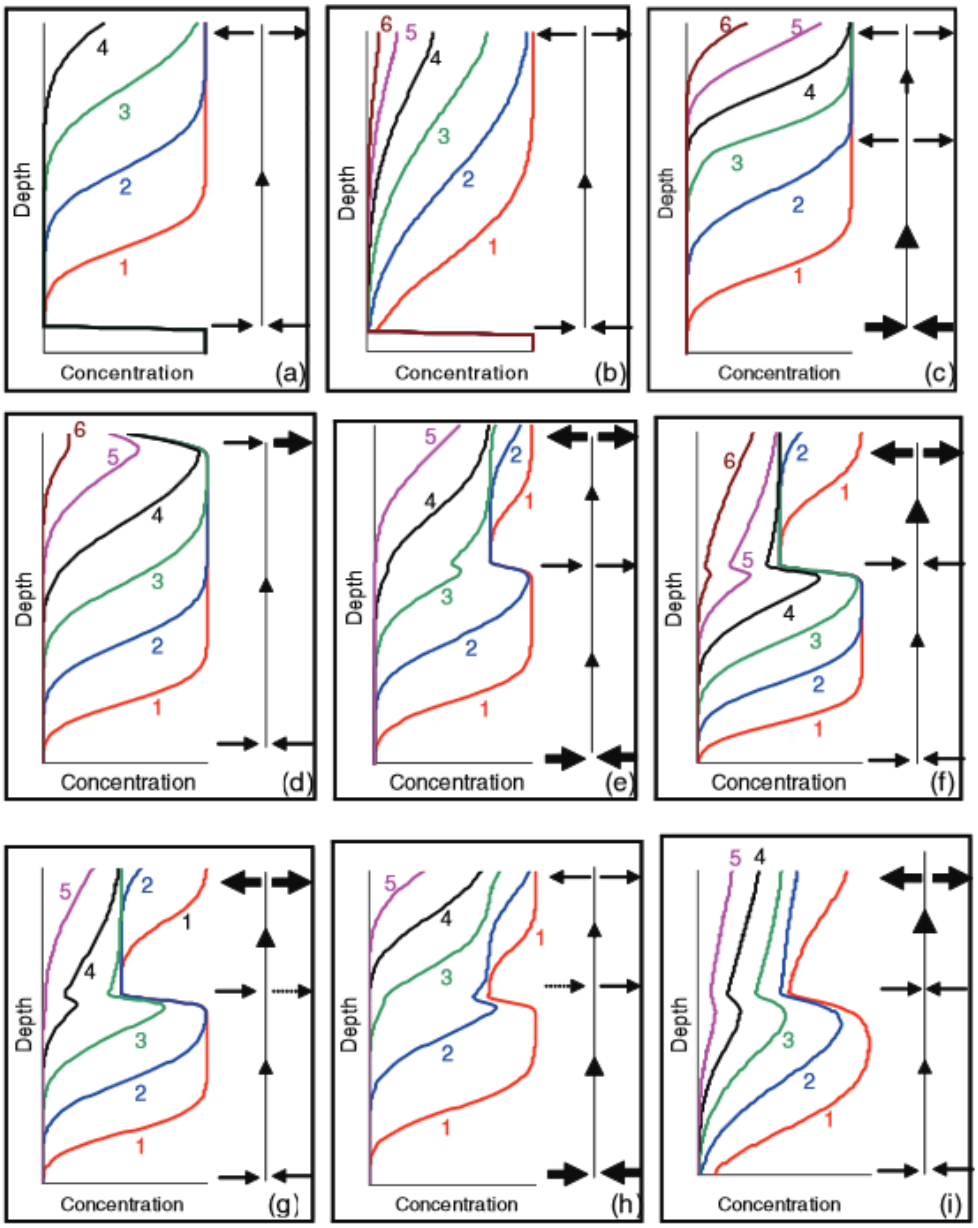

Figure 17: Theoretical SBDT results in boreholes with different types of vertical flows (see figure 16), showing the decrease of salt concentration at different times after salt injection. (Source: Maurice et al., 2011).

3.3.2 Calculations used in the interpretation of electrical conductivity development

When interpretating the results from the electrical conductivity development in a borehole in the field, both the average electrical conductivity from measured values, $EC_{measured,average}$, and the expected average electrical conductivity $EC_{expected,average}$ are calculated and presented Given the calibration factor k (-), inital salt mass m (g), borehole radius r (dm), borehole length l (dm), and electrical conductivity at ambient background conditions $EC_{background}$ (µS/cm), an expected average value of the electrical conductivity

$EC_{expected,average}$ (µS/cm) reached after injection could be calculated according to equation 7.

$$EC_{expected,average} = \frac{l \times \pi \times r^2}{k} + EC_{background} \tag{7}$$

3.3.3 Calculating Darcy flow velocity

By means of calibration, the electrical conductivity can be converted into salt concentration through the following formula:

$$Salt\,concentration = Electrical\,conductivity \times Calibration\,factor \tag{8}$$

The remaining salt quantity in the borehole can be calculated using the following formula:

$$Salt\,quantity\,[g] = (Depth_2\,[m] - Depth_1\,[m]) \times \pi \times r^2 \times \frac{Concentration_1\,[mg/l] + Concentration_2\,[mg/l]}{2} \tag{9}$$

This computation is done for each of the measured depth intervals. All values are then added together into the total salt quantity in the borehole. Doing this procedure for measurements taken at different times, the salt quantity development in the borehole can be determined.

The calculated salt concentrations can help determine the filtration velocity at each depth interval. By calculating the natural logarithm of the salt concentration over time at a specific depth, the data can be linearly adapted (Pitrak et al., 2007). Ogilvi (1958) showed the following linear relation between the natural logarithm of the salt concentration $ln(C_i)$ and the time ti:

$$\ln C_i = -\frac{2v_a}{\pi \times r} t_i + \ln C_1 \tag{10}$$

where C_i is the salt concentration at time t_i after the salt application, C_1 is the salt concentration directly after the salt application, r is the borehole radius and v_a is the apparent filtration velocity. Using the slope of regression line k obtained from the natural logarithmation, the apparent velocity can be expressed as:

$$v_a = \frac{k \times \pi \times r}{2} \tag{11}$$

In order to calculate the actual filtration velocity, the apparent filtration velocity should be divided by a drainage coefficient. According to Pitrak et al. (2007) a drainage coefficient of 2 should be used (Pitrak et al., 2007).

$$v_f = \frac{v_a}{2} \tag{12}$$

Formula (10) is based on the assumption that there are no vertical groundwater movements in the well. In practice, however, this is only true for completely homogeneous aquifers. In this master thesis, the SBDTs are carried out in two karst aquifer wells and three gravel aquifer wells. As described in the introduction,

karst aquifers are highly heterogeneous. The actual filtration velocity calculated for the karst aquifer wells should therefore be seen as indications and not as absolute velocity values. Just as with the graphs displaying the electrical conductivity development, possible cavity areas in the karst aquifer well can be localized through analysis of the Darcy flow velocity.

Alternative adjustments for calculation of filtration velocity

ln C_i for each depth along the filter section is plotted in a graph, with time t (h) along the x axis. Figure 18 shows an example of such a graph (based on data from a SBDT in measuring well 2301). As noted, a linear regression is fitted to the curve. The linear constant k of the regression is used for calculations of the filtration velocity v_f (m/h). However, the data row may not fit to one linear regression solely. In these cases, several regressions have to be made. The different regressions result in different k values, and therefore different alternative filtration velocities. The results from the different combination of regressions, or adjustments, are compared with each other. When several adjustments have been made, an average of the filtration velocity of the adjustment is calculated.

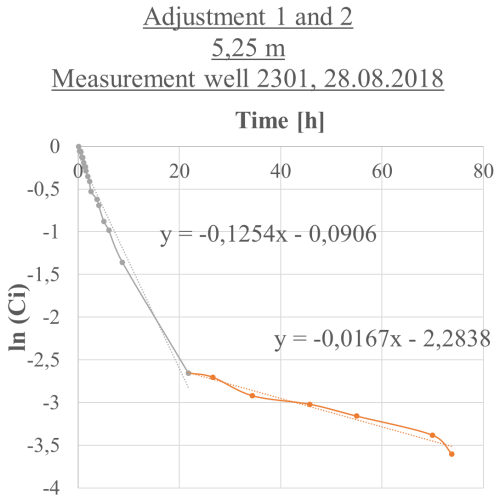

Figure 18: Example of adjustments in the calculation of the filtration velocity.

Chapter 4

Results and Discussion

The borehole dilution tests were executed between August 2018 and January 2019. In addition, data from a field test executed in December 2017 was used. The first step of each test was to measure the electrical conductivity at ambient background conditions. Subsequently, the salt quantity for the salt injection was prepared either by inserting a specific mass of salt into a nylon stocking (Stocking method), filling a hosepipe with salt solution of a specific salt concentration (Hosepipe method) or filling the point injection device with 250 ml of salt solution with a specific salt concentration (Point injection).

After the salt injection, the values of the electrical conductivity were measured with the electrical conductivity meter at different depth and time intervals. The values were noted by hand and later transferred to Microsoft Excel. The data were analyzed by plotting graphs that show the **development of the electrical conductivity** in both space and time, i.e. displaying the eletrical conductivity at different depths as well as different times. This gives an idea of the depths at which there is a higher or lower horizontal groundwater flow. A section with a rapid decrease in electrical conductivity indicates that the section is subject to high horizontal flow, whereas a section with a particularly slow decrease indicates that the section has a weak connection to the surrounding aquifer. The graph can also reveal vertical flows in a borehole, for example when the peak of electrical conductivity appears and moves up- or downwards along the borehole as time goes by.

For each of the SBDTs in the field, the electrical conductivity values were translated into salt quantities at different depth sections along the borehole by using a calibration factor described in section 3.2.4. From this, the **total salt quantity development** in a borehole can be calculated. For the SBDTs in the field where the stocking method was used, calculations of the **filtration velocity (Darcy flow velocity)** throughout the borehole were made by using the calculation method described in section 3.3.3.

Since the PET pipe, used as borehole for tests in the lab, has no in- or outflow of water as well as no filter, there is no filtration velocity to be calculated. The total salt quantity in the pipe will stay the same, since no salt can exit from it. Due to this, the total salt quantity development will not be calculated or further discussed for the tests executed in the lab.

4.1 SBDT in the lab

In the lab, a total number of nine SBDTs were executed from end October to mid January. The tests are presented in Table 5. For the tests presented with a parantesis the injection was accidentally not carried out in a correct way, making it hard to analyse their results. These tests are therefore not further analysed or described.

Table 5: Summary of input data for SBDTs executed in the lab. Tests presented with parentesis were not further assessed, due to failure in test execution.

Injection method	**Date and Time of Salt Input**	**Duration of salt input [min]**	**Salt input quantity [g]**	**Number of measurements**
Stocking method	30.10.2018 15:55-15:57	2	65	6
Stocking method	15.11.2018 15:24-15:34	10	65	12
Hosepipe method (type 1)	13.11.2018 13:07-13:08	1	65	13
Hosepipe method (type 2)	14.01.2019 13:37-13:42	5	151	9
Point Injection	31.10.2018 14:58-14:59	1	25	11
Point Injection	05.11.2018 13:00-13:01	1	50	15
(Point Injection)	(15.11.2018 13:03-13:04)	(1)	(12,5)	(16)
(Point Injection)	(17.12.2018 13:50-13:51)	(1)	(12,5)	(15)
(Point Injection)	(20.12.2018 09:40-09:41)	(1)	(12,5)	(13)

Since the purpose of the SBDTs executed in the lab was to evaluate the injection method and possible density effects from the salt, the results from the early measurements are the most interesting to look at. For the figures that display the electrical conductivity development further on in this chapter, the data rows have been assigned with different shades of blue; data collected during early measurement are displayed with darker shades, whereas late measurements have lighter shades. The electrical conductivity at ambient background conditions are black, and the electrical conductivity at first measurement after injection is red. In order to make it easier to compare two SBDTs using the same injection method, the electrical conductivity values corresponding to the same time after injection have another color such as yellow or purple.

Since the water added into the water pipe before each test was tap water from the same tap, a calibration of the borehole water at initial conditions (before salt injection) only had to be made once. The result is shown in Figure 19. A linear adaptation of the results shows a calibration factor of 0,5177. As described in section 3.3.3, the factor is used for calculation of salt concentration and Darcy flow velocity from the measured values of electrical conductivity.

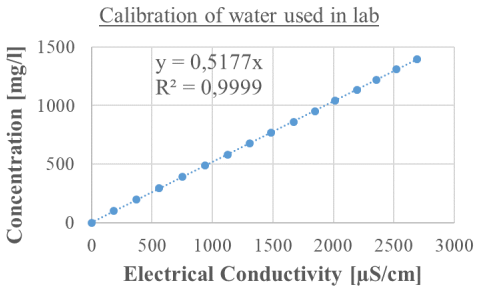

Figure 19: Calibration of water used in lab.

4.1.1 Stocking method

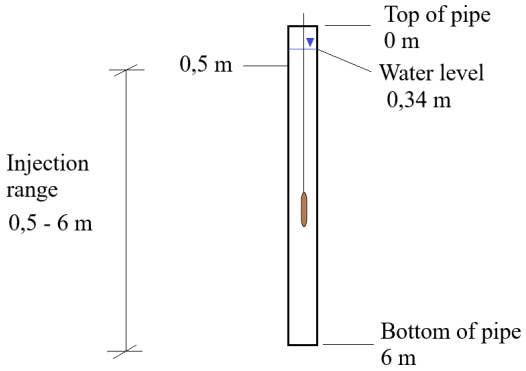

Figure 20: Illustration of injection with the stocking method in the lab.

Electrical conductivity development

The SBDTs with the stocking method were executed at two different occasions. The same salt quantity was used for both tests (65 g). The salt dissolved quickly in the test on 30.10.2018 (2 min) and relatively slowly in the test on 15.11.2018 (10 min). The reason behind the difference in dilution duration is not clear.

The results of the electrical conductivity measurements for the tests are shown in Figure 21 and 22. The water initially has an electrical conductivity of almost 600 µS/cm. The values directly after the injection lie between approximately 1700-2600 µS/cm (30.10.2018) and approximately 1500-2500 µS/cm (15.11.2018). Gernerally, it is difficult to get an equal distribution of salt with the stocking method. However, the electrical conductivity changes relatively smoothly along the borehole. I.e., between single depths, the electrical conductivity only varies a bit. Even though a uniform distribution can not be obtained, valuable conlusions regarding the electrical conductivity development can be achieved, due to its smooth pattern.

For the test on 30.10.2018, the salt distribution from the injection can be divided into two sections, as seen in Figure 21. The first section ranges between 0,5 and 3,25 m of depth and has a relatively equal salt distribution with electrical conductivity values of approximately 1700-1800 µS/cm. The second section ranges from 3,25 to 5,5 m of depth and has electrical conductivity values that are significantly higher (approximately 1800-2600 µS/cm). Over the measurement duration (17,37 h), the electrical conductivity did

not change much from the initial values (M1). The distribution of salt at measurement 6 (M6) can be divided in the same sections as measurement 1 (M1).

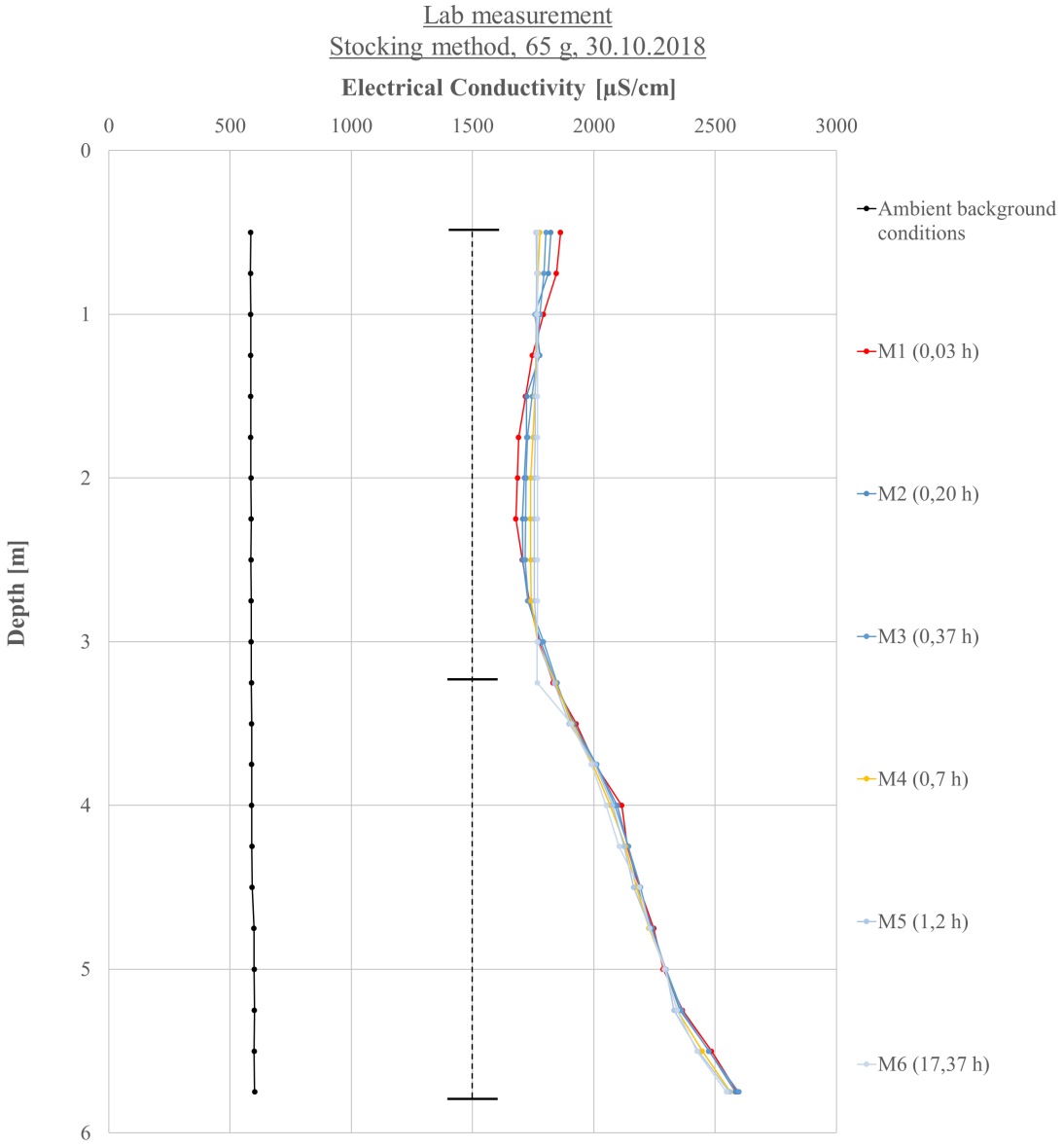

Figure 21: Electrical conductivity development, stocking method 1 of 2 in the lab.

For the test on 15.11.2018, the salt distribution can be divided into three sections, see Figure 22. Two sections have electrical conductivity values of approximately 1700-2500 µS/cm, ranging between 0,5 - 2,25 and 4,25 - 5,5 m, respectively, of depth. The third section ranges between 2,25 and 4,25 m of depth and shows electrical conductivity values of approximately 1500-1700 µS/cm.

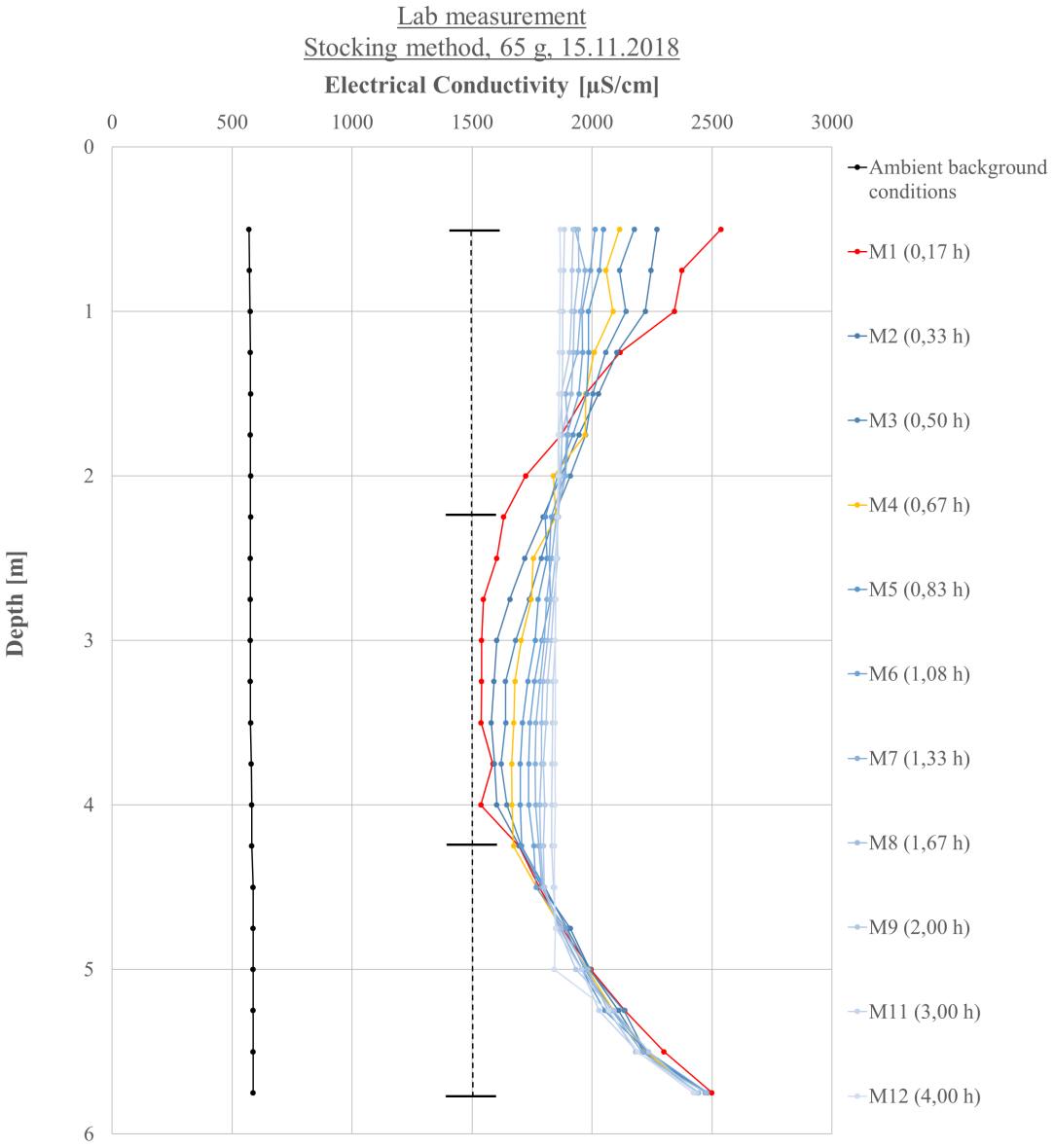

Figure 22: Electrical conductivity development, stocking method 2 of 2 in the lab.

Compared to the test on 30.10.2018, the electrical conductivity values in the second test vary more between the first and last measurement at the depth range 0,5 - 4,25 m. The reason is probably that the injection in the test on 15.11.2018 resulted in a less uniform salt distribution than the test on 30.10.2018.

For the first test (30.10.2018), additional measurements of the electrical conductivity were executed at 0,7 h and 1,2 h after salt injection, using a CTD-Diver. Figure 23 displays the measured electrical conductivity values from the CTD-Diver as well as from the Electrical Conductivity Meter. The difference in measured values between the CTD-Diver and Electrical Conductivity values is probably due to a different calibration in the devices.

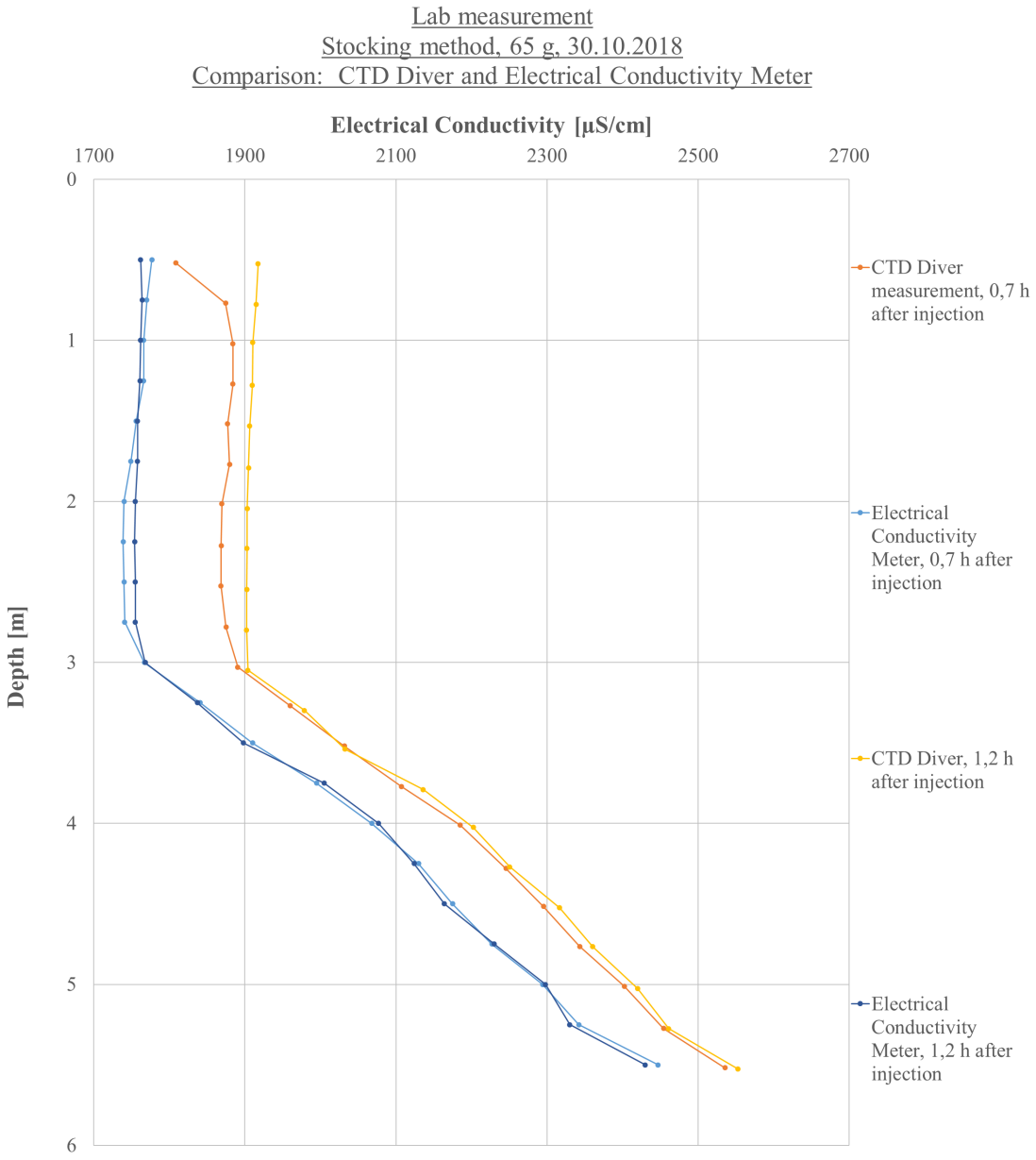

Figure 23: Comparison of measurement values from Electrical Conductivity Meter and the CTD-Diver.

The CTD-Diver measures the electrical conductivity at an exact time. When using the Electrical Conductivity meter, the electrical conductivity is paired with an approximate time, i.e. the start time of each measurement. Since the CTD-Diver calculates the depths based on the water pressure, the measured depth should be exact. With the Electrical Conductivity Meter, the water depth is measured manually with a simple measure tape, resulting in approximate values. Calculations from the data shown in Figure 23 show that the differences in electrical conductivity between 0,7 h and 1,2 h for the CTD-Diver and the Electrical Conductivity Meter, respectively, are different. The average difference of electrical conductivity between 0,7 h and 1,2 h was approximately 25,2 µS/cm for the CTD-Diver, and approximately 0,14 µS/cm for the Electrical Conductivity Meter. Taking this difference into account and the fact that CTD-diver is supposed to measure the electrical conductivity accurately, it means that the measured values from the Electrical

Conductivity Meter do not exactly correspond to the real values.

When it comes to handling, the CTD-Diver has some advantages. It is a small device (22mm in diameter and 150 mm long), and can measure the electrical conductivity values much faster than the Electrical Conductivity Meter. Based on the measurements in the lab hall, the CTD-Diver was able to measure the electrical conductivity throughout the 6 m long borehole in less than 2 minutes. The corresponding time for measuring the electrical conductivity with the Electrical Conductivity Meter was 4 minutes. In addition, CTD-Diver is able to measure the electrical conductivity at much smaller intervals than the Electrical Conductivity Meter. Using the CTD-Diver instead of the Electrical Conductivity also reduces documentation work, since it transforms the measured values directly into an Excel-file. For the Electrical Conductivity Meter, the values have to be read from the device display and written down, and then manually transferred into Excel. Alternatively, a computer has to be brought into the field so that the data can be written directly into an Excel file, however, it is impractical to handle the computer at the same time as doing measurements with the Electrical Conductivity Meter. In the case of the CTD-diver, some additional work has to be done in Excel in order to calculate the water pressure values into corresponding water levels, however, this work is small compared to the documentation work that the Electrical Conductivity Meter requires.

All data obtained with the CTD-Diver can not be displayed until after the field measurement, since it takes some time for the data to process into an Excel file. When using the Electrical Conductivity Meter, the measured values can be studied after each measurement. Due to this, an estimation of suitable times between measurements throughout the test duration can be made. For example, it can directly be seen if the electrical conductivity changes quickly, and if so, be decided that the duration between measurements has to be shorter. Also, the point at which the electrical conductivity has gone back to background conditions can easier be detected. When that happens, there is no need for more measurements, and the test can be finished. With a CTD-Diver, nothing of this can be detected until after the end of all the measurements. A CTD-Diver is suitable to use for boreholes where SBDTs already have been executed and where there is already a knowledge of the electrical conductivity development as well as the approximate duration for the injected salt to totally disappear from the borehole. Then, the time frequency chosen for the measurements with the CTD-diver can be based on previous experience from the borehole. Important is, however, to use the CTD-Diver in a SBDT where the same salt quantity as in at least one previous SBDTs has been used, since the duration of salt disappearance varies with the quantity of injected salt.

4.1.2 Hosepipe Method

Electrical conductivity development

The hosepipe method was only carried out in the lab and not in the field due to time limitation. It was executed at two different occasions: one with hosepipe type 1 on 13.11.2018 and one with hosepipe type 2 on 14.01.2019. The injected salt solution volume was calculated by multiplying the water filled depth (corresponding to the total depth range for the injection) with the bottom area of the hosepipe. The inner diameter for hosepipe type 1 is 2,5 cm and 0,9525 cm for hosepipe type 2. Given that the water depth was approximately 6 m in the lab, hosepipe type 1 had to be filled with a total volume of salt solution of approximately 10,72 liters whereas hosepipe type 2 had to be filled with approximately 1,71 liters. As noted, the volume for hosepipe 1 is ten times bigger than for hosepipe 2. For hosepipe type 1 a total salt input

of 65 g was chosen, corresponding to an approximate salt concentration of 6,06 g/l. For hosepipe type 2 a salt quantity of 180 g was used, corresponding to an approximate salt concentration of 100 g/l. Figure 24 illustrates the injection setup for the two executed hosepipe tests.

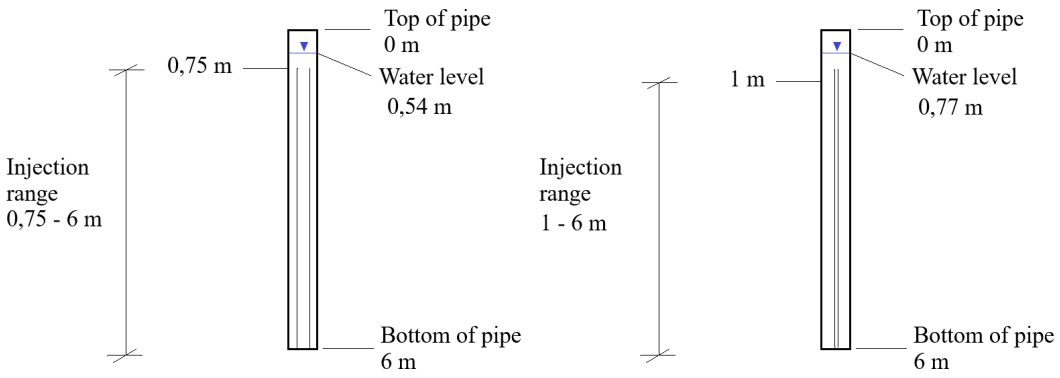

(a) Type 1. (b) Type 2.

Figure 24: Illustration of injection with the hosepipe method in lab.

Hosepipe, type 1

When studying the electrical conductivity measured directly after salt injection with hosepipe type 1, three main sections can be defined. The first section ranges between 0,5 and 4,5 m and has electrical conductivites of approximately 1400-1900 µS/cm. Section 2 ranges between 4,5 and 5,35 m and has electrical conductivity values of approximately 1900-3100 µS/cm. Section 3 is located from 5,35 to 6 m of depth and has electrical conductivity values of approximately 1600-1900 µS/cm. By studying the result, it seems as if too small quantites of salt solution was injected in section 3, and that the salt instead got released in section 2.

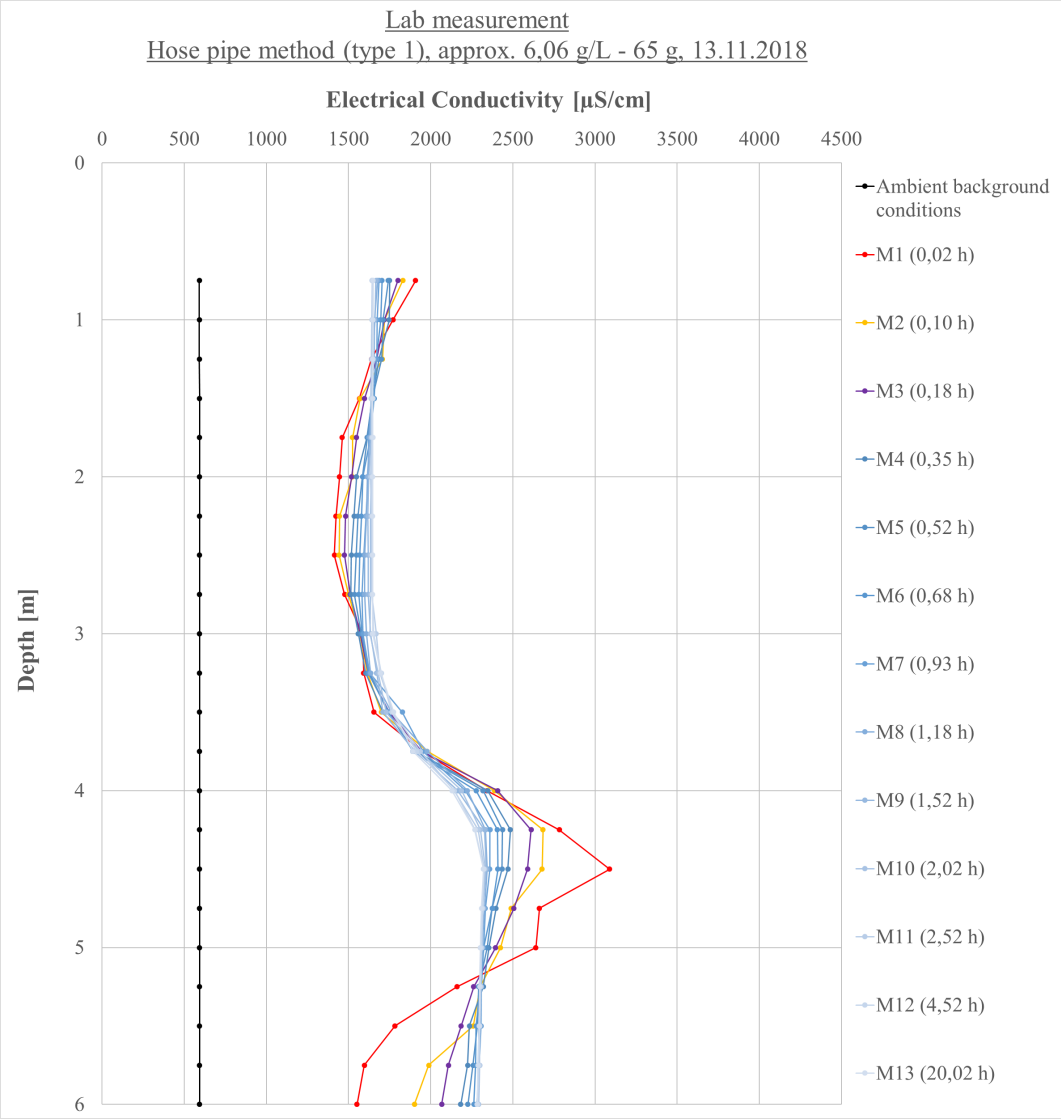

Figure 25: Electrical conductivity development, hosepipe method (type 1) in the lab.

Hosepipe, type 2

In the test with hosepipe type 2, the electrical conductivity differs from around 3200 to 4200 µS/cm as shown in Figure 26. Compared to the results from test with hosepipe type 1 shown in Figure 25, no clear sections can be pointed out for the first measurement after injection.

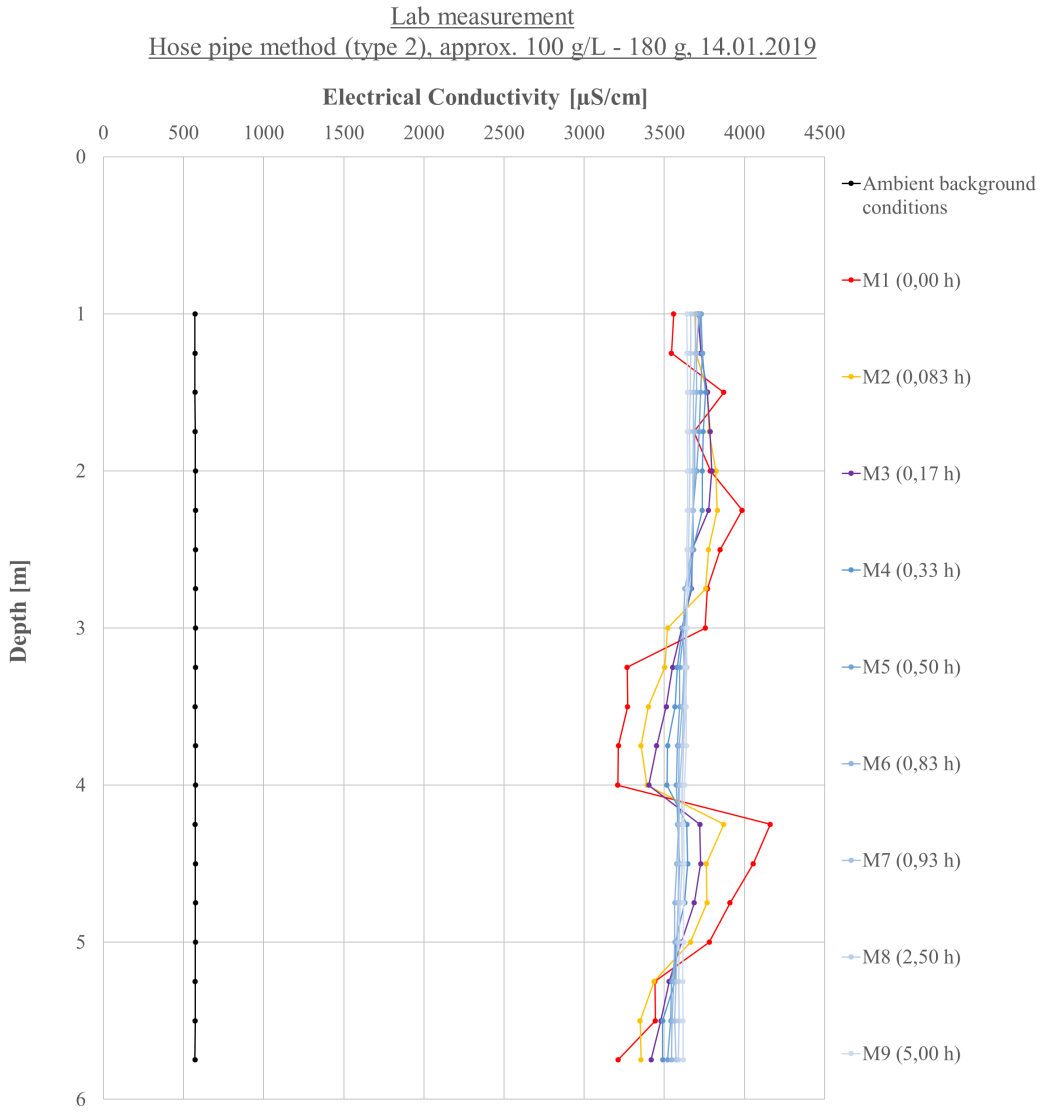

Figure 26: Electrical conductivity development, hosepipe method (type 2) in the lab

The total variation of electrical conductivity directly after injection is 1700 µS/cm for the hosepipe type 1 test and 1000 µS/cm for the hosepipe type 2 test. Looking at the whole pipe length, it means that the injection with hosepipe 2 achieved a more equal salt distribution than with hosepipe 1. Looking at the whole borehole, the test with hosepipe type 2 has a more equally distributed salt injection than the test with hosepipe type 1. However, the electrical conductivity in type 1 varies smoothly, whereas the electrical conductivity development with type 2 follows a "zigzag" pattern. The electrical conductivity development from a smoothly distributed salt injection along with the borehole as in hosepipe type 1 may be easier to analyze. When focusing on that fact, hosepipe type 1 might be a better alternative. A final conclusion of which of the hosepipes that is most suitable as injection method can, however, not be drawn from only two tests. Several tests should be done of each of the hosepipe methods, combining different salt solutions. The results from the two tests in this master thesis should be used as indications for the planning of future tests in the lab.

4.1.3 Point Injection

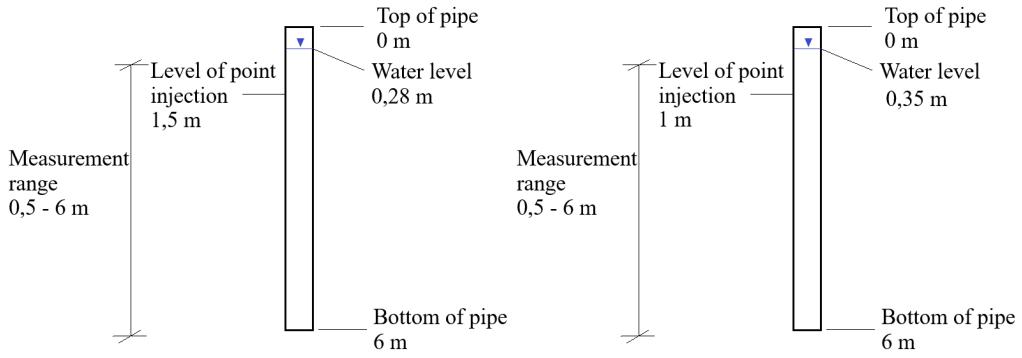

(a) 31.10.2018. (b) 05.11.2018

Figure 27: Illustration of injection with the point injection method in the lab.

In the lab, five SBDTs with point injection were executed. In three of those, the salt was injected too high up in the water well due to imperfections in the point injection device, making it hard to get the injection at one specific and desired point. Because of the injection failure, the salt dilution development above and below the injection point could not be compared. Those three SBDTs are therefore not included in the detailed analysis. Due to the imperfect device, another, improved injection device will be developed and used in future experiments.

The point injection of the two relevant SBDTs were carried out on 31.10.2018 and 05.11.2018. The first test was carried out with a salt solution of 100 g/l and the second test with a salt solution of 200 g/l. Given that the volume of salt solution in the point injection device is 250 ml, this means that the first test had a total amount of 25 g salt and the second test 50 g. Figure 27a and 27b shows an illustration of the injection for each test.

Electrical conductivity development

As expected, the second test (05.11.2018) resulted in higher electrical conductivity values than the first test (31.10.2018). The peak of electrical conductivity directly after injection reached around 2900 µS/cm in the first test and 3700 µS/cm in the second test. The injection was done approximately 1,5 m below the water surface for the first test and approximately 1 m below the water surface for the second test. As long as the injection was not made too high up or too deep down, the difference in injection level does not play an important role. For the early electrical conductivity measurements, the peak of electrical conductivity does not significantly move downwards in the borehole. This can be seen through the thick black points in Figure 28 and 29. This indicates that density effects from the salt does not have any important impact on the results.

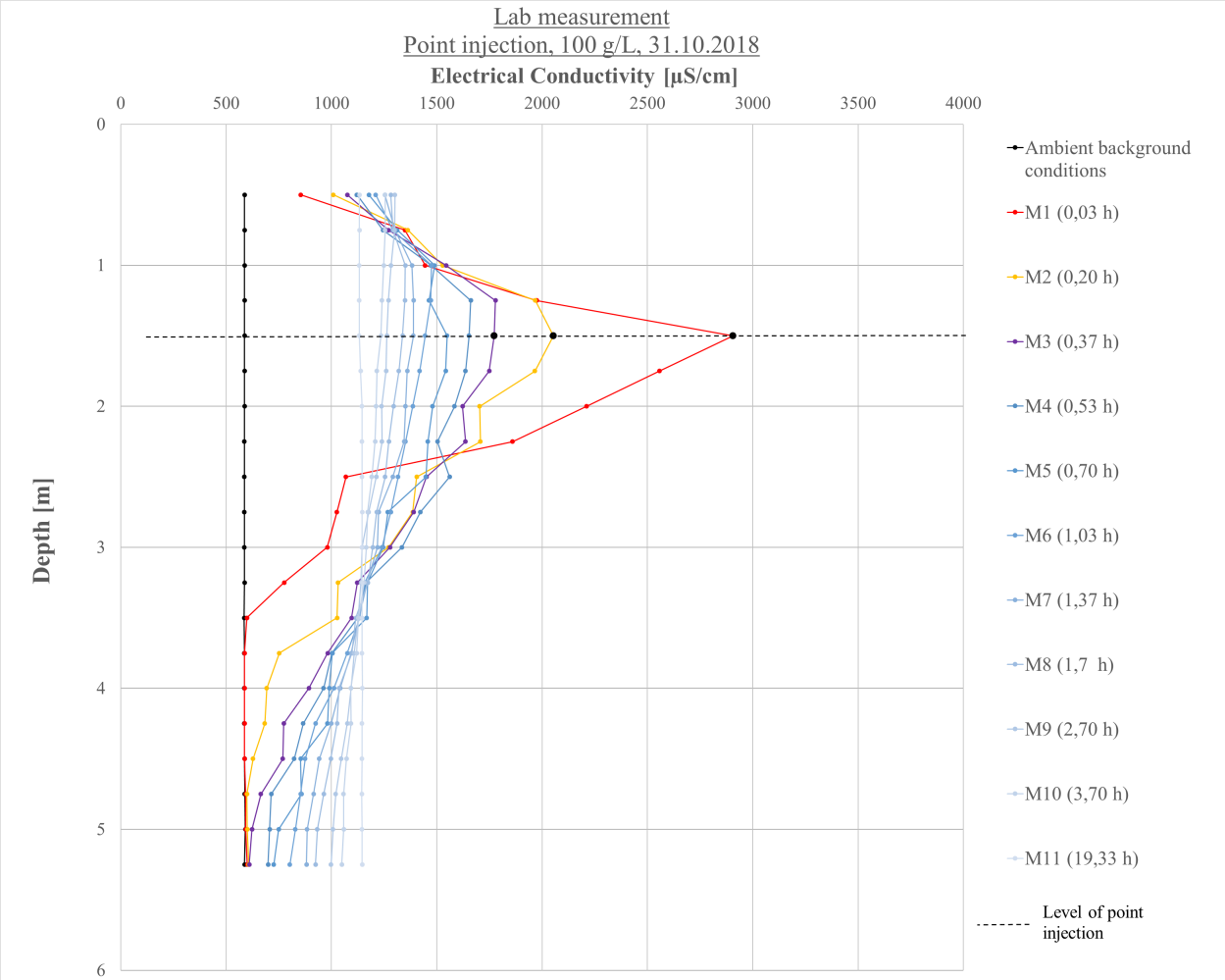

Figure 28: Electrical conductivity development, point injection 1 of 2 in the lab.

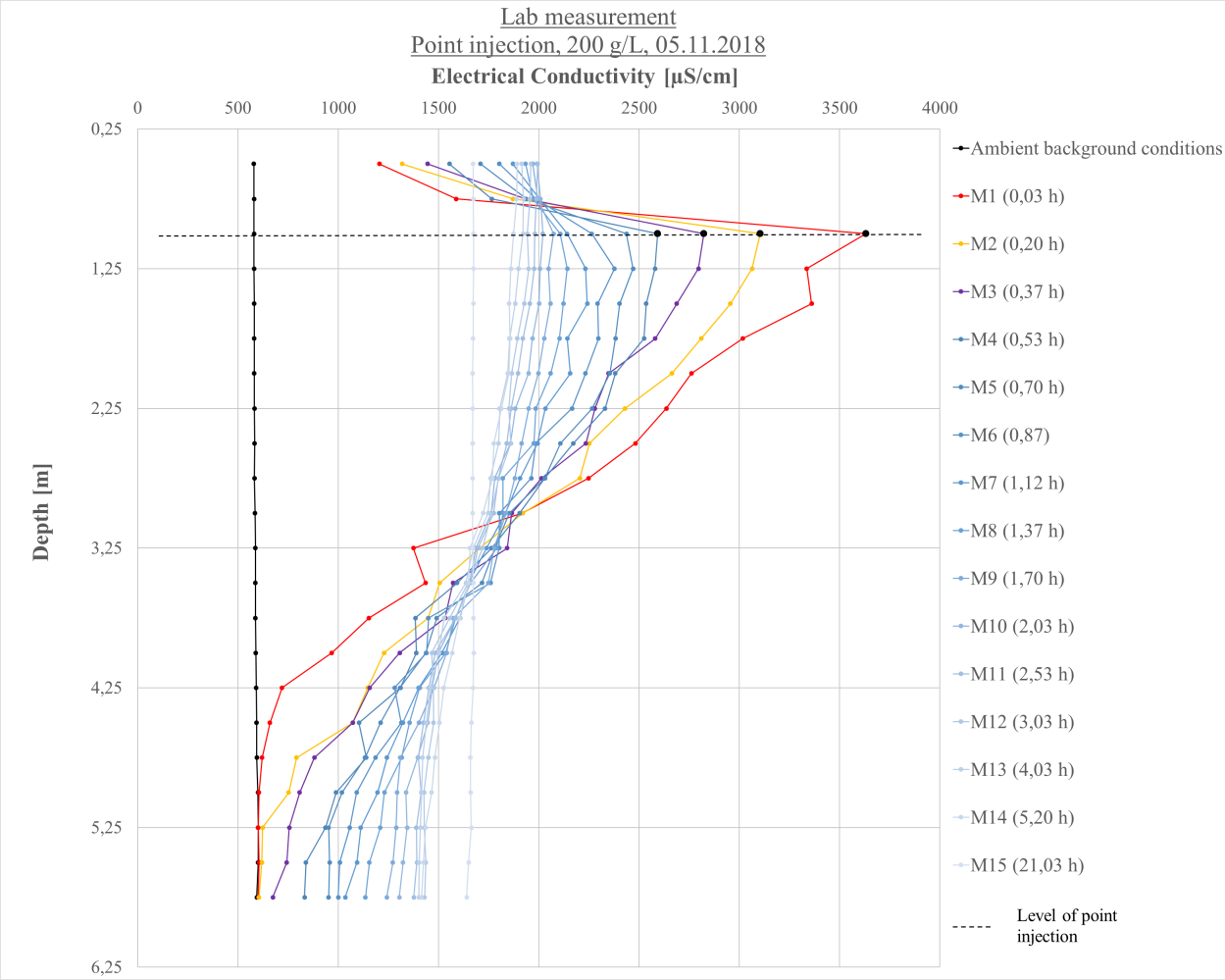

Figure 29: Electrical conductivity development, point injection 2 of 2 in the lab.

4.2 SBDT in the field

In the field, a total number of eight SBDTs were made from end of August to the middle of December, all presented in Table 6. The location of each borehole is shown in Appendix 6.

Table 6: Summary of input data and filtration velocities for SBDTs executed in the field.

Well number	**Method**	**Date and Time of Salt Input**	**Duration of salt input (min)**	**Salt input quantity (g)**	**Number of measure-ments**
2301	Stocking	28.08.2018 10:50-11:08	18	50	25
2301	Stocking	02.12.2017 10:28-10:30	2	25	8
5303	Point Injection	28.11.2018 10:35-10:36	1	50	15
5303	Point Injection	12.12.2018 10:51-10:52	1	12,5	23
5312	Point Injection	28.11.2018 13:33-10:34	1	50	13
7721	Stocking	17.10.2018 11:26-11:32	6	800	20
7721	Stocking	18.10.2018 09:00-09:26	26	800	16
7733	Point Injection	07.11.2018 11:04-11:05	1	50	22

The tests were carried out in late summer, autumn, and winter. Due to seasonal variations, the conditions such as groundwater flow and groundwater level thereby differed between the tests. For example, the groundwater level for the area, in which the measurement wells listed above are located, varied from 462 m.a.s.l. in August 2018 to 461,3 m.a.s.l. in December 2018. In December 2017, the level reached 461,5 m.a.s.l. The summer of 2018 was exceptionally dry and hot in southern Germany, resulting in a bit lower groundwater levels in the Donauried-Hürbe than the average level measured between 1980-2013 (Landwasserversorgung, 2018). For measurement well 2301, one test was carried out in late August and one test in the beginning of December. The results from 2301 can therefore be used for comparing SBDTs between late summer and winter. The point injection tests in measurement well 5303 were carried out on 28.11.2018 and 12.12.2018, making the seasonal conditions similar. This makes it possible to compare the tests based on factors connected to the injection characteristics, such as salt input quantity. The first SBDT (stocking method) in 7721 was executed one day before the second one, basically resulting in the same background conditions. As the second test was initiated, there was, however, still salt from the first test in the well, resulting in slighty higher electrical conductivity values during the measurements. In order to prevent uncertainties followed by remaining salt in measurement well 7733, the tests should be executed with one or two days inbetween.

By studying results from previously executed SBDTs, further comparison between tests for the same borehole is possible. This is particularly valuable for measurement well 5312 and 7733, since only one point injection for each of them was carried out in this master thesis. Important to remember is that this master thesis is part of a bigger research project and that the results will be useful for the analyses of future tests.

For each borehole a detailed illustration of the actual groundwater level, borehole features, and injection depths follows along with the results. For the tests with the stocking method, the filtration velocity is only presented for depths within the filter section. For tests with point injection, the filtration velocity is only presented for a few meters above and below the injection point.

4.2.1 Measurement point 2301

For measurement point 2301, located in the gravel aquifer, two SBDTs with the stocking method were analyzed. One was carried out within the frame of this master thesis on 28.08.2018, and one was carried out on 02.12.2017 by the research group at the Institute of Applied Geosciences at Karlsruhe Institute of Technology. Two different salt input quantities were used: 25 g (02.12.2017) and 50 g (28.08.2018). The salt dissolved relatively quickly on 02.12.2017 and relatively slowly on 28.08.2018, resulting in a big difference in the salt input duration: 2 minutes (02.12.2017) and 18 minutes (28.08.2018). A description of the injection in both tests is illustrated in Figure 30.

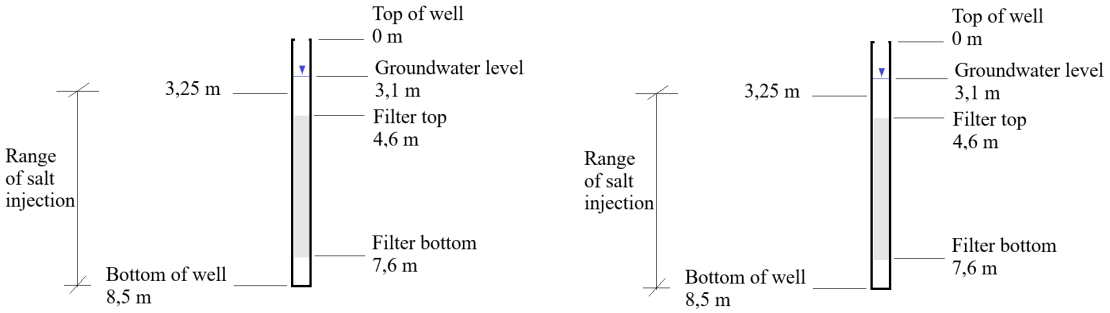

(a) 02.12.2017 (b) 28.08.2018

Figure 30: Illustration of injection in borehole 2301.

Electrical conductivity development

The development of the electrical conductivity for the two SBDTs is presented in Figure 31 and 32. Both figures show a relatively equally distributed salt injection between 4,6 and 8 m, with an electrical conductivity variation of approximately 300 µS/cm. From 3 - 4,6 m in the first test (02.12.2017), the electrical conductivity is lower directly after injection, indicating that the salt did not dissolve as fast as in the lower part of the well, which has probably is due to the fact that it belongs to the non-filtered section of the borehole. Within the filtered section, the electrical conductivity seems to decrease faster further down, indicating that the groundwater flow is higher deeper down in the aquifer. The expected average value was approximately 1400 µS/cm for the first test and 2200 µS/cm for the second test. The average electrical conductivity for the measurement directly after salt injection is 1300 µS/cm for the first test and 2200 µS/cm for the second test.

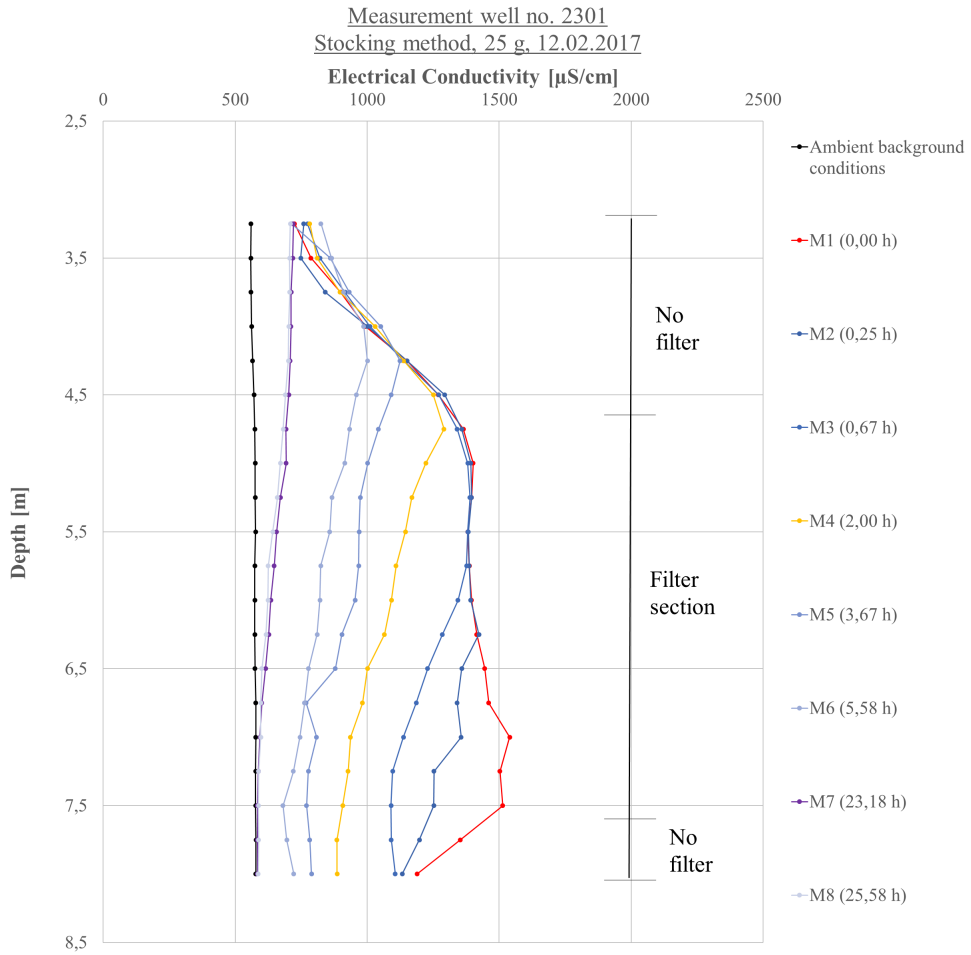

Figure 31: Electrical conductivity development, stocking method 1 of 2 for measurement well 2301.

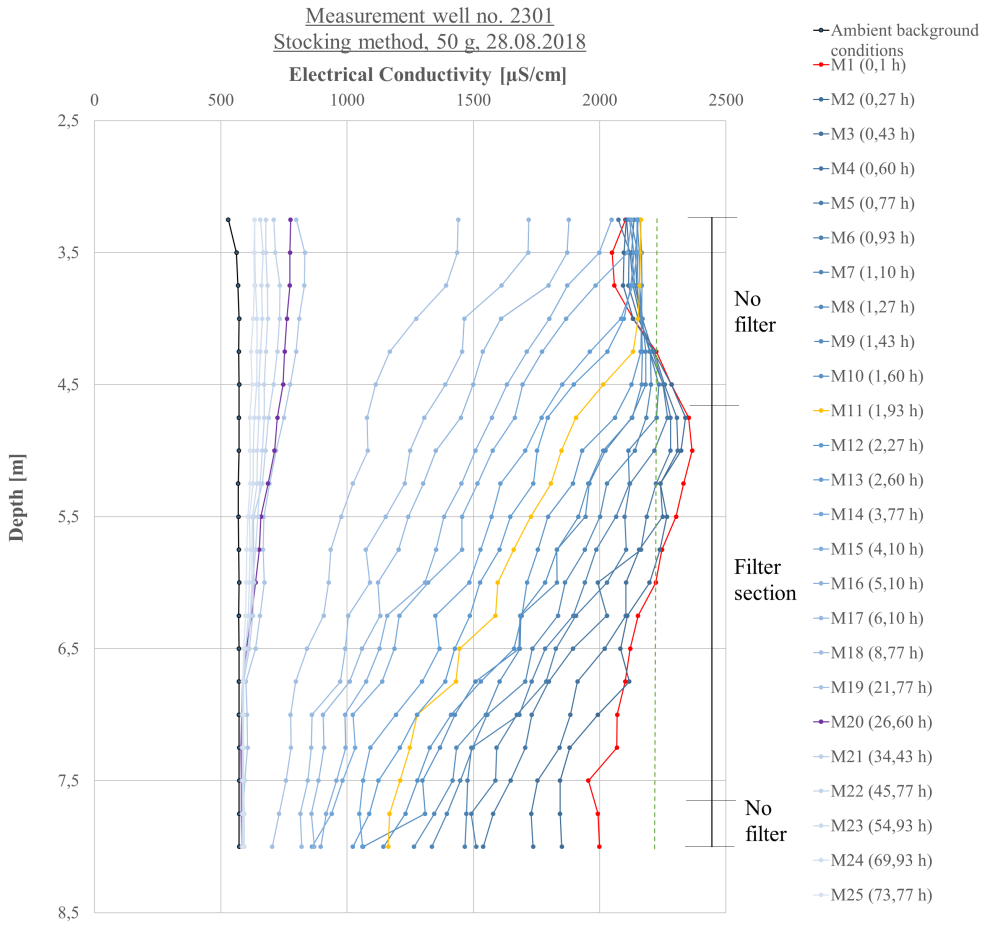

Figure 32: Electrical conductivity development, stocking method 2 of 2 for measurement well 2301.

Salt quantity development

The calibration factor used for calculating the salt quantity in measurement well 2301 is 0,487, see Figure 33.

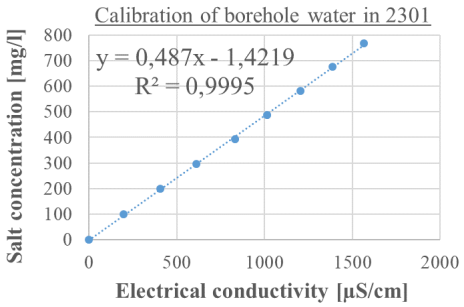

Figure 33: Calibration for measurement well 2301.

Figure 34a and 34b show the total salt quantity development in the borehole during the tests. Both graphs have been adapted with the natural logarithm. In the first test, it took approximately 3,8 hours for the salt to decrease with 50 %, and approximately 26 hours for the salt to decrease with 87 % of the

injected salt quantity. In the second test, it took approximately 4,5 hours for the salt to decrease with 50 %, and approximately 21,8 hours for the salt to decrease with 88 % of the injected quantity. According to the natural logarithm regression, the injected salt of 25 g disappeares from the borehole around 850 hours after injection in the first (calculated by setting y to zero in the ln equation). For the second test, the injected salt of 50 g disappears, according to the ln regression, after 73 hours. All numbers mentioned are summarized in Table4.2.1. As seen, the reliability of the regression is relatively low for the first test (R^2=0,7267), and high for the second test (R^2=0,9629). A better regression might have been obtained with more frequent measurements, and if measurements would have been closer to the point at which the electrical conductivity had gone back to background conditions. However, due to time limits at the day of test execution this was not possible to do for the first test.

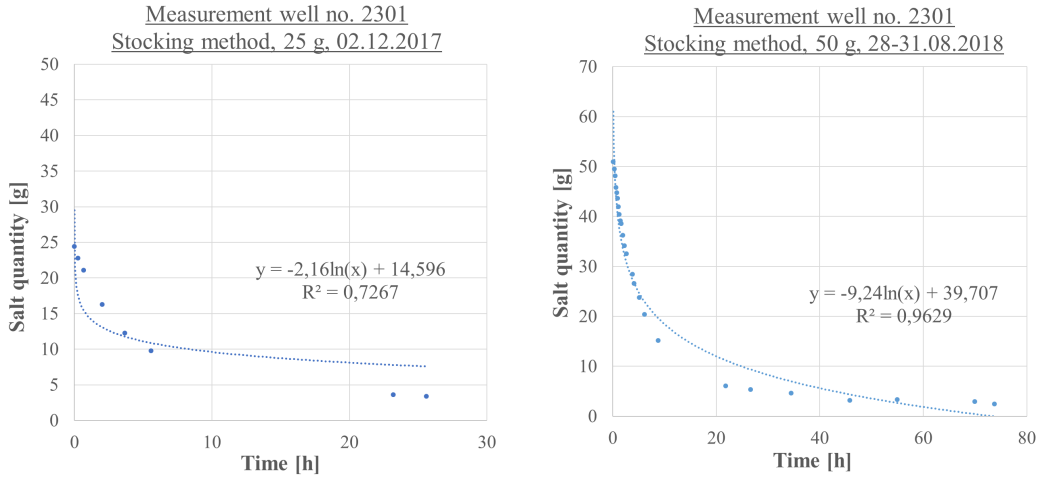

(a) Salt injection quantity: 25 g.

(b) Salt injection quantity: 50 g.

Figure 34: Salt quantity development, stocking method for measurement well 2301.

Table 7: Summary of salt dilution durations for measurement well 2301.

Test	**Duration 50 % decrease (h)**	**Duration 87-88 % decrease (h)**	**Duration 100 % decrease (h)**
02.12.2017 (25g)	3,8	26	not reliable
12.12.2018 (50 g)	4,5	21,8	73

Filtration velocities

In Figure 35a and 35b the calculated filtration velocity for each depth along the filter section are displayed. The average filtration velocity and maximum filtration velocity for each test are summarized in Table 8. The filtration velocities are similar for both tests. There is an overall increase of the filtration velocity as the depth increases. I.e., the groundwater flow is bigger further down in the aquifer.

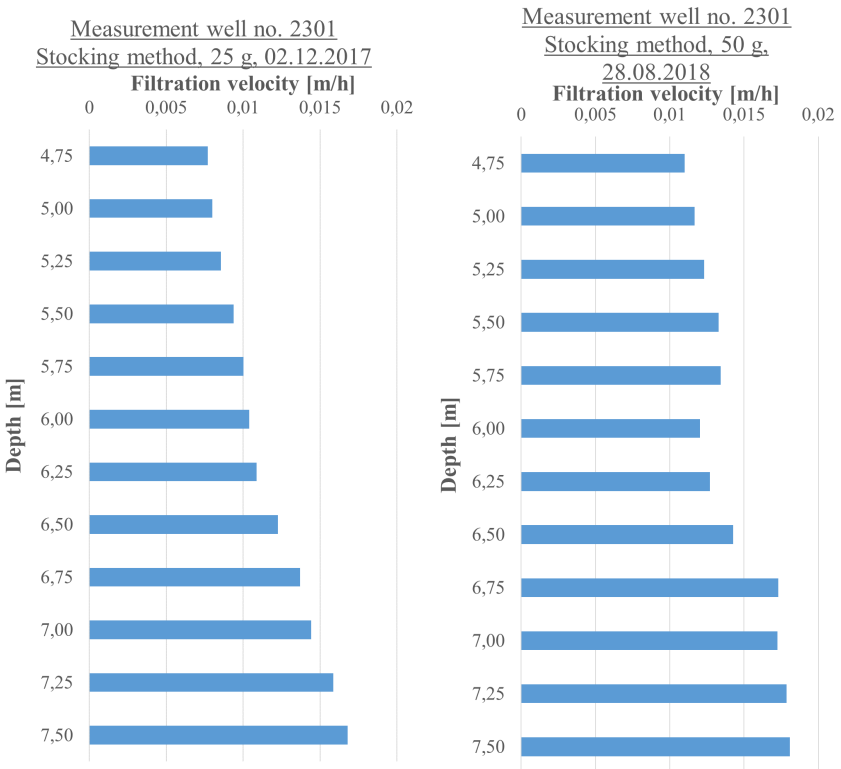

(a) Salt injection quantity: 25 g.

(b) Salt injection quantity: 50 g.

Figure 35: Filtration velocity, measurement well 2301.

Table 8: Average and maximum filtration velocity from tests for section 4,75-7,50 m in borehole 2301.

Test	**Average filtration velocity (m/h)**	**Maximum filtration velocity (m/h)**
12.12.2017 (25 g)	0,012	0,017
28.08-2017 (50 g)	0,013	0,019

4.2.2 Measurement point 5303

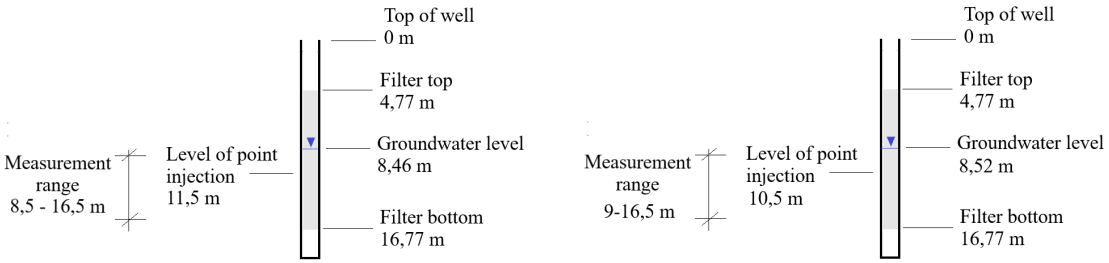

(a) 28.11.2018 (b) 12.12.2018

Figure 36: Illustration of injection in borehole 5303.

In measurement well 5303, located in the gravel aquifer, two point injections were executed: one with a salt solution of 200 g/l (28.11.2018) and one with a salt solution of 50 g/l (12.12.2018). Since the total volume of salt solution injected in each test is 250 ml, that corresponds to 50 g respectively 12,5 g of salt. The first test was measured during a total time of 2,1 hours and the second test during a total time of 4,1 hours. The measurements of the electrical conductivity were all done within the filter section of the borehole. The injection was done at similar depths: in the first test at a depth of 11,5 m, and in the second at a depth of 10,5 m, as seen in Figure 36.

Electrical conductivity development

Due to the differences in injected salt quantity, the first test, compared to the second test, reached a higher peak in electrical conductivity directly after injection: 6173 µS/cm compared to 1948 µS/cm. For both tests, there seems to be a vertical flow moving downwards in the well. This can be seen for example by the electrical conductivity peak that moves downwards with time, illustrated with thick, black dots in Figure 37.

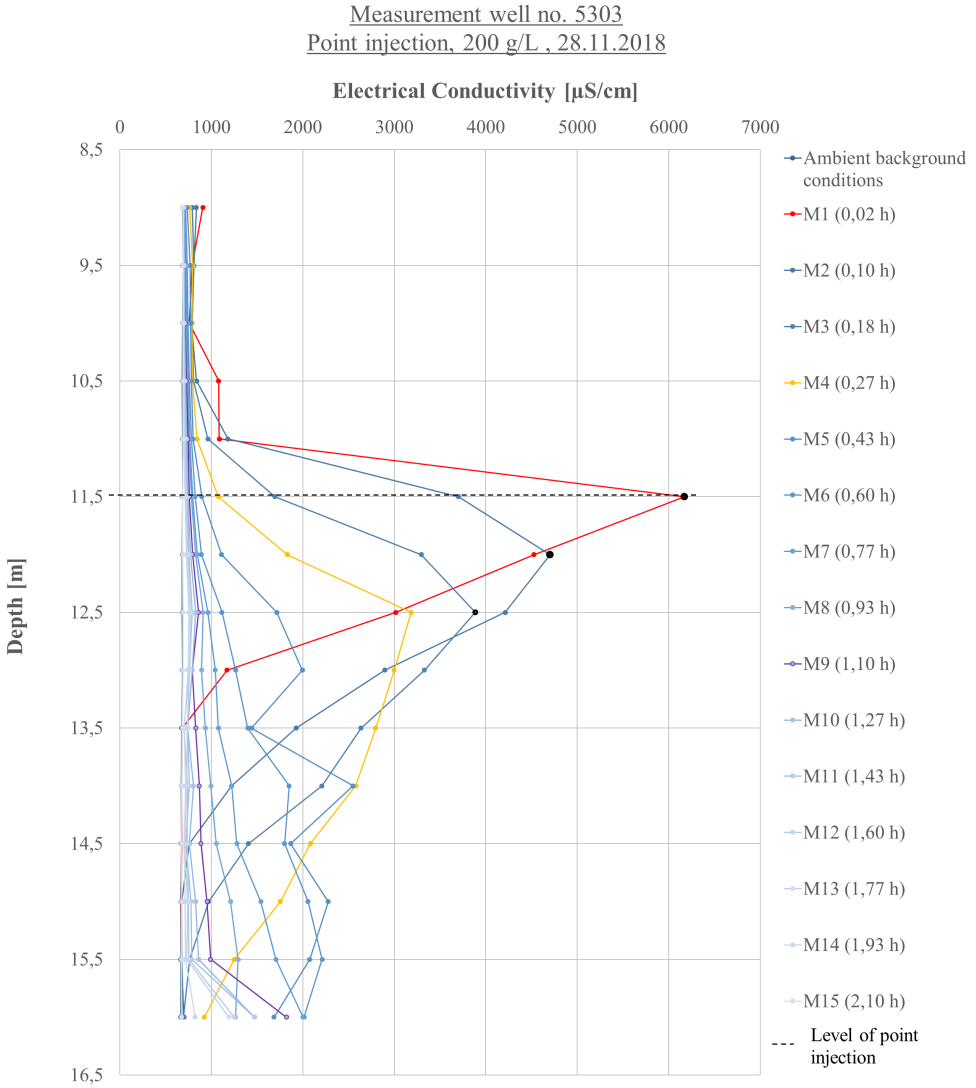

Figure 37: Electrical conductivity development, point injection 1 of 2 for measurement well 5303.

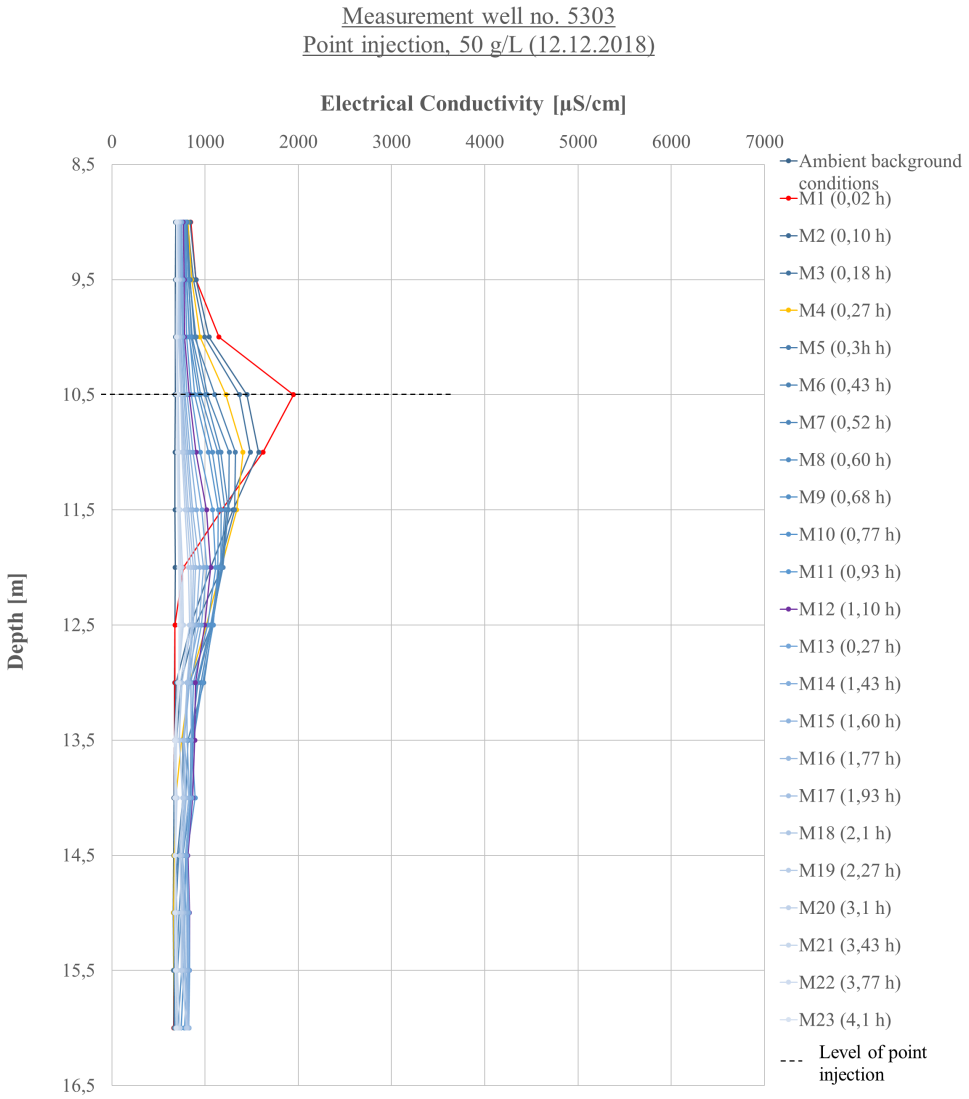

Figure 38: Electrical conductivity development, point injection 2 of 2 for measurement well 5303.

Salt quantity development

The calibration factor used for calculating the salt quantity in measurement well 5303 is 0,5271, see Figure 39.

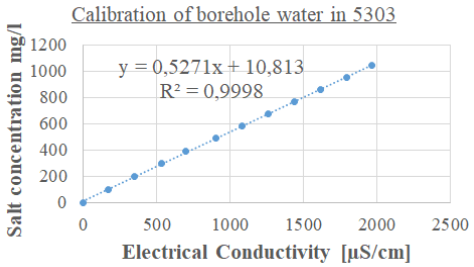

Figure 39: Calibration for measurement well 5303.

The salt quantity development for each of the two point injections are presented in Figure 40a and 40b. Both data sets show a similar pattern, since they both follow a x^2 adjustment. The salt disappeared faster in the first test than in the second one. At around 2 hours, almost all of the salt in the first test had disappeared, according to the x^2 regression. Meanwhile, it took, according to the x^2 regression, approximately 4,2 hours until the salt quantity in the second test had disappeared. In the first test, it took between 0,5 - 1 hours for 50 % (25 g) of the salt to disappear. In the second test, 50 % (6,25 g) of the initial salt quantity had disappeared after almost 2 hours. Furthermore, it took approximately 1,4 hours for 90 % (40 g) of the salt to disappear in the first test, and approximately 3,8 hours for 90 % (11,25 g) of the salt to disappear in the second test. The mentioned numbers are summarized in Table 9. The ln regressions for both tests are well fitted for the measured data (R^2=0,9905 and R^2=0,9708). However, in the first graph the regression increases again at around 1,8 hours, which would not be logical since the salt quantity decreases and should reach zero. The model therefore seems to work well up for x values between 0 and 1,8. However, with a brief estimation when studying the actual measured point, the assumption of total salt dilution at approximately 2 hours can be done. For the second test, the regression shows that 100 % salt would disappear after around 4,2 hours.

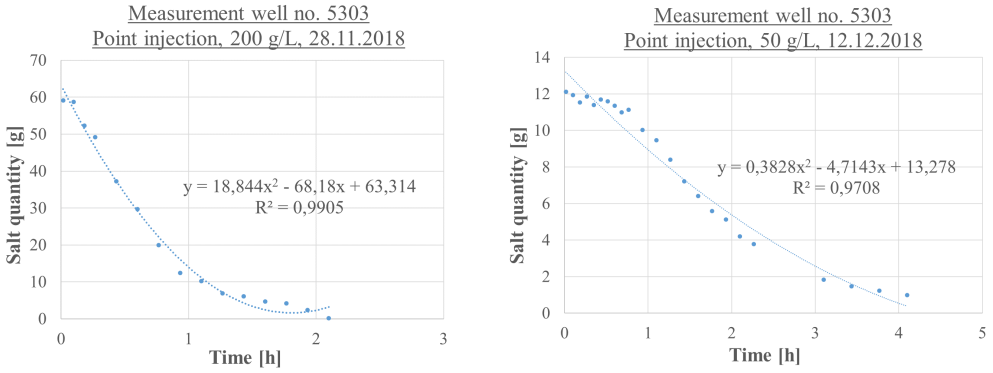

(a) Salt injection concentration: 200 g/l.

(b) Salt injection concentration: 50 g/l.

Figure 40: Salt quantity development, point injection for measurement well 5303.

Table 9: Summary of salt dilution durations for measurement well 5303.

Test	**Duration 50 % decrease (h)**	**Duration 90 % decrease (h)**	**Duration 100 % decrease (h)**
28.11.2018 (200 g/l; 50 g)	0,5-1	1,4	2
12.12.2018 (50 g/l; 12,5 g)	2	3,8	4,2

Previous SBDTs executed in borehole 5303 also show a relatively fast decrease in total salt quantity. In one test, where the stocking method and an initial salt quantity of 60 g was used, 50 % of the salt had disappeared after approximately 0,3 hours, and 90 % had disappeared after approximately 0,8 hours. In another test, where the stocking method and an initial salt quantity of 70 g was used, 50 % of the salt had disappeared after approximately 0,45 hours and 90 % after approximately 1,1 hours. In a test where the hosepipe method and a total inital salt quantity of 50 g was used, 50 % had disappeared after 0,6

hours (Fromm, 2018). The results from 28.11.2018 and 12.12.2018 in combination with the results from the previously executed SBDTs all show a fast total salt quantity decrease, indicating that the borehole has a strong connection to the surrounding aquifer, and that it is relatively well suited as input point for tracers in tracer tests.

Filtration velocity

For the test on 28.11.2018, the filtration velocity was calculated for the section around the injection point (10,5-12,5 m), see Figure 41a and Table 10. For the test on 12.12.2018, the filtration velocity was calculated for the section around the injection point (9,5-11,5 m), see Figure 41b and Table 10.

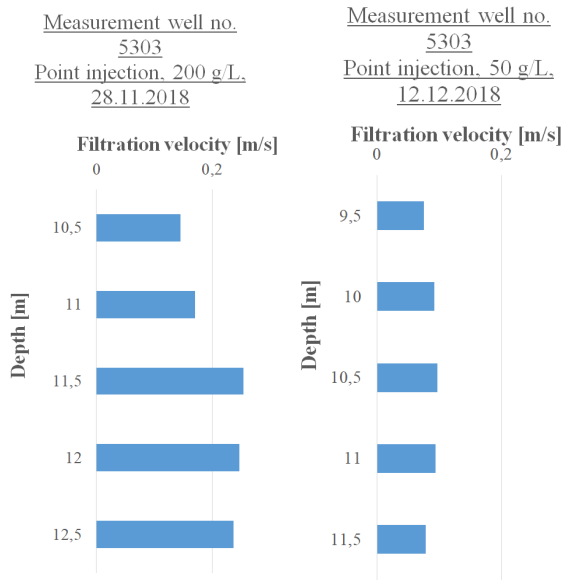

(a) Test on 28.11.2018, at depth section 10,5-12,5 m

(b) Test on 12.12.2018, at depth section 9,5-11,5 m

Figure 41: Filtration velocity in measurement well 5303.

Table 10: Average and maximum filtration velocity for depth section 10,5-12,5 m from test on 28.11.2018, and depth section 9,5-11,5 m from test on 12.12.2018 in borehole 5303.

Test date	**Average filtration velocity (m/h)**	**Maximum filtration velocity (m/h)**
28.11.2018 (200 g/l; 50 g)	0,210	0,254
12.12.2018 (50 g/l; 12,5 g)	0,088	0,097

Results from previous SBDTs showed an average filtration velocity of 0,258, 0,18 and 0,216 m/h along the whole filtered section of borehole 5303 (Fromm, 2018). The filtration velocity calculated from the test on 28.11.2018 corresponds well to the previous results, whereas, the test on 12.12.2018 shows values more than half as big. The reason why the second test deviates from the other results is not clear. More point

injection tests should be done in the borehole in order to evaluate what is a legitimate filtration velocity for the section around 9,5-12,5 m.

4.2.3 Measurement point 5312

In measurement well 5312, located in the gravel aquifer, one point injection was executed on 28.11.2018. The salt concentration was 200 g/l, corresponding to a total salt quantity of 50 g. The salt was injected at a depth of 11 m and the measurements were carried out during a total time of 3,43 hours. An illustration of the injection can be seen in Figure 42.

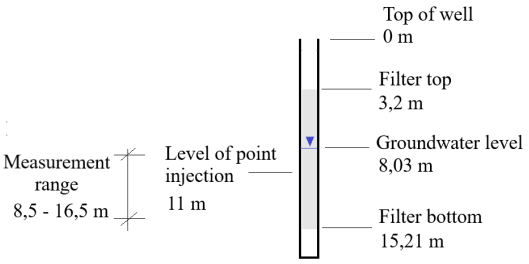

Figure 42: Illustration of injection in borehole 5312.

Electrical conductivity

The maximum electrical conductivity reached 4614 µS/cm directly after injection. After 1 hour, the maximum value had decreased to 1693 µS/cm. After 3,43 hours, the electrical conductivity was between 577 and 935 µS/cm. By studying the downward movement of the electrical conductivity peak, there seems to be a tendency of downward vertical flow below 11 m . Results from a previously executed SBDTs with the stocking method show that there is a higher horizontal groundwater flow between 12,25 - 15,5 m (Engel, 2017; Fromm, 2018). Due to this, the salt from the above section moves downwards and dilutes into water at the lower section.

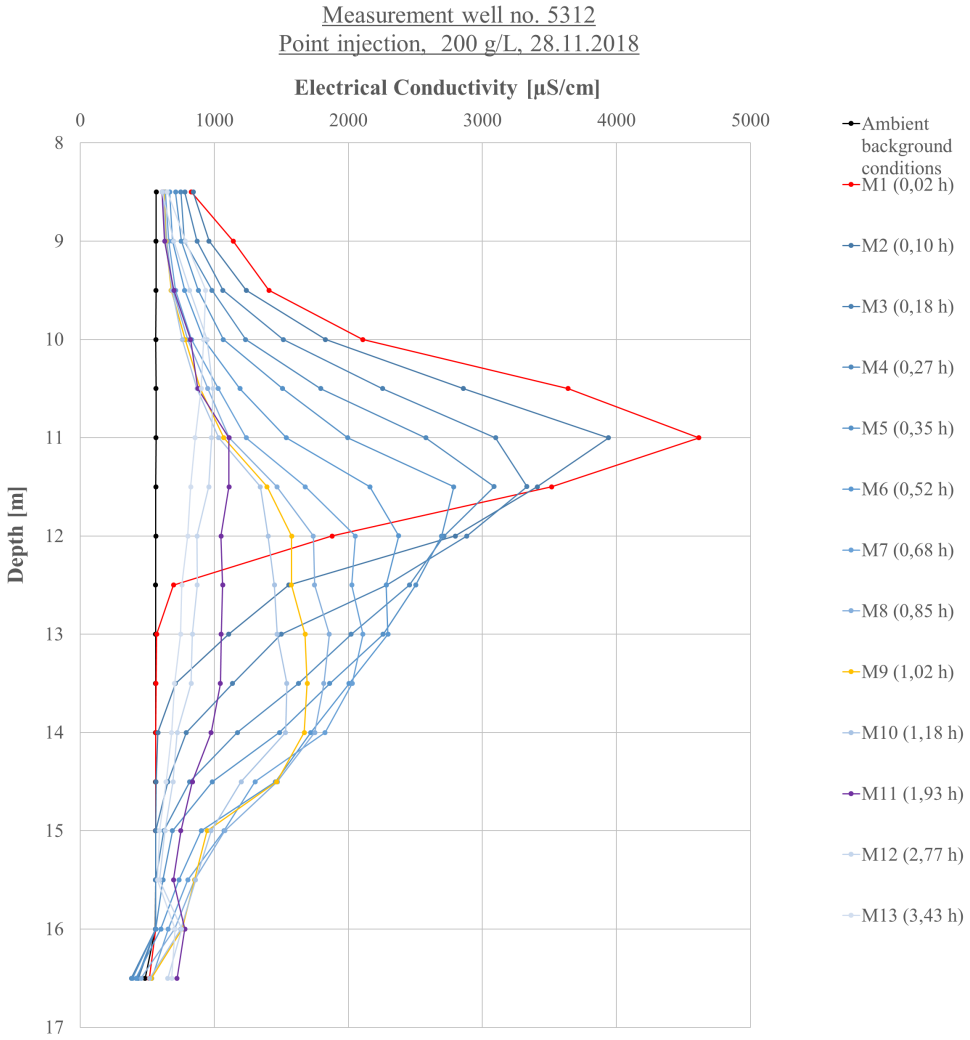

Figure 43: Electrical conductivity development, point injection 1 of 1 for measurement well 5312.

Salt quantity development

The calibration factor used for calculating the salt quantity in measurement well 5312 is 0,5342, see Figure 44.

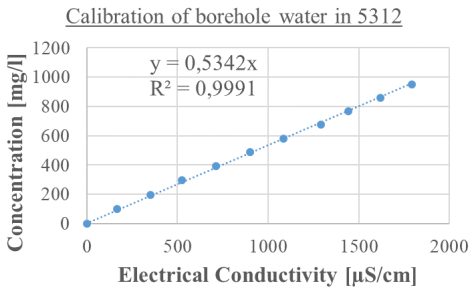

Figure 44: Calibration for measurement well 5312.

According to the results in Figure 45, the amount of salt in the borehole was more than 50 g for the

first five measurements. The reason of this, might be that too much salt was added when preparing the salt solution, resulting in a concentration that was actually higher than 200 g/l. The amount of salt in the borehole decreased by 50 % (35 g) during the first hour. Afterwards, the decrease of salt went much slower; it took another hour for the salt to decrease from 35 to 20 g, i.e. it took approximately two hours for the salt to disappear by 70 %. The mentioned numbers are summarized in Table 11. From the results it is not possible to estimate the time it would take for the salt to totally disappear from the borehole. In order to do so, the measurements of the electrical conductivity should have been done over a bit longer time, until the electrical conductivity is closer to background conditions. Due to time limitation on the day of the experiment, this was, however, not possible. However, it can still be concluded that the salt disappears relatively quickly, indicating that borehole 5312 has a good connection to the surrounding aquifer and therefore suitable as input point in tracer tests.

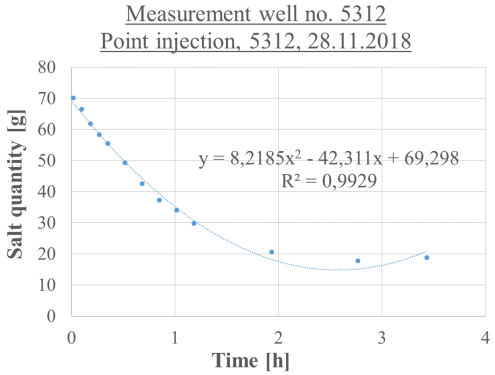

Figure 45: Salt quantity development, point injection for measurement well 5312.

Table 11: Summary of salt dilution durations for measurement well 5312.

Test	**Duration 50 % decrease (h)**	**Duration 90 % decrease (h)**	**Duration 100 % decrease (h)**
28.11.2018 (200 g/l; 50g)	1	1,8	-

In the previous SBDTs with the stocking method, the injected also disappeared quickly. In one of them, which had an injected salt quantity of 60 g, 50 % had disappeared after approximately 0,7 hours and 90 % after approximately 1,5 hours. In the other one, where same salt quantity was used, 50 % had disappeared after approximately 0,9 hours and 90 % after approximately 1,8 hours (Fromm, 2018). These results confirm the conclusion that 5312 is well suited for tracer tests.

Filtration velocity

The filtration velocity was only calculated for the depths close to the injection level, see Figure 46.

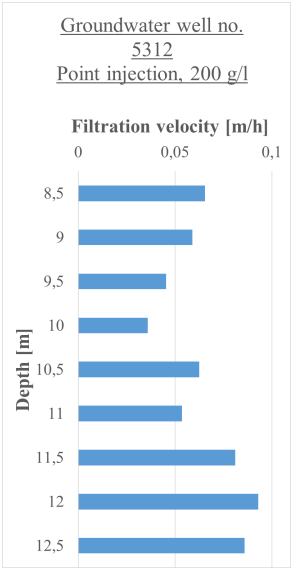

Figure 46: Filtration velocity for depth section 8,5-12,5 m in measurement well 5312

The calculated average filtration velocity and maximum filtration velocity for each adjustment as well as the average from all four filtration velocities are presented in Table 12.

Table 12: Filtration velocity for depth range 8,5-12,5 m from test on 28.11.2018 in borehole 5312.

Test	**Average filtration velocity (m/h)**	**Maximum filtration velocity (m/h)**
28.11.2018 (200 g/l)	0,065	0,093

The results from the two previously executed SBDTs showed an average filtration velocity of 0,091 m/h and 0,08 m/h, respectively. This would indicate that the filtration velocity is smaller in depth section 8,5-12,5 m depth than the average velocity of the well. This would comply with previous results, that say that there is a higher horizontal flow at 12,5-15 m (Fromm, 2018).

4.2.4 Measurement point 7721

In well 7721, located in the karst aquifer, two SBDTs with the stocking method were executed: one on 17.10.2018-18.10.2018 and another on 18.10.2018. By carrying out the tests close in time to each other, it is possible to compare different tests based on the same surrounding conditions. The injection for the two tests are illustrated in Figure 47. In the second test, it took much more time for all the salt to dissolve (26 minutes) compared to the first test (6 minutes). The reason for this is not fully clear, however, since the two injections were made by two different persons, eventual differences in technique handling may have played a role. It is less likely that the difference in dilution rate would depend on temperature, background concentration, and in- and outflow rate, since these factors were the same for both tests.

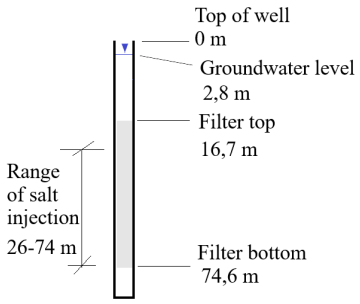

Figure 47: Illustration of injection in borehole 7721 for tests on 17-18.10.2018 and 18.10.2018.

Electrical conductivity development

Since the injections in the tests were executed only approximately 22 hours after each other, the electrical conductivity had not totally gone back to ambient background conditions at the start of the second test. On average, the electrical conductivity was approximately 25 µS/cm higher than the values at ambient background conditions in the first test (17-18.10.2018).

The injection was carried out over a total depth range of 48 m (from 26 to 74 m depth). At 71-74 m depth, the electrical conductivity reached values far above the ones in the rest of the well during ambient background conditions. The explanation might be that the lowest part of the well is sediment clogged, resulting in almost no horizontal or vertical groundwater flow. Particles from the surrounding as well as salt from previous SBDTs may have gotten trapped there, resulting in high electrical conductivity. Due to these uncertainties, the results from 71-74 m will not be further analyzed nor discussed. The first upper meter that was measured, i.e. 25-26, is located above the filter section. The "nick" that occurs at 26 m in Figure 48 and Figure 49 is therefore not due to any cavities in the karstic rock, but rather due to the fact that the filter starts there.

Given the calibration factor, borehole radius, borehole length and electrical conductivity at ambient background conditions, an expected average value of the electrical conductivity reached after injection could be calculated: approximately 3300 µS/cm for both SBDTs. This expected value is visualised as a green, dashed line in Figure 48 and 49. The average of the measured values directly after salt injection (M1) was approximately 2900 µS/cm for the first test and approximately 2600 µS/cm for the second test, visualised with a brown, dashed line in Figure 48 and 49. This may indicate that already at M1, salt has left the borehole. However, the difference in actual average and expected could also be caused by uncertainty in the lowest part of the well (71 - 74 m depth).

In both tests, a particularly high horizontal flow occurs at around 36 m. Here, the electrical conductivity decreases faster compared to most other sections of the well. This can be seen in the form of a "nick" in Figure 48 and 49. A previously executed SBDT with the stocking method shows similar patterns (Fahrmeier, 2016).

In the lower part of the well, vertical groundwater flow can be observed. In Figure 48 this is visualized through the electrical conductivity peak moving downwards. After 1,35 hours (M5), the peak has already moved from 55 to 65 m. In Figure 49 it is visualized through the changing angle between the later graphs and graph M1.

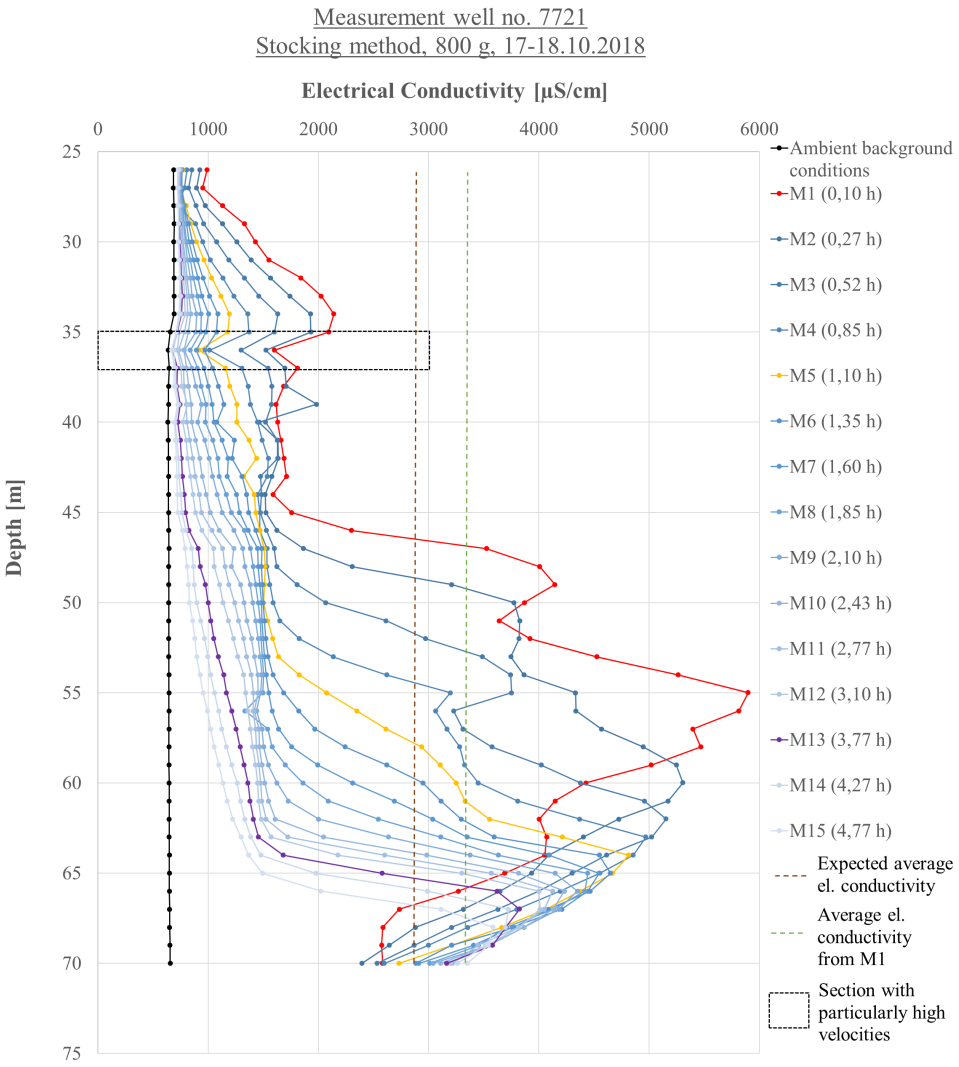

Figure 48: Electrical conductivity development, stocking method 1 of 2 for measurement well 7721.

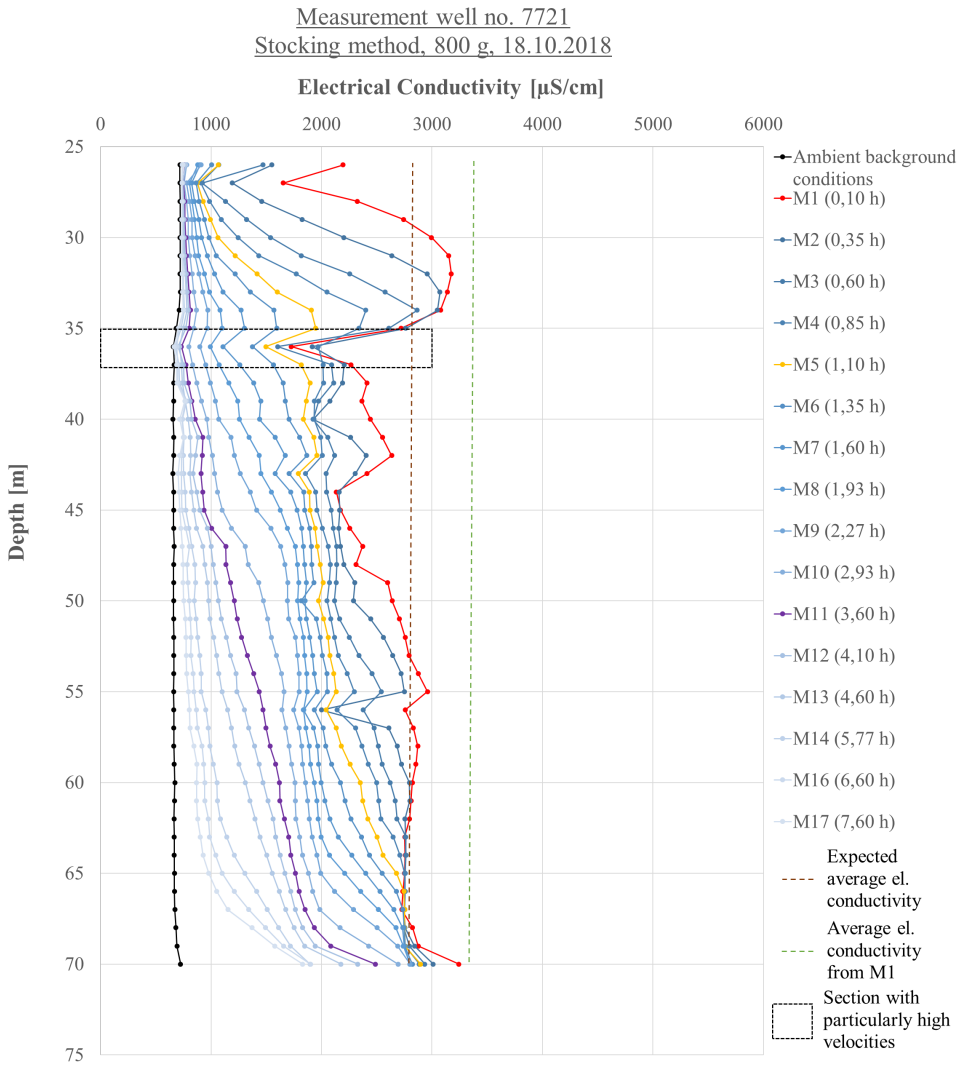

Figure 49: Electrical conductivity development, stocking method 2 of 2 for measurement well 7721.

Salt quantity development

The calibration factor used for calculating the salt quantity in measurement well 7721 is 0,52, see Figure 50.

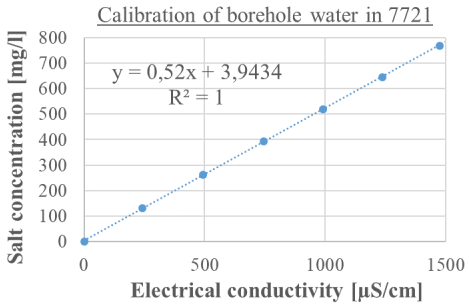

Figure 50: Calibration for measurement well 7721.

The salt quantity development shows a similar pattern for both tests, with a natural logaritm adjustment

for the salt quantity values. This is logical given that the tests were executed with the same quantity and under the same surrounding conditions. The difference between the factor in front of *ln* (-148,1 respectively -187,4) can be explained by the difference in the injection process and the presence of salt from the first test still in the borehole during the second test. In the first test, it took approximately 1,3 hours for the initial salt quantity to decrease with 50 %, and around 8 hours for the salt to decrease with 90 %. In the second test, the corresponding times are similar: approximately 1,4 hours and approximately 7,6 hours, respectively. Setting y to 0 in both ln equations, the duration for the salt to totally disappear could be estimated to 18 and 12 hours, respectively. The mentioned numbers are summarized in Table 13. The relatively fast decrease in total salt quantity indicates that borehole 7721 is well connected to the surrounding aquifer, and therefore a suitable injection point for tracer tests.

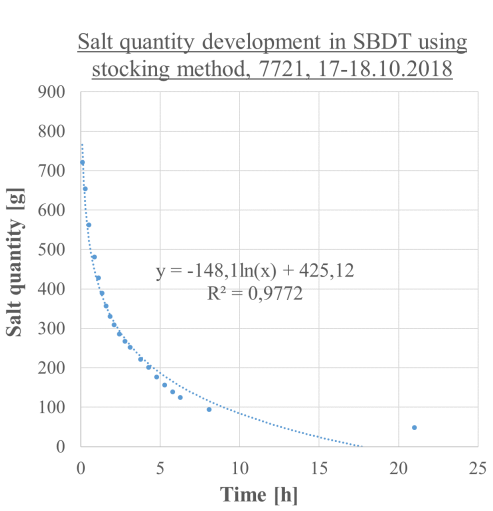

(a) Salt injection quantity: 800 g.

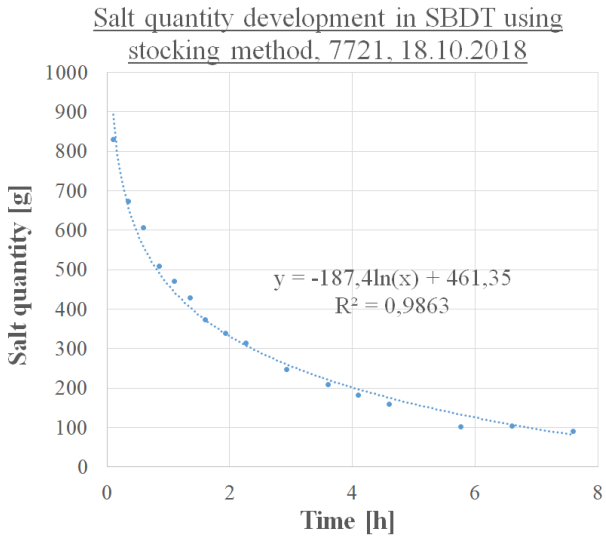

(b) Salt injection quantity: 800 g.

Figure 51: Salt quantity development, stocking method for measurement well 7721.

Table 13: Summary of salt dilution durations for measurement well 7721.

Test	**Duration 50 % decrease (h)**	**Duration 90 % decrease (h)**	**Duration 100 % decrease (h)**
17-18.10.2018 (800 g)	1,3	8	18
18.10.2018 (800 g)	1,4	7,6	12

Filtration velocity

In order to avoid any incertainties caused by the shift between non-filtered and filtered section at around 26 m, the filtration velocity was only calculated starting from 27 m. In the first test, the data was hard to interpret into filtration velocities below 64 m of depth. Due to this, the filtration velocities were only calculated until 64 m depth. In order to make the two tests comparable, the filtration velocity in the second

test is also only presented for depths up to 64 m. The filtration velocity from the test on 17-18.11.2018 is presented in Figure 52a, and the filtration velocity from the test on 18.10.2018 is presented in Figure 52b.

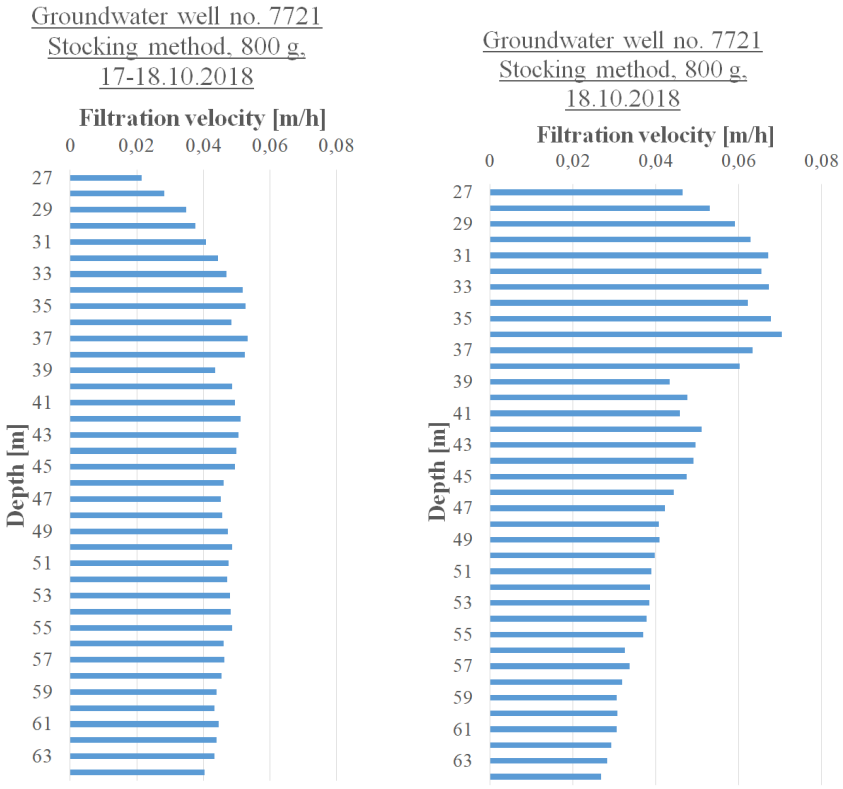

Figure 52: Filtration velocity for depth section 27-64 m in measurement well 7721.

The average and maximum filtration velocities are presented in Table 14.

Table 14: Filtration velocity for depth section 27,5 - 33,5 m from test on 07.11.2018 in borehole 7721.

Test	**Average filtration velocity (m/h)**	**Maximum filtration velocity (m/h)**
17-18.10.2018 (800 g)	0,045	0,053
18.10.2018 (800 g)	0,046	0,070

The average filtration velocity calculated in the adjustments are similar, making the final, calculated value of the average filtration velocity reliable. From a previously executed SBDT with the stocking method, the average filtration velocity from 23-74 m was calculated to 0,047 m/h, which is similar to the values calculated from the SBDTs executed on 17-18.11.2018 and 18.11.2018 (Fahrmeier, 2016).

4.2.5 Measurement well 7733

The point injection in measurement well 7733, located in the karst aquifer, was executed on 07.11.2018 with a salt solution of 200 g/l. As the point injection has a volume of 250 ml, this corresponds to a total salt quantity of 50 g.

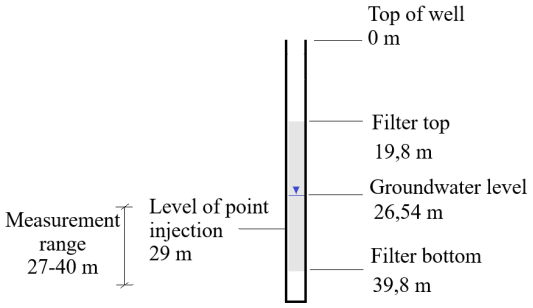

Figure 53: Illustration of injection in borehole 7733.

Electrical conductivity development

The measurements of the electrical conductivity were done between 27 and 40 m depth. The highest electrical conductivity measured was 4272 µS/cm at the injection level (29 m of depth). At the last measurement (M23, i.e. 6,93 h after injection) the electrical conductivity had almost gone back to ambient background conditions. At the two first measurements (M1 and M2), the electrical conductivity peaks at the injection level (29 m). However, already after the second measurement, the peak changes place to above or below the injection level. According to the results from a previously executed SBDT with the stocking method and the hosepipe method, the well has its highest horizontal flow at around 29 - 29,5 m (Fahrmeier, 2016; Engel, 2017). This explains the fact that the electrical conductivity decreases faster at around 29 m than for the sections above and below (at 30 - 31 m respectively 27,5 - 28,5 m of depth). Since the horizontal flow is particularly high at 29 m, the real maximum electrical conductivity can be expected to have reached a slightly higher value than the one measured. During the time between injection and the measurement, some salt may already has disappeared. Since the test was carried out as point injection, no conclusions can be drawn regarding groundwater flow in the lower part of the well.

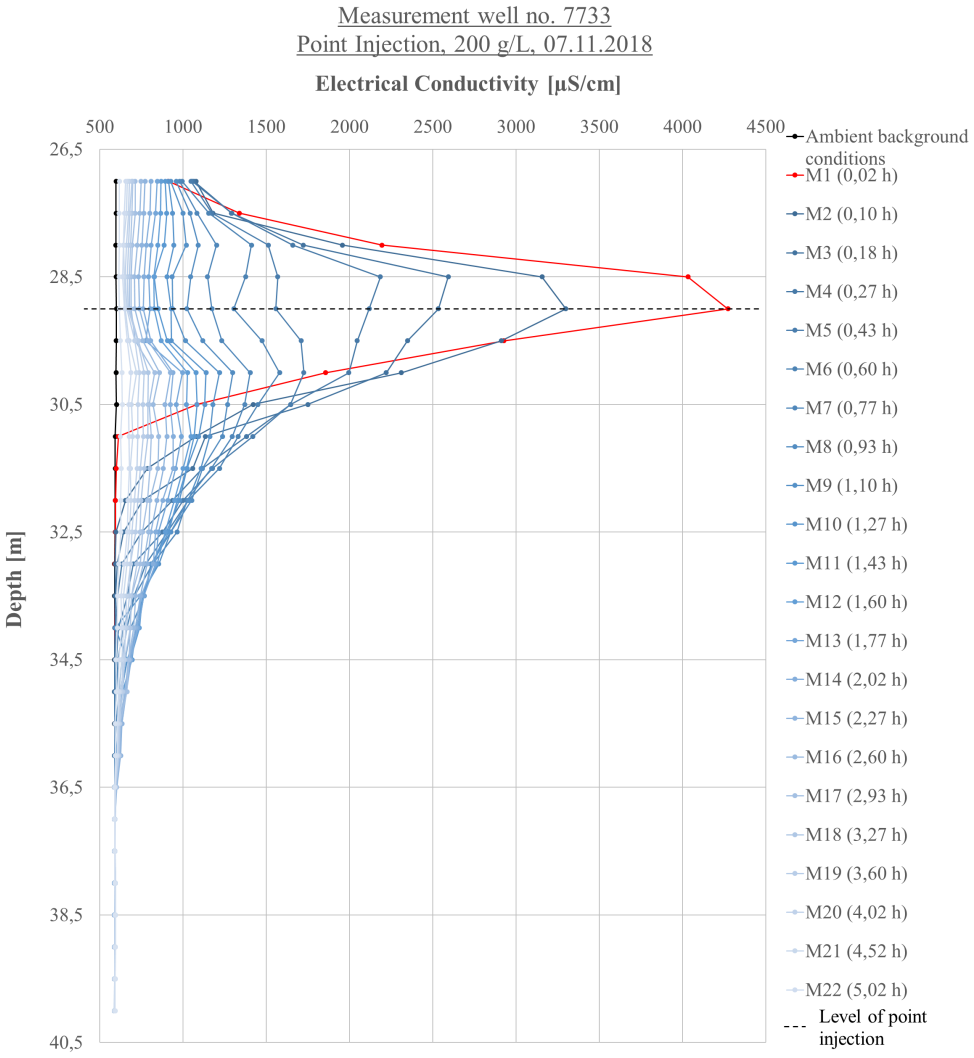

Figure 54: Electrical conductivity development, point injection 1 of 1 for measurement well 7733.

Salt quantity development

The calibration factor used for calculating the salt quantity in measurement well 7733 is 0,5294, see Figure 55.

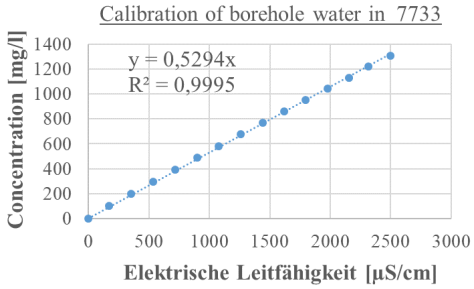

Figure 55: Calibration for measurement well 7733.

Figure 56 displays the total salt quantity development during the SBDT. The total quantity at the first measurement after injection (M1) was 45,5 g. This affirms the theory that some salt already had disappeared from the borehole during the time between injection and the first measurement. After 0,5 hours, approximately 50% of the initial salt (50 g) had disappeared and after 2 hours, approximately 75 % of the initial salt (50 g) quantity had disappeared. After 4 and 6 hours, approximately 90 % and 97 %, respectively, had disappeared. The ln regression has a relatively high reliability (R^2=0,9365)The time it would take for the salt to totally disappear is calculated by setting y to 0 in the ln regression equation and calculate the x value, which here was equal to approximately 8,5 hours. The mentioned values are summarized in Table 15. Rapidly decreasing salt quantities along the borehole were also previously noted in the SBDT executed by Fahrmeier (2016) and Engel (2017). This suggests that the measuring point is well connected to the surrounding aquifer, and thereby suitable as an input point for tracer tests.

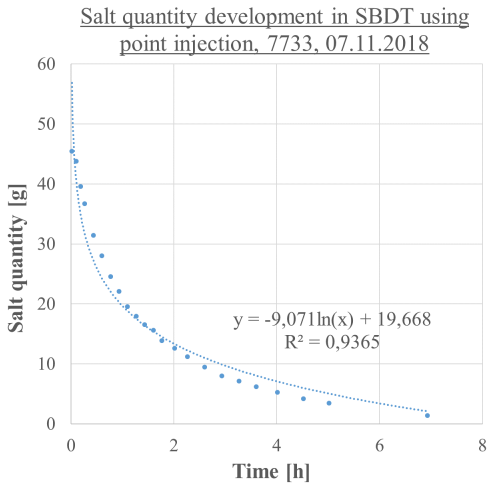

Figure 56: Salt quantity development, point injection for measurement well 7733.

Table 15: Summary of salt dilution durations for measurement well 7733.

Test	Duration 50 % decrease (h)	Duration 75 % decrease (h)	Duration 90 % decrease (h)	Duration 97 % decrease (h)	Duration 100 % decrease (h)
07.11.2018 (200 g/l)	0,5	2	4	6	8,5

Filtration velocity

The filtration velocities at different depths from 27,5 to 30,5 m are presented in Figure 57, and the average of these as well as the maximum are presented in Table 16.

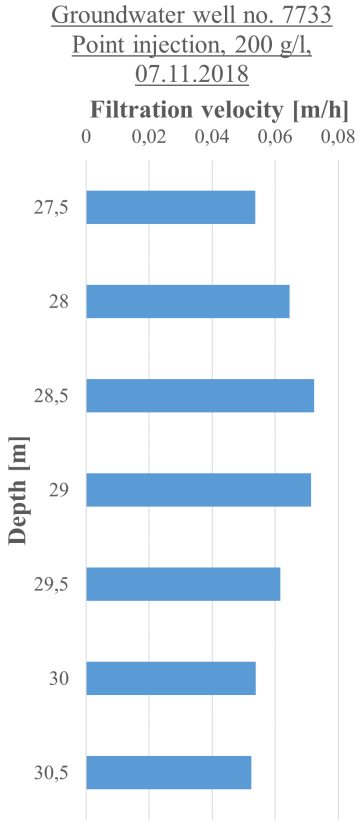

Figure 57: Filtration velocity for depth section 27,5-33,5 in borehole 7733.

Table 16: Filtration velocity for depth section 27,5 - 33,5 m from test on 07.11.2018 in borehole 7733.

Test	**Average filtration velocity (m/h)**	**Maximum filtration velocity (m/h)**
07.11.2018 (200 g/l)	0,061	0,072

Previously executed SBDTs in borehole 7733 showed an average filtration velocity of 0,043 m/h for the section between 26 and 40 m (Fahrmeier, 2018). Since the results from the electrical conductivity both from the test on 07.11.2018 and from previous tests indicate that the borehole has its highest horizontal flow around 29-29,5 m, it is logical that the filtration velocity is higher in the section between 27,5 and 33,5 m than the average filtration velocity between 26 and 40 m.

4.2.6 Summary of results in the field

Table 17 displays a summary of the results presented in this chapter.

Table 17: Summary of results from salt quantity development and filtration velocity for SBDTs executed in the field.

Well nr.	**Method**	**Test date and salt quantity/ salt concentration**	**Average filtration velocity (m/h)**	**Max. filtration velocity (m/h)**	**Duration 50 % salt dilution (h)**	**Duration approx. 90 % salt dilution (h)**	**Duration 100 % salt dilution (h)**
2301	Stocking	28.08.2018 (50 g)	0,012	0,017	4,5	26	not reliable
2301	Stocking	02.12.2017 (25 g)	0,013	0,019	21,8	21,8	73
5303	Point Injection	28.11.2018 (50 g)	0,210	0,254	0,5-1	1,4	2
5303	Point Injection	12.12.2018 (12,5 g)	0,088	0,097	2	3,8	4,2
5312	Point Injection	28.11.2018 (50 g)	0,065	0,093	1	1,8	-
7721	Stocking	17-18.10.2018 (800 g)	0,045	0,053	1,3	8	18
7721	Stocking	18.10.2018 (800 g)	0,046	0,070	1,4	7,6	12
7733	Point Injection	07.11.2018 (50 g)	0,061	0,072	0,5	4	8,5

Despite problems with the injection in some tests, for example with the stocking method in measuring well 2301 and 7721, valuable conclusions from the results could be obtained. Wells 5303, 5312, 7721 and 7733 can be identified as measuring wells suitable as input point of tracers or measurement of tracers in a tracer test due to particularly fast decrease in total salt quantity and high Darcy flow velocities. In some wells, sections with particalarly high groundwater flow could be detected. If a tracer test is executed in such a well, these sections are particularly suited for tracer injection. Well 2301 proved to have the lowest filtration velocities and longest salt dilution duration of all studied wells, and would probably be less suited for tracer tests. The results did not differ depending on the type of aquifer (karst or gravel aquifer). The filtration velocity in gravel well 2301 was smaller than the filtration velocity in the karst aquifer wells whereas the filtration velocity in gravel aquifer 5303 and 5312 was higher. Therefore it is not possible to conclude whether karst or gravel wells are more suitable as input points for tracer tests.

Chapter 5

Conclusion

Through two point injection SBDTs performed at the lower part of the filtered section, porous aquifer well 5303 proved to have an average Darcy flow velocity of 0,088-0.210 m/h. Porous aquifer well 5312, in which another point injection SBDT was performed at the lower part of the filtered section, the Darcy flow velocity measured 0,065 m/h. Karstic aquifer well 7721 showed, from two stocking method SBDTs, an average Darcy flow velocity of 0,45-0,46 m/h. For karstic aquifer well 7733, a point injection SBDT performed at the lower part of the filtered section showed a Darcy flow velocity of 0,0614 m/h. Through two stocking method SBDTs, porous aquifer well 2301 proved to have 0,012-0,013 m/h in average Darcy flow velocity. From these results, it seems as if four of the five studied wells (5303, 5312, 7721 and 7733) are suitable as inputs point and measurement points in a tracer test due to high Darcy flow velocities. Porous aquifer well 2301 has a relatively low Darcy flow velocity, and is due to this perhaps less suitable for tracer tests. The Darcy Flow velocity results obtained from a SBDT already gives an indication of potential contamination transport paths that exist in the protection area, however, tracer tests will give more precise results.

Even though the calculation of Darcy flow velocity mainly should be used for porous aquifers, it could still give a good estimation whether a specific karst aquifer well has good connection to the surrounding aquifer. So far, three SBDTs have been carried out for measurement well 7721, and they all showed a similar filtration velocity. The filtration velocity calculated for 7733 also complied well with previous results. This might indicate that the calculation method works for the well 7721 and 7733 and could work also for other karst aquifer wells.

In order to evaluate the three different SBDT injection methods (stocking method, hosepipe method and point injection method) and two different SBDT measurement methods (Electrical Conductivity Meter and CTD-Diver), experiments were executed in a lab hall. Salt was injected by using either the stocking method, two different types of the hosepipe method, or the point injection method in a water filled, vertically positioned 6 meter long PET pipe. A major problem when it comes to the stocking method, is to get an equal distribution of the injected salt. Tests with the hosepipe method did not result in any particular improvements compared to the stocking method. The stocking method is therefore preferred, since it also is cheaper, easier to handle and easier to prepare. Both the stocking method and the hosepipe method type 1 resulted in a smoothly distributed salt injection, whereas hosepipe method type 2 resulted in an injection with "zigzag" patterns. When analyzing the results, it might be easier to analyze a smooth graph for the

electrical conductivity development. A major challenge in the tests that included the point injection, was to get the injection at a desired level, since the point injection device turned out to have some technical imperfections. Due to this, an improved point injection device will be developed and used in future SBDTs. According to the results from the point injections, density effects caused by the salt can be neglected, since the salt did not dissolve particularly faster below than above the point of injection.

Using a CTD-Diver instead of an Electrical Conductivity Meter has several advantages. It is smaller and therefore easier to handle, measures faster and is thereby more time effective, and requires less work load on documentation. Even though some additional work has to be done with converting water pressure values to water depths, the CTD-Diver is preferred. However, for measurement wells where a SBDT has not yet been executed and where the groundwater flows are not yet known, it is better to use to the Electrical Conductivity Meter. The reason for this, is that it is possible to observe the results during the the test when using the Electrical Conductivity Meter, which facilitates the estimation of the required measurement frequency as well as total measurement duration of the SBDT. However, the best option would be if the research group at KIT would invest in a handy system in which the results from a CTD-Diver can be observed directly during the test.

Chapter 6

Recommendations

A regression curve was fitted to the graph of the results of the total salt quantity development, making it possible to describe the groundwater behaviour inside and around the borehole. Through the function calculated from the regression curve, an estimated time it takes for the salt to totally disappear from the borehole could be determined. For some tests, it was difficult to find a suitable regression curve due to too few data points. If the electrical conductivity values would have been measured more frequently in time and closer to the point at which the electrical conductivity returns to background values, a more reliable function, and therefore calculation of total salt dilution duration, could probably have been found. Even though conclusions whether the studied wells suitable for tracer tests can be drawn, it is still not possible to decide exactly where in the area a tracer test should be executed. In order to decide that and thereby maximize the potential outcome of a tracer test, SBDT data would need to be achieved for more wells in the area. In that way, a better understanding regarding the groundwater flow connections within the whole area can be achieved.

For future SBDTs, it is recommend to execute "pairs" of tests in a specific borehole, where only one factor differs. For example: two tests with the same injection method and the same salt quantity but in different seasons, or two tests with the same injection method and executed only some days after each other (resulting the same background conditions) but with different salt quantities. Then, it would be easier to compare results. Hosepipe method type 2 has so far only been carried out in the lab, so it is recommended to try the method in the eld in order to see how it behaves in a real hydrogeological situation.

Bibliography

Bakalowicz, M. (2005). *Karst groundwater: a challenge for new resources.* Hydrogeology journal, 13(1), 148-160.

Chen, Z., Auler, A. S., Bakalowicz, M., Drew, D., Griger, F., Hartmann, J., Jiang, G., Moosdorf, N., Richts, A., Stevanovic, Z.,Veni, G., Goldscheider., N. (2017). *The World Karst Aquifer Mapping project: concept, mapping procedure and map of Europe.* Hydrogeology Journal, 25(3), 771-785.

Drost, W., Klotz, D., Koch, A., Moser, H., Neumaier, F., and Rauert, W. (1968). *Point dilution methods of investigating ground water flow by means of radioisotopes.* Water Resources Research, 4(1), 125-146.

Encyclopedia Britannica. (2009). *Riss-Würm Interglacial Stage, Geology.* The Editors of Encyclopedia Britannica. https://www.britannica.com/science/Riss-Wurm-Interglacial-Stage

Engel, P. (2017). *Durchführung und Vergleich von Bohrlochverdünnungsversuchen mit verschiedenen Injektionsmethoden.* Fakultät für Bauingenieur-, Geo- und Umweltwissenschaften am Karlsruher Institut für Technologie.

Europea, U. (1995). *Hydrogeological aspects of groundwater protection in karstic areas*, Final report (COST action 65), 446 pp.

Fahrmeier, N. (2016). *Hydrogeologische Charakterisierung des Karstgrundwasserleiters im Einzugsgebiet der Landwasserversorgung. Fakultät für Bauingenieur-, Geo- und Umweltwissenschaften am Karlsruher Institut für Technologie.*

Fitts, C. R. (2002). *Groundwater science.* Elsevier.

Ford, D., and Williams, P.D. (1989) *Karst hydrogeology and geomorphology* (Vol. 601). London: Unwin Hyman.

Fromm, L. (2018). *Durchführung von Bohrlochverdünnungsversuchen unter Einsatz eines Bohrlochpackers und Vergleich verschiedener Eingabemethoden.* Fakultät für Bauingenieur-, Geo- und Umweltwissenschaften

am Karlsruher Institut für Technologie.

Gaspar, E. (1987). Modern trends intracer hydrology (Vol. II). CRC Press; Boca Raton, FL.

Glötzl Baumeßtechnik: *Probenahmegerät* für Flüssigkeit. Typ: PNF-MD 40, Art-Nr.: 86.10. (2002). Retrieved from: http://www.gloetzl.de/fileadmin/produkte/4_Sondergeraetebau/P_086.10_Probenahmegeraet_de.pdf

Goldscheider, N. (2005). *Karst groundwater vulnerability mapping: application of a new method in the Swabian Alb, Germany.* Hydrogeology Journal, 13(4), 555-564.

Goldscheider N, Madl-Szonyi J, Eross A, Schill E (2010) Review: *Thermal water resources in carbonate rock aquifers.* Hydrogeol J 18:1303–1318

Goldscheider, N., Drew, D. (2007). *Methods in karst hydrogeology.* Taylor and Francis, London.

Halevy, E., Moser, H., Zellhofer, O., and Zuber, A. (1967). *Borehole dilution techniques: a critical review. In Isotopes in hydrology. Proceedings of a symposium.*

Hölting, B., and Coldewey, W. G. (2013). *Allgemeine Hydrogeologie.* In Hydrogeologie (pp. 7-238). Spektrum Akademischer Verlag, Heidelberg.

Landwasserversorgung Stuttgart Kommunaler Zweckverband (HRSG.). (2012). Landeswasserversorgung. 100 Jahre Trinkwasser für Baden-Württemberg 1912 – 2012. Stuttgart.

Lamontagne, S., Dighton, J., and Ullman, W. (2002). *Estimation of groundwater velocity in riparian zones using point dilution tests.* CSIRO Land and Water.

Landesamt für Geologie, Rohstoffe und Bergbau Baden-Württemberg, Freiburg i. Breisgau (Bearbeiter: Plum, H., Prestel, R., Schloz, W. und Rausch, R.) und Landesamt für Umweltschutz, Baden-Württemberg, Karlsruhe (Bearbeiter: Kolokotronis, V.) (2002): *Hydrogeologische Karte von Baden-Württemberg. Ostalb. Erläuterungen.*

Zweckverband Landwasserversorgung. (2017). *Wir stellen uns vor.* Retrieved from: https://www.lw-online.de/fileadmin/lwonline/redaktion/pdf-dateien/publikationen/LW_UP_2015_Internet.pdf

Landwasserversorgung. (2018). *Grundwassermessstelle Langenau-Simontal.* Retrieved from: https://www.lw-online.de/fileadmin/lwonline/redaktion/aktuelle_messwerte/GWStand_Simontal.pdf

Langguth, H.R., and Voigt, R. (2004). *Hydrogeologische Methoden 2.* Springer Verlag, Berlin und Heidelberg.

Maurice, L., Barker, J. A., Atkinson, T. C., Williams, A. T., and Smart, P. L. (2011). *A tracer methodology for identifying ambient flows in boreholes.* Groundwater, 49(2), 227-238.

Ogilvi, N. A. (1958). *Electrolytic method for the determination of the ground water filtration velocity.* bulletin of science and technology news, (4).

Pitrak, M., Mares, S. and Kobr, M. (2007): *A simple borehole dilution technique in measuring horizontal ground water flow.* In Ground Water 45, No. 1, S. 89-92.

Pixabay. (n.d.). *Deutschland Karte Alle Bundesländer Ländesgrenze*n. https://pixabay.com/de/deutschland-karte-alle-bundesl%C3%A4nder-2431250/

Regierungspräsidium Freiburg, Landesamt für Geologie, Rohstoffe und Bergbau (Bearbeiter:Schloz, W., Armbuster, V., Preste, R. und Weinzierl, W.) (2007): *Hydrologisches Abschlussgutachten zur Neuabgrenzung des Wasserschutzgebiets Donauried-Hürbe für die Fassungen des Zweckverbands Landwasserversorgung im württembergischen Donauried und bei Giengen-Burgberg.*

Schloz, W. (1993). *Zur Karsthydrologie der Ostalb. Karst und Höhle.* Journal of Zhejiang University SCIENCE B, 9(3), 227-231.

Solinst: Model 107 TLC Meter. (N.d.). (Termperature, Level, Conductivity).
Retrieved from: https://www.solinst.com/products/level-measurement-devices/107-tlc-meter/datasheet/

Udluft, P., Bühlmeier, C., Schäfer, U., Wimmer, M., Kus, G., Aulbach, E. und Winter, J. (2000): *Das Grundwasser im Schwäbischen Donautal. Hydrologisch-hydrogelogische Untersuchung mit Erstellung eines Grundwassermodells im Maßstab 1:25 0000/50 000 im Donauzsl zwischen Ulm/Neu-Ulm und Neuburg an der Donau.* In Schriftenreihe der Bayerischen Sand- und Kiesindustrie, Heft 11/2000.

Van Essen Instruments. (2016.) *Product Manual, Diver®.* https://www.vanessen.com/images/PDFs/Diver-ProductManual-en.pdf

Vesper, D. J., Loop, C. M., and White, W. B. (2001). *Contaminant transport in karst aquifers.* Theoretical and Applied Karstology, 13(14), 101-111.

Zhu, Y., Balke, K.D. (2008). *Groundwater protection: What can we learn from Germany?.* pp 119-134, 9 Abb. München.

Appendix

Appendix 1 - Land-use map

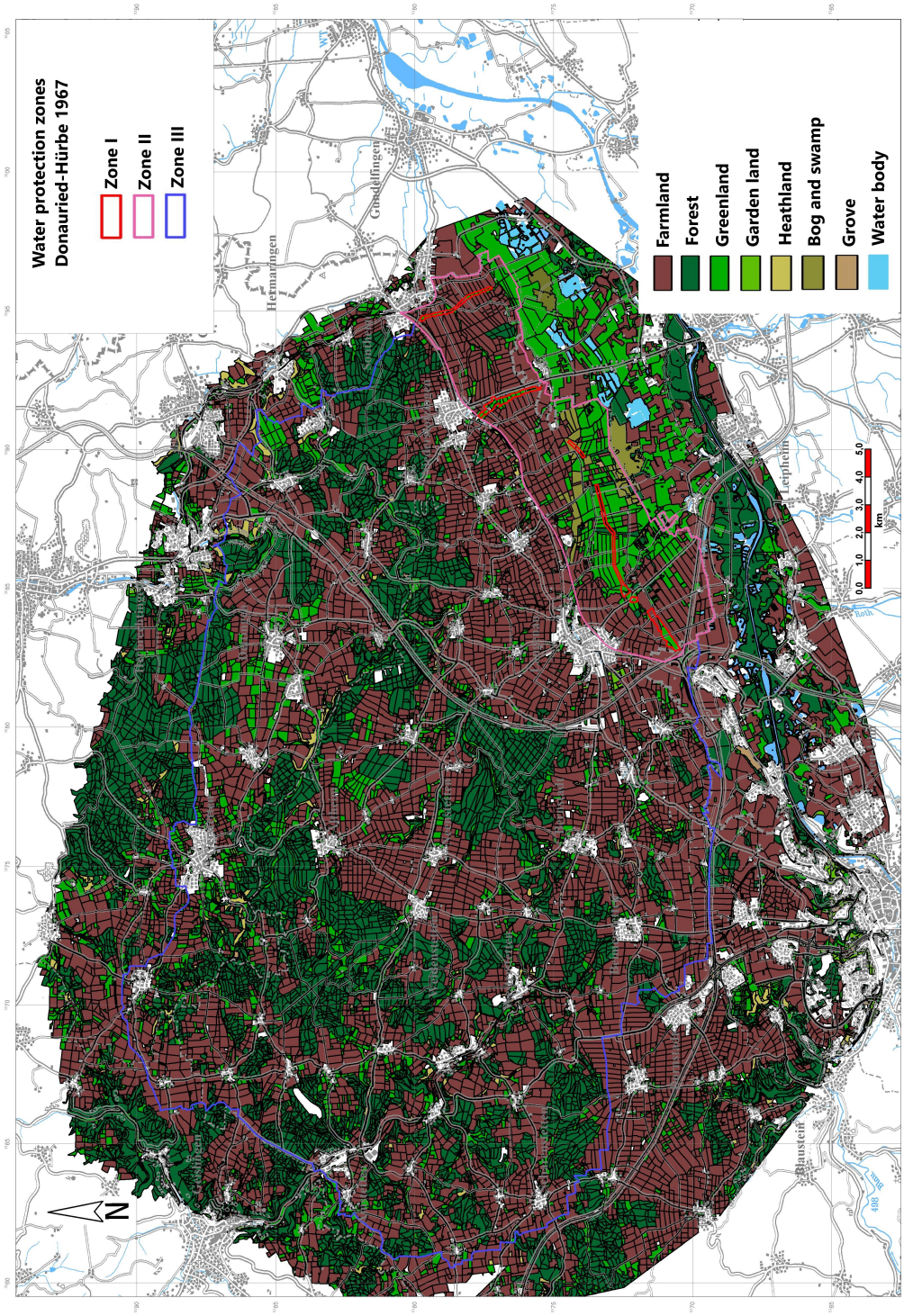

Figure A1: Land usage in the study area. (Source: Regierungspräsidium Freiburg Landesamt für Geologie, Rohstoffe und Bergbau, 2007; Anlage 31)

Appendix 2 - Geological overview map

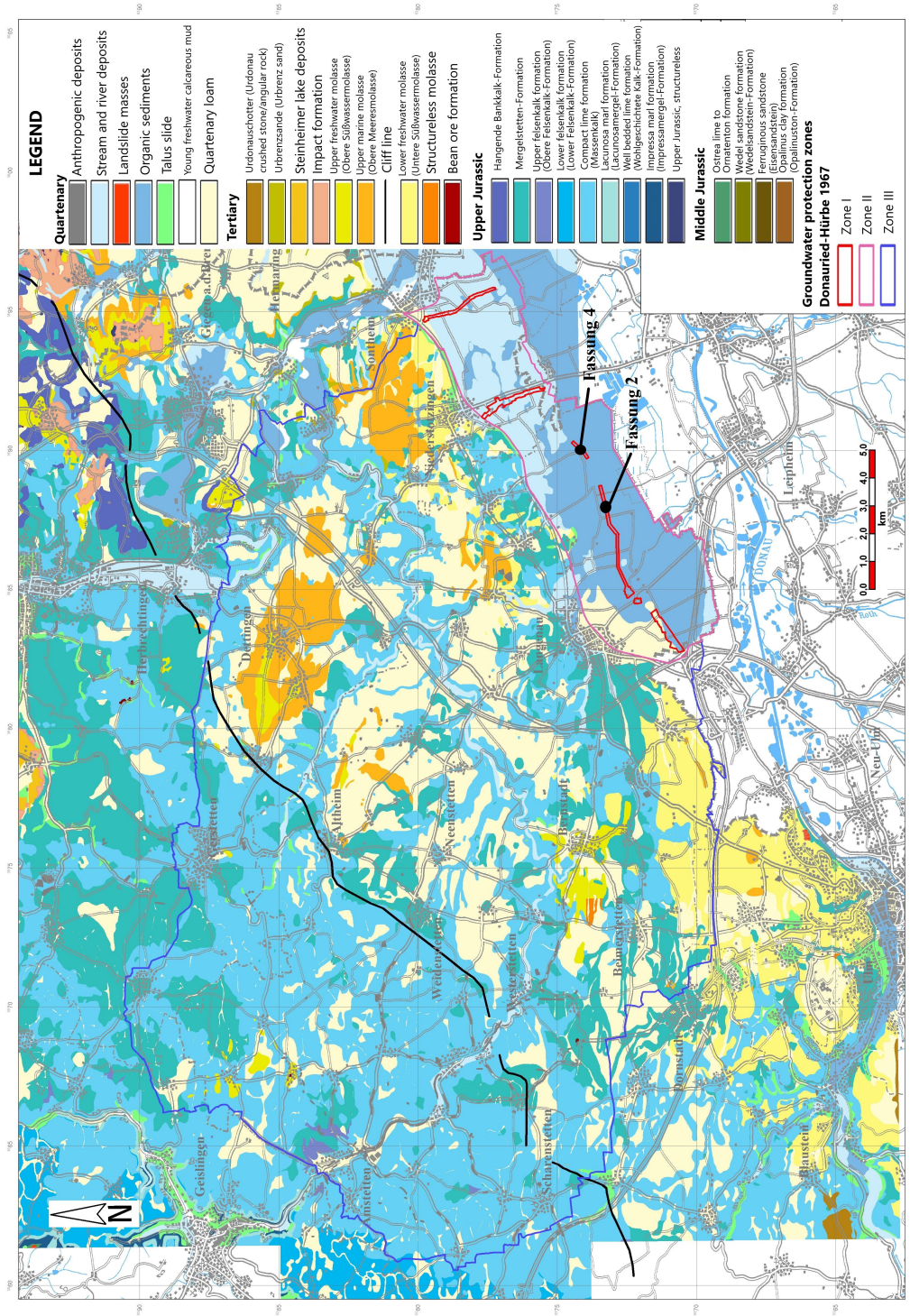

Figure A2: Geological overview map of study area. (Source: Regierungspräsidium Freiburg Landesamt für Geologie, Rohstoffe und Bergbau, 2007; Anlage 2

Appendix 3 - Summary of Geological Abbreviations

J2	Jüngere Nagelfluh	fluviatile pebbles from Upper Jurassic limestone - a type of conglomerate only existing in southwestern Germany
jOM	Massenkalk-Formation	unstratified sponge-algae limestone; massive dolomite stone, with holes when recalcitized (perforated rock), with alternating strong fissures and karstification
ki1	Lacunosamergel-Formation	dark grey marlstones with limestone and limestone marlstone banks
ki2	Lower Felsenkalk-Formation	light grey, banked limestones with mostly thin marlstone joints
ki3	Upper Felsenkalk-Formation	light grey, banked limestones with thin marl joints, pebble nodules
ki4	Liegende Bankkalk-Formation	light grey layered limestones with marlstone interlayers
ki5	Zementmergel-Formation	dark grey marl, limestone marl and limestones
tBM	Brackish Wassermolasse	Kirchberg strata (fine-grained deposits with organic layers and pyrite), Grimmelfingen strata (marley sands with partly high pyrite contents)
tOM	Upper Meereswassermolasse	yellow-brown and greenish micaeous fine-grained coarse-grained sands, clayey sands, sand marls
tOS	Upper Süßwassermolasse	freshwater limestone, greenish marl, fine-grained yellow-brown-greenish grey sands, sand marls
tUS	Lower Süßwassermolasse	yellow to greenish-grey clays and silt, yellow-brown fine grained sands, sandy marls, freshwater lime

Appendix 4 - Water protection zones map

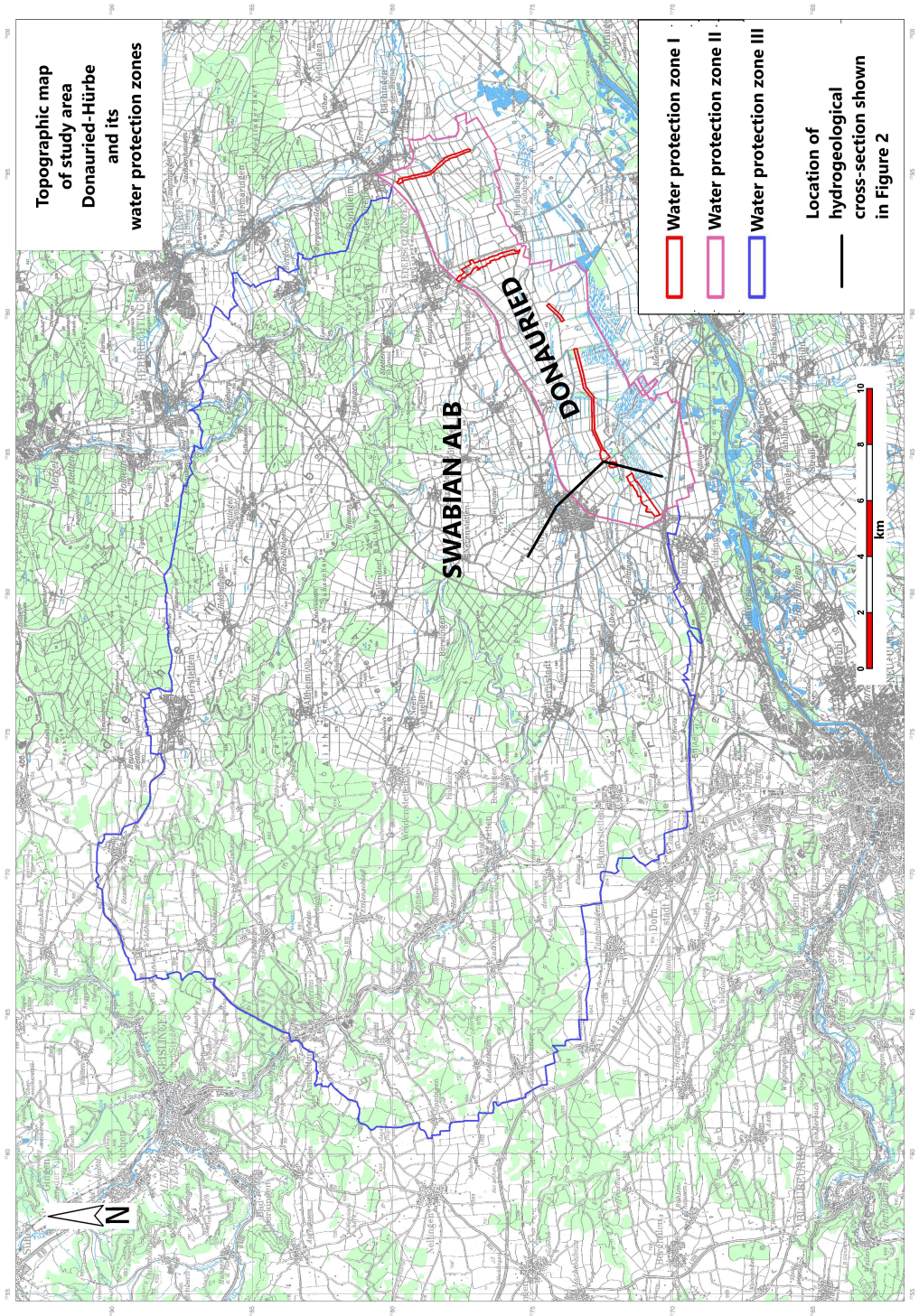

Figure A3: Overview map of the study area with its water protection zones. (Source: Regierungspräsidium Freiburg Landesamt für Geologie, Rohstoffe und Bergbau, 2007; Anlage 8.1)

Appendix 5 - Selected boreholes

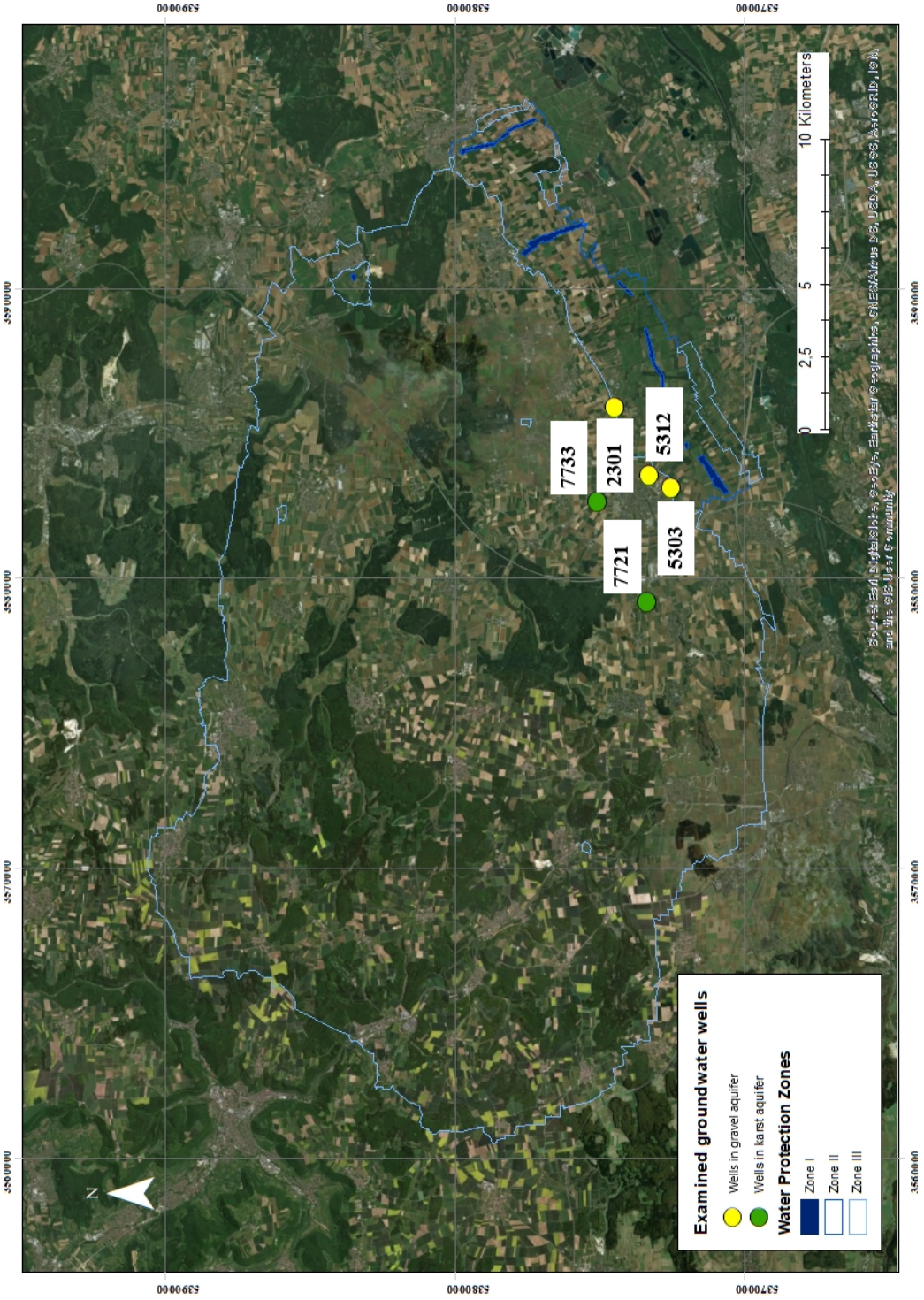

Figure A4: Selected measurement wells for the SBDTs in this master thesis.